Polytechnic University of Marche
Ph.D. School in Engineering Science
Curriculum in Integrated Facility Engineering and Resilient Environments

---

Automated OMA and Damage Detection: an Opportunity for Smart SHM Systems

Ph.D. Dissertation of:

Francesca Bianconi

Advisor

Prof. Francesco Clementi

Co-Advisor

Prof. Stefano Lenci

Curriculum Supervisor

Prof. Francesco Fatone

XXXV Cycle - 2019/2022

Università Politecnica delle Marche
Scuola di Dottorato di Ricerca in Scienza dell'Ingegneria
Curriculum in Integrated Facility Engineering and Resilient Environments

---

OMA e Rilevamento dei Danni Automatizzati: un'Opportunità per i Sistemi SHM Intelligenti

Tesi di Dottorato di:

Francesca Bianconi

Tutor

Prof. Francesco Clementi

Co-Tutor

Prof. Stefano Lenci

Coordinatore del corso

Prof. Francesco Fatone

XXXV Ciclo - 2019/2022

Università Politecnica delle Marche
Dipartimento di Ingegneria Civile-Ambientale, Edile e Architettura
Via Brecce Bianche - 60131 - Ancona, Italy

A me e alle persone che amo

"Chi ha un perché abbastanza forte, può superare qualsiasi come"
F. W. Nietzsche

Acknowledgements

Writing acknowledgements is never easy. There is always the feeling of not saying enough.

At the end of this journey, at first unwanted, then desired, sometimes suffered, but in any case "well lived", I want to thank myself primarily.
The person who we necessarily have to live with all our lives is ourselves. Sometimes we love ourselves, sometimes we hate ourselves, but the most important aspect is always to accept ourselves and never stop improving.
Each of us has our own battles. They do not necessarily have to be faced alone. There is a whole world to discover behind each person around us. I wish everyone who reads these pages to believe in themselves.

I would like to sincerely thank my tutor, Prof. Francesco Clementi. You gave me an opportunity that not everyone has and, despite my initial doubts, I am happy to have started this journey. Your guidance was fundamental. You have been a point of reference, not only on a professional level, but also on a human level. I wish you never to lose the infinite patience you showed me and all the other guys. Sometimes you might think it is a kind of weakness, but it is not.

A big thank you also goes to co-tutor Prof. Stefano Lenci.
To the Portuguese tutors, Prof. Daniel V. Oliveira and Prof. Nuno Mendes of the University of Minho, for their support both during the months spent at your university and in continuing the work from afar.
To Prof. Nuno Mendes and Prof. Enrique García Macías, of the Universidad de Granada, a big thank you for spending time carefully reviewing this thesis, suggesting improvements and useful hints for reflection.

I thank all the guys and colleagues in the department. From those closest to me, Ersilia, Gianluca, Mattia, with whom I started on this journey, to those

passing through or recently met, Angela, Giorgio, Nico and all the others.
Ersilia, with your simplicity and delicacy you always manage to find a way to say the right thing.
Gianluca, without your precious and concrete help, it would have been much more difficult to get to this point. Thank you for the time you spent for me. You once said: "We are a group, we help each other". I agree with you, but that does not mean that a big thank you is not due.
Mattia, together we completed our Master's degree. Together we started this PhD, we experienced the period abroad and now, together again, we conclude this chapter. Thank you for your presence.

The most special and sincere thanks go to my parents. Your constant support and encouragement has been important.
Mum, every day you fight for what you truly believe is important and what you love to do. I wish you to continue to do so. You often fight with those around you because you do not understand how one cannot try to do the best one can for others and not for oneself. Your sensitivity is sometimes a weapon for yourself, but keep guarding it strongly, without it you would not be you.
Dad, you are the backbone of the family. A bit of a tough character, introverted, but even with your manner, you never say no to a request for help. I think there is no limit to what you would do for your three women. I think of you and hope, one day, to be for my family what you are for me and Federica.

Federica. The relationship we have been creating for some time now, I treasure it strongly in my heart. You are a strong, independent and headstrong girl. But your presence and support are never in question. You know how to be sweet, but also firm. Tender at times, but also concrete. Unlike me, you show little of your emotions and that is not always a bad thing. But don't let people who are less than honest with you preclude you from new and perhaps beautiful acquaintances. Feelings and emotions are what make us who we are, so let the people around you see more.

Gian Luca. You are present in all my thank-you pages.
We met when we were very young and totally inexperienced about what it meant to share life, in all its aspects, with someone. We grew up together facing, with a few exceptions, very different life experiences. Throughout these years there have been many difficult moments that we probably still carry with

us, but now we are facing real life together, or at least we are trying to learn how to do it. Nothing will ever be easy and nothing will ever be given to us. To reach an objective, a goal, whether personal or as a couple, you have to work constantly, every day, because days spent waiting, without making decisions, are days lost.
Thank you for always being by my side in times of need, and thank you for choosing to stand by me even when it was not necessary.
You are a man, and like a man you have your frailties, which I have come to know and I hope you will be less afraid of having me by your side. I may not always be the perfect shoulder to rest on, but if you look for me, have no doubt that I will be there beside you doing my best. You are honest, generous and clear. There is never any malice in what you do for others. You are definitely stubborn, but at the same time you always have questions because you don't want to let anyone down. You don't want others to get into difficult situations. You can never please everyone, you can never satisfy everyone. Be as good as you have always been and those who want to get to know you and stand by you will do so regardless of any mistakes you may have made.
These have been very very complicated months. Only you and I know. Only you and I know the constant efforts that have been required of us. The commitment that I demanded of you because I was and I am convinced it was the right thing and the commitment that I demanded of myself and that you demanded of me. Now we are stronger, weaker, I don't know. But we are certainly more aware. I wish you the serenity you deserve. I am here to encourage you. No one's words should make you waver. Be proud of who you are, because I am extremely proud.

Thanks to my grandparents, all four of them, Costanza (you are always in my heart) and the rest of my family. The distance that separates us is only physical.

Thanks to all the people I have met so far. Each, in their own way, has left me something.
Thanks to those who have been there always. To the old friends, to those lost and then re-found, and to the more recent ones. The unit of measurement of bonds is quality and not quantity.
I would also like to thank those who have judged me without knowing me. To those who have assumed to understand who I am and how I am based on a situation, a sentence, a gesture. I don't know myself, imagine if you can. You

have made me realise that I don't want to be a girl who stops at appearances. Thanks to the 'library guys'. It's crazy how hours and hours of conversation over coffee, breakfast, drinks or dinner with you guys is never enough. The purity, with no ulterior motive, of what we have established I hope lasts for a long time.
I wish you all a life fully lived. Sincere and full of meaningful presences. It is always a pleasure to have people at one's side who are ready to support us.

Francesca

Abstract

Structural monitoring aims to develop systems that can monitor a structure by allowing its inspection and detection of damage with minimal human intervention. It therefore represents a process of implementing a damage identification strategy through which, by observing a structure with a certain periodicity, it is possible to arrive at an evaluation of specific characteristics of the system, to define its current state of health.
Its first application was in fields other than civil engineering. In fact, it was a technique mainly used in mechanical, aeronautical, and aerospace engineering. It later became evident that it was a strategy that, if correctly adapted, could be of great help in the control of all civil structures in the area.
It can be developed as an autonomous integrated system on big infrastructures (such as bridges, dams, etc.) with the aim of monitoring the response of the structure under stress during construction to modify designs if necessary. Also, on these types of structures, it can maintain constant control during its life cycle to implement timely interventions before irreversible and dangerous situations can arise.
In addition, structural monitoring can be used, as will be shown in this thesis, to monitor the structural health of historical buildings belonging to cultural heritage. This heritage is spread in Europe and particularly in Italy. We are talking about buildings even of considerable size (such as enormous churches), built in very distant epochs, the conservation of which is now the focus of many researchers. The case study that is the subject of the present work is the bell tower of a church in the Marche region, Italy, whose historical traces date back to around 1330, with numerous subsequent interventions and remodelling up to the present day.
With the technique of structural monitoring, it is possible to assess the dynamic behaviour of the (monitored) structure through the identification of its main modal parameters from the analysis of the acquired data. The term 'dynamic identification' of a structure means all those techniques, both analytical and

experimental, through which it is possible to identify the dynamic response of the structure itself by extrapolating natural frequencies, corresponding modal shapes and damping coefficients.
Focusing on this concept, the work was initially set up by implementing an automatic procedure for processing the output data from the monitoring and thus defining the modal parameters of the structure under examination purifying them from the effects of environmental actions such as temperature, average wind speed and humidity. By removing these external factors from the results, a prediction of the evolution of the modal characteristics can be obtained. Comparing them with the actual behaviour of the structure, any anomalies can be highlighted.
Regarding the above, it is nowadays of fundamental importance, to be able to recognise and predict the progressive failure of a structure. This may occur due to natural degradation of materials, or because of unexpected vibrations (earthquakes, explosions, etc.). Focusing on this concept, the identification of damage based on the evaluation of changes in modal parameters, purified of the influence of external agents, can be a time-consuming process. On the contrary, being able to know almost instantaneously the "new" behaviour of the construction, is an aspect that must be taken into well consideration both for safeguarding people's lives and for the accurate and timely implementation of improvements. Being prompt in critical situations, makes it possible to avoid reaching conditions where it is necessary to interrupt the operability of the structure for a long time to recover it, if it is possible. In the present work, methods based on the direct processing of data acquired from the continuous monitoring system were used. In this way, the computational burden was reduced. It was not necessary to elaborate the acquired data to extract the modal characteristics of the system, and almost instantaneous feedback of changes in dynamic behaviour was obtained. These aspects are significant when the purpose is to develop "sustainable monitoring" from both an economic and timing perspective.

Sommario

Il monitoraggio strutturale si propone di sviluppare sistemi che siano in grado di monitorare un'opera permettendone l'ispezione ed il rilevamento dei danni con il minimo intervento antropico. Esso rappresenta dunque un processo di implementazione di una strategia di identificazione dei danni attraverso la quale, osservando una struttura con una determinata periodicità, è possibile pervenire alla valutazione di alcune caratteristiche del sistema, in modo tale da definirne il suo stato attuale di salute.
La sua prima applicazione ha interessato campi differenti da quello dell'ingegneria civile. Infatti, era una tecnica impiegata prevalentemente in ambito meccanico, aeronautico e nell'ingegneria aerospaziale. Successivamente è risultato evidente come fosse una strategia che, se correttamente adattata, poteva essere di grande aiuto per il controllo di tutte le strutture civili presenti sul territorio.
Può essere sviluppata come un sistema autonomo integrato su grandi infrastrutture (come ponti, dighe, ecc.) con l'obiettivo di monitorare la risposta della struttura sotto delle sollecitazioni durante la costruzione per modificare i progetti se necessario. Sempre su questo tipo di strutture, può mantenere costante il controllo durante il suo arco di vita per attuare tempestivamente interventi prima che possano crearsi situazioni irreversibili e pericolose.
Inoltre, il monitoraggio strutturale può essere impiegato, come verrà mostrato in questa tesi, per il monitoraggio della salute strutturale di edifici storici, appartenenti al patrimonio culturale. Questo patrimonio è diffuso in Europa ed in particolare in Italia. Si parla di edifici anche di notevole entità (come grandi chiese), costruite in epoche molto lontane, la cui conservazione è oggi il focus di molti ricercatori. Il caso studio oggetto del presente lavoro è la torre campanaria di una chiesa nelle Marche, in Italia, le cui tracce storiche risalgono a circa il 1330, con numerosi interventi e rimaneggiamenti successivi fino ad arrivare ai giorni nostri.
Con la tecnica del monitoraggio strutturale è possibile valutare il comportamento dinamico della struttura (monitorata) attraverso l'identificazione dei

suoi principali parametri modali a partire dall'analisi dei dati acquisiti. Con l'espressione "identificazione dinamica" di una struttura si intendono tutte quelle tecniche, sia analitiche che sperimentali, attraverso le quali è possibile appunto individuare la risposta dinamica della struttura stessa andando ad estrapolare frequenze naturali, corrispondenti forme modali e coefficienti di smorzamento. Soffermandoci su questo concetto, il lavoro è stato inizialmente impostato implementando un processo automatico per l'elaborazione dei dati in uscita dal monitoraggio e quindi per la definizione dei parametri modali della struttura sotto esame depurandoli dagli effetti delle azioni ambientali quali temperatura, velocità media del vento ed umidità. Rimuovere questi fattori esterni dai risultati, permette di ottenere una previsione dell'evoluzione delle caratteristiche modali. Dal loro confronto con il comportamento reale della struttura si possono evidenziare eventuali anomalie.

In riferimento a quanto appena detto, risulta oggigiorno di importanza fondamentale riuscire a riconoscere e prevedere il progressivo deterioramento di una struttura. Questo può avvenire per naturale degrado dei materiali, o dopo aver subito vibrazioni impreviste (terremoti, esplosioni, ecc). Focalizzandosi su questo concetto, l'identificazione del danno basata sulla valutazione delle variazioni dei parametri modali, depurati dell'influenza di agenti esterni, può essere un processo lungo. Al contrario, poter conoscere quasi istantaneamente il "nuovo" comportamento della costruzione, è un aspetto da tenere bene in considerazione sia per salvaguardare la vita delle persone, sia per attuare in maniera precisa e puntuale interventi di miglioramento. Essere tempestivi in caso di situazioni critiche, permette di evitare di arrivare a condizioni tali per cui è necessario interrompere l'operatività della struttura per molto tempo pur di poterla recuperare, se possibile. Nel presente lavoro si sono utilizzati metodi basati sull'elaborazione diretta dei dati acquisiti dal sistema di monitoraggio in continuo. In questo modo l'onere computazionale è stato notevolmente ridotto. Non è stato necessario elaborare i dati acquisiti per estrarre le caratteristiche modali del sistema e si è ottenuto un feedback quasi istantaneo di variazioni nel comportamento dinamico. Tali aspetti, risultano significativi quando l'obiettivo è di sviluppare un "monitoraggio sostenibile" sia da un punto di vista economico che di tempistiche.

Contents

List of Figures

List of Tables

Abbreviations

ANPSD Averaged Normalized Power Spectral Density

AVT Ambient Vibration Test

BFD Base Frequency Domain

CL Centre Line

CMIF Complex Mode Indication Function

DAQ Data-Acquisition

DFT Discrete Fourier Transfer

DOF Degree of Freedom

DR Dynamic Range

EFDD Enhanced Frequency Domain Decomposition

EM Experimental Model

EMA Experimental Modal Analysis

FA Factor Analysis

FDD Frequency Domain Decomposition

FEM Finite Element Model

FFT Fast Fourier Transform

FIR Finite Input Response

FRF Frequency Response Function

FVT Forced Vibration Tests

IEPE Integrated Electronics Piezo-Electric

IRF Impulse Response Function

LCL Lower Control Limit

LF Loss Function

LS Least Squares

LTI Linear-Time Invariant

MAC Modal Assurance Criterion

MDOF Multiple Degree of Freedom

MEMS Micro Electro Mechanical Systems

MRA Multiple Regression Analysis

NI Newness Index

OMA Operational Modal Analysis

PC Principal Component

PCA Principal Component Analysis

PP Peack Picking

PSD Power Spectral Density

SDOF Single Degree of Freedom

SHM Structural Health Monitoring

SNR Signal-to-Noise Ratio

SSI Stochastic Subspace Identification

SSI-Cov Covariance-driven Stochastic Subspace Identification

SSI-Data Data-driven Stochastic Subspace Identification

SV Singular Value

SVD Singular Value Decomposition

UCL upper Control Limit

VBDIM Vibration-Based Damage Identification Methods

ZOH Zero Order Hold

Chapter 1

Introduction

1.1 Research context

Italian history shows how in our country, periodically, events occur that severely test the entire built environment, both the most recent and modern as well as the oldest [1–5].
In recent decades, sensitivity to the issue of building conservation and structural safety has increased considerably, leading to the development of highly efficient techniques and procedures, first and foremost ***Structural Health Monitoring (SHM)*** [6, 7].
SHM is presented as a set of techniques for the detection, localisation, characterisation and quantification of structural damage. In this sense, it is proposed as a useful tool to predict the residual life of the structure [8]: following the evolution of the damage over time allows to understand if the mechanism is in place or if it has stopped and therefore if the construction under examination still has adequate resistance.

The widespread use of SHM derives in part from the need to compensate seismic analyses performed on numerical models that are extremely simplified. The construction of these, in fact, requires knowledge of structure characteristics that are difficult to acquire. Therefore, the evaluation of the dynamic behaviour is a very difficult task and the numerous uncertainties and approximations that are necessarily introduced can lead to insignificant or erroneous results.
In this context, the SHM provides very meaningful results that can be used, for example, to calibrate the aforementioned numerical models.

In addition to the evolution of the damage over time, the SHM is a useful tool to allow a rapid post-event (earthquake) assessment without necessarily having to schedule in-situ visual inspections by qualified operators. These, in fact, also imply high costs and inconvenience for the users of the structural system under investigation since they may require significant actions (removal of partitions, false ceilings, etc.). Furthermore, if there are many buildings to be inspected, and given the possibility that qualified inspectors are not immediately available for the investigation, it is obvious to assume that the timeframe is necessarily long. In thiS sense, the results of a SHM system can be considered as accurate information on the dynamic behaviour of the structure and on the basis of this the engineers can target inspections to specific areas.

Another very significant use of the SHM technique concerns the possibility of integrated installation of monitoring equipment already in the early stages of construction of a structure. This allows a continuous control of the structural system from the "first moments of life" and thus the possibility of making corrections to projects in a timely manner.

In this general overview presented, it has been highlighted how SHM can be applied on different types of structures and with different purposes.
Thinking of the Italian territory, but also extending the look to other countries, the attention was strongly focused on the conservation of cultural and architectural heritage, which is present in a very significant way. This has always played a very important cultural, economic and political role in society. Given its age and the typical construction system (masonry), a punctual and systematic structural assessment is required: the intrinsic characteristics of masonry buildings easily lead to cracking and, often, collapse, following seismic events [9–12]. The needs are: to prevent unforeseen failures that imply the interruption of usability, to diagnose previous pathologies and, above all, to plan maintenance in an appropriate and cost-effective manner. What is to be avoided is irreversible damage that compromises the overall structural integrity. In addition to this, the high seismic risk of the area has made the needs just presented even more important. In addition, it has led to the research and implementation of methodologies for the control of the structural state of health, exploiting the vibration characteristics of structures, which have undergone significant development in recent decades.

Monitoring tools, involving non-destructive methods, allow a very reliable characterisation of the statics and dynamics of systems while respecting the historical value of the construction.

As is well known, the evaluation of the structural condition of a system begins with the execution of a dynamic test. To do this, the structure under investigation can be subjected to externally imposed or environmental/operational load scenarios.
These tests can be classified into two categories:

1. ***Forced Vibration Tests (FVT)***, in which the structure is artificially excited, in a controlled manner and using specific instrumentation. The imposed stress is then known;

2. ***Ambient Vibration Test (AVT)***, in which the modal parameters are extracted using the dynamic response of the structure under environmental loads (micro-tremors induced by traffic, wind, operational loads, etc.), which are always present. The stress remains unknown. This second type of test certainly is suitable for continuous data analysis.

Dynamic tests are usually adopted to perform the identification of modal parameters (natural frequencies, mode shapes and modal damping ratios) from measured structural responses. This can be done through:

1. ***Experimental Modal Analysis (EMA)***, a input-output modal analysis method directly related to the *FVT*s [13];

2. ***Operational Modal Analysis (OMA)***, a output-only modal analysis method directly linked to the *AVT*s [14–17], which can be performed in the time domain [18] or frequency domain [19].

For a more detailed discussion of aspects concerning one or the other technique, advantages and disadvantages, please refer to chapter 3.

The discussion presented here refers to the second identification methodology and it is based on the concept of vibrations induced by white noise (environmental agents or human activities), which allow the extrapolation of dynamic characteristics under *operating conditions* (without interrupting the operability and without inducing "abnormal" vibrations). This is certainly a very significant aspect when considering the fact that using specific instrumentation to

excite a large infrastructure or cathedral is expensive, can cause further damage and in many cases is impractical [20]. Finally, output-only methods are definitely the best choice when considering a continuous monitoring system, which can last for years and requires a constantly excited structure.
The well-known possibility of easily measuring modal quantities has favoured their use as indicators of *structural damage* in many fields of engineering [15, 21, 22].

Vibration-Based Damage Identification Methods (VBDIM) starting from the knowledge of nodal responses, are based on the well-known consideration that the modal parameters of a structure are its intrinsic properties, closely dependent on physical properties. Therefore, since the occurrence of damage is often associated with a reduction in the overall stiffness of the structure, this also implies a consequent decrease in, for example, frequency values. Ultimately, changes in dynamic properties can be a reflection of structural damage [23, 24].
It should be emphasised that the identification of structural anomalies is not always easy because modal estimates are influenced by environmental factors (e.g. temperature, humidity and wind). This is still the focus of many researchers today.

Initial interest was shown in methods that took frequencies as an indicator of damage [25]. Over time, however, it became apparent that these failed to provide spatial information about damage and the nominal value of the frequency was strongly influenced by environmental factors, to the extent that it masked real variations due to real damage [26]. To overcome this second problem, methods based on mode variations and/or modal curvatures were developed due to their lower sensitivity to environmental conditions and dependence on the nodal coordinates of the system. In this case, however, it is not always feasible to excite the higher modes through vibration tests [27] In addition to these more classical methods, other procedures have been developed and are under development, e.g. based on the updating of unknown structural model parameters [28], the use of statistical properties of random signals (non-modal methods) [29], wavelet analysis, neural networks, genetic algorithms [30] or interferometry [31].

As just mentioned, at the base of the mentioned methods is the need to perform

dynamic identification of the structure under investigation. Referring again to the assumption that variations in modal characteristics imply the presence of damage, attention is drawn to a newer and faster warning strategy. This, in fact, allows the assessment of modal parameter variation by excluding the identification phase and analysing monitoring data directly [32, 33]. In the practical application, recordings made considering a reference state of the structure, assumed to be undamaged, and those made in the "current" state, i.e. the state in which I want to know whether there are variations in the modal parameters, are considered. The comparison that is then made is statistical. For more details, please refer to chapter 4.

Summarising all the issues proposed up to now, which will be analysed in more detail in the chapters of this paper, a classical approach to vibration-based monitoring can be represented as in figure 1.1 and describes as in the three macro topics listed below.

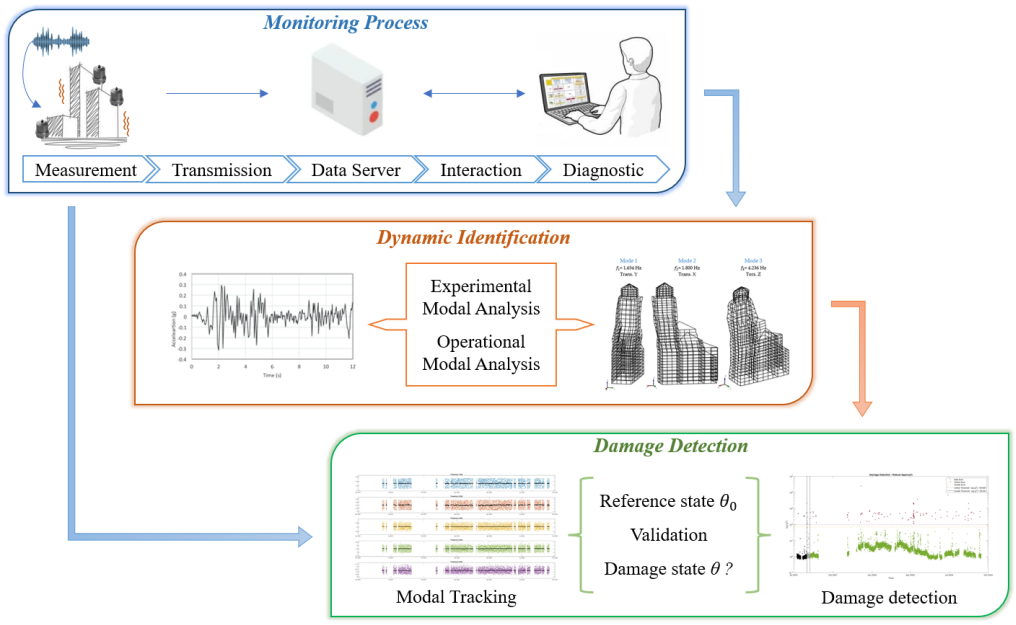

Figure 1.1: *Classical approach to vibration-based monitoring*

- Measurement of structural response by sensors measuring accelerations, velocities or displacements.
- Extraction of modal parameter estimates through dynamic identification

techniques that allow the conversion of the collected time series into dynamic characteristics.

- Tracking the time evolution of modal estimates (with removal or minimisation of environmental/operational effects to obtain results that depend only on structural conditions) to implement damage detection procedures based on changes in structural dynamic behaviour and automatically report anomalies.

1.2 Objectives and main contributions

The work that will be presented is based on the use of OMA techniques in the context of a continuous SHM, more than a year old and still active on a church in the Marche region, which is known to be subject to seismic phenomena.

A scenario like this certainly requires the development of an automatic system capable of constantly processing the large amount of data output from dynamic monitoring. Therefore, the first issue addressed was the implementation of an automatic procedure to manage the continuous monitoring of the structure.
Acquisitions are made through MEMS accelerometers. These sensors interpret the excitation in a fully electronic way. They are certainly less efficient than other types of sensors, but what we wanted to check was their effectiveness in returning good results that could be used for subsequent damage identification. An important issue is indeed the possibility of developing *sustainable monitoring*. The use of highly specialised but also highly expensive instrumentation certainly means that these processes are not widely used.
The automatic procedure processes the data to perform a modal tracing. It proceeds with the removal of environmental effects from the results and makes it possible to obtain a prediction of the evolution of the main modal characteristics to be compared with actual behaviour and thus highlight any anomalies.

In order to expand the application of these tools as far as possible in order for them to be an easy-to-use and immediate resource, a *subspace-based damage identification* procedure was also implemented in this work by directly analysing the collected time series. In this way, a precise localisation or quantification of the damage was not obtained, but an *alarm* is returned if the system registers

a significant change in the dynamic behaviour of the structure. Thinking about a possible diffusion of this methodology, it is easy to imagine how a physical signal (an alarm) can be easily read even by less experienced people. In the occurrence of an anomaly, it will then be the task of a technician to assess the actual significance of the alarm itself.

1.3 Structure of the thesis

This thesis is developed as follows:

- Chapter 2: a general introduction to structural monitoring is proposed. Its strengths are analysed and the necessary steps for its correct application are described. Then, all its possible classifications and applications in the field of structural engineering are shown. Finally, attention is drawn to specific issues that must be taken into account before applying a monitoring technique in order to derive the greatest benefit from it.

- Chapter 3: OMA is discussed in detail, starting with the basics of structure dynamics and ending with a presentation of all the possible techniques that can be used today to achieve dynamic identification of a structure, both in the time domain and in the frequency domain.

- Chapter 4: explores the close relationship between the SHM technique and OMA. Automatic algorithms for the extrapolation of modal parameters are presented; the important issue of removing the influence of environmental factors on the dynamic characteristics is addressed by proposing various methods existing today; it discusses the problem of damage identification by presenting a classic tool used today, the control chart, and then proceeds with an in-depth discussion of the basis on which the procedure for identifying structural anomalies, based on the detection of variations in dynamic behaviour, was implemented.

- Chapter 5: is proposed as a practical insight into dynamic monitoring. The various instrumentation required, such as acquisition hardware and transducers on the trade, and the importance of signal processing are presented.

- Chapter 6: presents the main topic of the thesis. The case study taken into consideration is presented in detail and all the subsequent analysis

steps are described with regard to the topics already set out in detail.
The general, historical and geometric presentation is followed by the description of investigations conducted over time through short-term monitoring. The numerical model realised with advanced calculation software is shown, which can be used for subsequent assessments of the structural health of the building.
With the description of the long-term monitoring campaign, the second part of the chapter opens. The implementation of the automated procedure for OMA is described with the results obtained even after the removal of the influence of environmental factors.
The discussion concludes with the automated procedure implemented to deal with damage detection. The results will show how the alarms obtained certainly reflect changes in dynamic behaviour, but at the same time are not permanent.

- Chapter 7: contains a summary of the main issues addressed, presenting the results critically and proposing possible future developments.

Chapter 2

Structural Health Monitoring (SHM): background and tools

2.1 Introduction to SHM

In its broadest sense, a structure is said to be damaged when it presents a change, more or less visible, capable of negatively influencing its current and future performance [3]. From this definition it is clear that the concept of damage is only consistent if one is able to make a comparison between two different states of the system under examination: the initial state, which may coincide with an undamaged state or more generally with the state of the structure at the time of the "first check", and the final state, which may be associated with damage caused by a particular event (e.g. an earthquake, or an explosion) or, after years, to check if the structural performance has undergone changes linked to the degradation of materials.
Structural damage affects all buildings, both the most common ones such as those for residential use, and strategic ones such as dams, bridges, power stations, as well as structures of the artistic and cultural heritage, which, as we all know, occur in very large numbers in our country, Italy. All these types of structures are an integral part of people's life and ensure the proper functioning of society [34].This is where the concept of **SHM** comes in. The basic idea is to develop systems that are able to monitor a structure by permitting its inspection and damage detection with minimal human intervention [35]. It therefore presents itself as a real process, periodic, of identifying and evaluating certain characteristics of the structure, sensitive to "damage", in order to define its state of health. The methodologies it can be performed with are different

depending on the needs and information to be collected.
One of the most relevant reasons why monitoring the performance of a structure is essential is because through a monitoring system it is possible to predict an imminent collapse of the structure. In addition, a structure must work properly and adequately to ensure its usability and the safety of its occupants, and SHM allows to provide a possible occurrence of unacceptable future performance with an acceptable notice.
The approach used for this research work, first initiated for industrial and aerospace engineering, then for civil engineering since the 1980s, is essentially based on ambient vibrations (Ambient Vibration Tests - AVT). These vibrations induced on the structure, caused by both environmental and anthropogenic factors, are analysed and from them it is possible to extract all those properties that make it possible to describe the dynamic behaviour of a structure. The basic idea is that the modal parameters of a structure (vibration frequencies, modal shapes and modal damping) are based on its intrinsic physical properties (stiffness, mass, damping), which will necessarily change if the structure itself is exposed to damage.
In the field of civil engineering, the information that can be obtained from SHM is useful for a variety of needs:

- Assessing structural integrity after a seismic event;
- Control of construction degradation;
- Planning requirements for focused maintenance to avoid interrupting the structure's operability;
- Rehabilitation of historic structures;
- Estimation of the remaining life of a structure.

2.2 Monitoring Steps

Monitoring a structure means observing it over time by extracting and analysing the characteristics that make it possible to establish its state of health.
The focus of the research carried out up to now and found extensively in the literature, which attests to the possibility of detecting structural damage from the study of vibrations, is to understand how the responses that a damaged

system provides can best be exploited. The aim is also to optimally define the number, as well as the position, of sensors required for signal acquisition, so that the greatest amount of information can be obtained [36].
It is possible to fix some steps in the monitoring process. It begins with a preliminary assessment, so that the conditions, both operational and environmental, of the system under investigation can be defined, and possible limitations of data acquisition are recognised based on the environment in which the structure is located. In this first phase, economic considerations are made, and it is defined what damage is expected and what may be of concern. All these considerations provide a way of adapting the data acquisition process to the specific characteristics of the system to be monitored.
Then we move on to the operational phase of data acquisition and subsequent data cleaning.
Subsequently, using different methods, we proceed with the extraction of the structure's characteristics.
Finally, there follows a phase of developing statistical models for implementing algorithms that act on the extracted characteristics to quantify the damage to the structure. In general, as suggested by Rytter (1993) [20], the damage state of a system can be described by answering a few queries [2]:

1. *Existence.* Is there damage in the system?
2. *Location.* Where is the damage in the system?
3. *Type.* What kind of damage is present?
4. *Extent.* How severe is the damage?
5. *Prognosis.* How much useful life remains?

By answering, in order, the above questions, it is possible to gain adequate knowledge about the damage state of the system under investigation. Statistical models also have the purpose of minimising false results: a false negative (I do not recognise the damage, but it is present) represents the most dangerous situation for safety, but a false positive can create inconvenience because subsequent decisions can be based on it (e.g., interrupting the operation of the structure, which certainly has economic implications, can affect the trust placed in the monitoring process).

2.3 SHM Classifications and Applications

Classifications

As mentioned in the previous paragraphs, the main purpose of structural monitoring is to obtain the information required to interpret the correct dynamic behaviour of a structure. It is possible to define different types of monitoring, considering different classification criteria. Depending on the duration and frequency of measurements, it is possible to speak of ***short-term monitoring*** [17] or ***long-term monitoring*** [10]. Short-term monitoring is used when the structural phenomenon must be evaluated at a specific moment in time. It may therefore be useful to make use of this solution in the case where the structural response is to be evaluated due to a change in the static scheme, but it is not recommended to use it in the case where phenomena, such as the opening of cracks or foundation settlements, are to be monitored, because the time frame in which these phenomena take place is longer and it is more appropriate to turn towards long-term monitoring. This type of monitoring is carried out for years or decades (if it were possible, it would be optimal to carry it out for the entire life of the structure). It is evident that in the case of short-term monitoring, the amount of data associated with it is much less than in the case of long-term monitoring, implying simpler data management. A particular setting that is normally applied when long-term monitoring is carried out is ***triggered monitoring***. This is activated at the time of the occurrence of a specific event, in other words when a certain parameter exceeds a set threshold (a practical example of this type of monitoring is the measurement of the time histories of earthquakes). Depending on the dynamic nature of the phenomena studied, the sampling interval for each data collection varies.

A further classification can be made according to the phenomena that are to be monitored: ***local monitoring***, if the focus is on, for example, measuring how a crack propagates to identify its position, severity and behaviour (in this case it is not possible to determine the health of the entire structure), or ***global monitoring*** if the intention is to study a structure in its entirety and thus to examine vibrations and deformations.

A final differentiation is made according to the loads applied. We can speak of ***static monitoring*** if we intend to monitor parameters that vary slowly over time (for phenomena such as deflection, settlement, slope, crack width, etc.). In this circumstance, a few measurements per minute or hour are sufficient to obtain information on a specific parameter. Or we speak of ***dynamic***

monitoring if we intend to record the time-history of mechanical vibrations. Generally, dynamic tests measure the required characteristics from external forcing or natural phenomena (i.e., environmental vibrations).

Applications

Over the time, the attention and interest in SHM has always increased. This is amply demonstrated in the literature but can also be seen in the numerous technical applications in which it is involved. Technological evolution has led to improvements in this process: it has been possible to reduce the size of the instrumentation while also lowering costs, and through the continuous development of the Internet, the continuous exchange of data and even the remote control of systems has been greatly simplified.
Today, an SHM system can have several applications:

- *During the construction phase of a structure.* In this case, monitoring can be provided already during the design phase. The purpose is to monitor the characteristics of the structure during construction in order to manage and reduce safety risks by mitigating the uncertainties that always accompany construction. Thus, during and after construction, it is possible to verify the correctness of the design hypotheses made in relation to the structure's statics and dynamics behaviour and, if necessary, implement timely design corrections. Once the construction work is complete, the system, which remains integrated into the structure, can continuously provide reports on the health of the structure.

- *For assessing the health of an existing building.* This application is currently the most widespread and used, especially in an area such as Italy, which is rich in cultural heritage buildings, whose constant monitoring and need to understand what interventions should be carried out for their conservation, represent an important topic for structural engineering. In this context, short-term monitoring can be implemented to obtain a "digital fingerprint" of the structure under examination, starting from its dynamic characteristics, and based on this, decisions can be made regarding the operability of the building, ordinary or extraordinary maintenance or repairs.

- *For the calibration of numerical models.* This third application is closely related to the previous one. In fact, the parameters extracted from short-term monitoring are then used to correctly set the numerical model of

the construction (implemented in complex software) by acting on the assigned material parameters. In this way, it is reasonably certain that the numerical model is close to reality. This model can then be subjected to all those linear and non-linear analyses necessary to identify and verify damage mechanisms in place, to assess the general state of the structure and to design and plan targeted interventions.

Trying to encompass all the applications described above, the recent innovation in the field of SHM is continuous monitoring with associated constant and automatic interpretation of the acquisition data. In this way, it is possible to have in real time the actual dynamic characteristics of the structure that are needed to implement a systematic process of updating the numerical models and thus verify the health of the structure continuously without interruption.

2.4 SHM General Methods

As already mentioned in paragraph 2.2, whatever use is to be made of the SHM, it must be defined in detail:

- requirements and needs;
- expected results;
- constraints of the monitoring project.

Having clearly defined these aspects, as described by [37], it is necessary to focus on some critical aspects that need to be evaluated.

I. Detailed characterisation of the structural system:
leads to a deep understanding of the structure under examination and the objectives of the monitoring application. It is therefore necessary to utilise all relevant design information and drawings. It is appropriate to develop numerical *Finite Element Model (FEM)* for the simulation of structural response, which can be further refined, then calibrated, using the data from an initial short-term SHM so that they accurately reproduce the actual conditions and mechanisms of the structure and can be used as the foundation for future evaluations of the structure's performance and health.

II. Identification of measurements:
meaning all those static or dynamic parameters (mechanical, electrical, chemical, etc.) that will characterise the phenomena of interest and that may include: forces and stresses, rotations and distortions, displacements and deformations, vibrations, but also natural (wind speed and direction, temperature, humidity) and anthropic (traffic) environmental parameters.

III. Choice of detection and data acquisition system:
this applies to the entire system but also to individual components, such as sensors, identification software, etc. For each one, the technical specifications concerning the methods and techniques to be used for installation and configuration must be considered, as well as the methodology for checking their operation.

IV. Quality assurance, data processing and storage:
given the presence of multiple possible sources of error and uncertainty in the field that can adversely affect the reliability of measurements, the methods that are chosen to be used should be developed and implemented at multiple levels of the signal path to ensure quality.

V. Data presentation and decision-making:
in this final phase, the focus must be on adopting methods of interpreting and presenting data in a concise and easily comprehensible form to facilitate subsequent decision-making operations. To give an example: we could use a system that automatically sends an alarm when it detects that the parameters under investigation have exceeded a specific threshold value, considered critical.

Chapter 3

Operational Modal Analysis (OMA) Technique

3.1 Introduction to Dynamic Identification

This expression refers to the techniques by which the dynamic characteristics of a structure (natural frequencies, corresponding modal shapes and damping coefficients) can be determined. Two different approaches can be distinguished through which these characteristics can be determined [38]: the *analytical approach* and the *experimental approach*.
Since some of the characteristics of the structure (geometry, distribution of masses and stiffnesses, type of materials) are assumed to be known a priori, the *analytical approach*, called the *direct approach*, allows the modal parameters of a structure to be determined by solving an eigenvalue problem.
The *experimental approach*, on the other hand, called the *inverse* or *indirect problem*, determines the characteristics of the structure from a known dynamic input (***EMA***) or unknown (***OMA***). The former technique operates in a deterministic context, the latter operates in a stochastic context [39].The difference between these two techniques will be discussed in more detail below.
The software used today for FEM allows for the realisation of very complex and detailed models, but they do not always faithfully reproduce reality and the results obtained may differ, even significantly, from the real structural response.
These discrepancies are due to the fact that by using a finite element analysis, a structure, which in reality is continuous, is discretized. Furthermore, it is not always easy to establish accurate material characteristics and damping. These

factors mean that there is a gap between the model and the real structure.
In this context, the operation of dynamic analysis becomes fundamental because, once the natural frequencies of the structure have been evaluated experimentally, these allow the calibration of the model itself: the characteristics of the elements are adjusted until the response of the numerical model is the same as the real structure (considering a small percentage of error as acceptable).
As mentioned above, the dynamic behaviour of a structure depends exclusively on its intrinsic characteristics (mass, stiffness and constraint) and not on the magnitude and/or type of load applied. Therefore both the EMA and OMA techniques allow the same conclusions to be reached, despite the technical differences.

At this point, to better understand the differences between EMA and OMA, it is useful to give some indication of the types of input that imply a dynamic response of a structure. It is possible to distinguish between *artificial excitation* and *environmental excitation.*
The former is an excitation that can be realised through the use of particular devices, even very large ones. Such devices are not always available, or in any case may also involve high costs. On the other hand, knowing and establishing the dynamic input makes it possible to work specifically on the frequency band of interest. The most commonly used instrument is the vibrodyn: it allows the delivery of unidirectional sinusoidal dynamic forces. A second instrument is the instrumented hammer: it generates excitation due to a direct impact with the structure. Magnitude and duration of the impulse depend on the weight of the hammer and the material of the striking part (steel, plastic or rubber), the dynamic characteristics of the surface and the speed at the moment of impact. Compared to vibrodyn, it is certainly easier to use and less costly, but in the case of large structures it may not be easy to generate the necessary vibrations.
Environmental excitation, on the other hand, includes all those vibrations caused by *"environmental loads"* (micro-motors induced by traffic, wind, service loads insisting on the structure, earthquakes, industrial activities, etc.). These unknown excitation cause vibrations in the subsoil that produce a fixed vibration of variable amplitude in the structure. The greatest advantage of this type of excitation is that it does not require any cost.
The use of artificial excitation ensures that the motion of a structure is better controlled. At the same time, however, they imply an interruption, although temporary, of its operation. This is not always possible, but in general, even if

it were possible, the interruption of operation can have consequences, economic and others. In addition, the induced vibrations may to some extent damage the structure, even if only slightly. In the case of OMA techniques, using an unknown dynamic input, it is not possible to calculate modal modal participation factors. On the other hand, they are certainly cheaper and quicker techniques since no instrumentation is required (or it is very small) and there is no interruption in the use of the structure. However, errors can occur in the analysis if the environmental excitation, defined as *white noise*, is superimposed by a non-random excitation.

3.2 Operational Modal Analysis

The topic of experimental identification of modal parameters began in laboratories for testing and analysing small structures in a controlled environment (mechanical engineering components), thus using the EMA technique, mentioned in the previous paragraph. From the earliest applications to the present day, the instrumentation and data processing methods have evolved, and this has allowed EMA to be used for civil engineering structures as well, especially on large structures such as bridges and dams. These tests, known as ***FVT***, also have, as already mentioned, the complication of causing the interruption of operation of the structure under examination, not forgetting that physically induced vibrations can cause damage, even if not significant. In this context, research focused on finding solutions to perform tests that were cheaper, more practical and with less impact on the structure itself: ***AVT***. The environmental forces are freely available in nature, and they replaced the dynamic excitation provided by large devices. The main advantage of these tests is that they allow to define the dynamic behaviour during operating conditions, thus permitting to obtain realistic results associated with real vibration conditions, and not due to extraordinary vibrations. They can also highlight anomalies or non-linearities that could not normally be obtained using artificially generated vibrations.

Although the AVT has numerous advantages over the FVT, this technique also has some negative aspects. As the input excitation is very low, the signal may have a high noise content. Therefore, the use of very sensitive sensors becomes necessary to obtain consistent results. In addition, the frequency content of the excitation may not cover the entire band of interest, so it is possible that not

all modes of the structure are well excited. Another disadvantage concerns the modal mass, which is not estimated: mode shapes are not uniquely defined or in any case not absolutely scaled.
Despite some disadvantages, this testing technique has continually evolved and improved due to the increasing interest in it, focusing on the undeniable advantage of obtaining excellent results only by measuring the response under operational conditions. This OMA, also known as ***Output-only Modal Analysis*** as it only measures outputs, is therefore based on the assumption that the necessary input excitation is always present and is represented by a *stochastic process* (defined as *"white noise"*), which has the characteristic of having a constant spectrum with constant intensity along the frequency range of interest.
Over the years, various dynamic identification techniques have been developed based on OMA procedures (classified as *parametric* and *non-parametric methods*) that operate in the frequency or time domain. The following sections will illustrate the use of these techniques in the context of dynamic monitoring under operating conditions.
The work carried out for this doctoral thesis focuses only on the use of OMA. Therefore, in this chapter, the dynamic system models adopted by identification methods are explained, a description of the available algorithms is provided, and finally, the most widely used and representative identification methods in Civil Engineering applications are described.

3.3 Structural Dynamic Models

In this section, the main concepts relating to the solution of a classical vibration problem are summarised: the mathematical models used to characterise the dynamic behaviour of linear systems are described. Initially, the classical formulation of the problem is presented, which is based on the solution of a system of second-order differential equations, showing its resolution in the time and frequency domain, and then the state-space model is shown. The advantages of using this model in identification problems are also discussed, as well as the main assumptions to be considered on the input excitation for the implementation of output-only identification techniques.

3.3.1 Spatial and modal models

The definition of the mathematical model depends on the distribution of mass, stiffness and damping, which are usually defined using a matrix representation derived from an initial spatial discretization of the system. Hence, the behaviour of the model is defined by a set of differential equilibrium equations (related to the discretization of the structure) that characterise the basis of the various models. These equations can be defined in continuous time (representing continuous models, in which the response is defined continuously over time) or discrete time (characterising discrete models, in which the response is obtained after a certain discretization).

Spatial formulation

Structural Dynamics is a branch of Structural Engineering through which it is possible to evaluate the deformations and internal stresses of systems subjected to an external force over time. Loads are a function of: time, so the structural response will also be dependent on it, elastic forces and inertia forces that oppose displacement and acceleration respectively, viscous damping forces (if present) that oppose velocity.

Figure 3.1 shows the schematisation of a linear dynamic system, the simple oscillator, also known as the *Single Degree of Freedom (SDOF)* system.

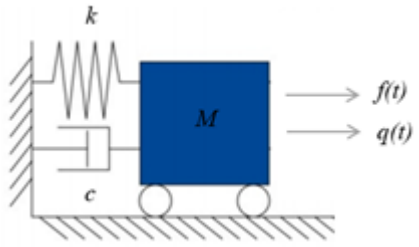

Figure 3.1: *SDOF System*

The only possible direction of movement is horizontal. The mass M is assumed to be all concentrated at one point. The characteristics of the system are the stiffness k, ideally represented by a mass-free spring, and the dissipation factor c, both of which represent energy dissipation mechanisms. All three parameters (M, k and c) determine the behaviour of the system under dynamic loads.

Real structures, however, are more complex systems and consequently have an infinite number of degrees of freedom. To study a continuous structure, it must be assumed that it consists of as many degrees of freedom as necessary to

guarantee sufficient accuracy of the schematised model. These types of systems are called *Multiple Degree of Freedom (MDOF)* (Figure 3.2).

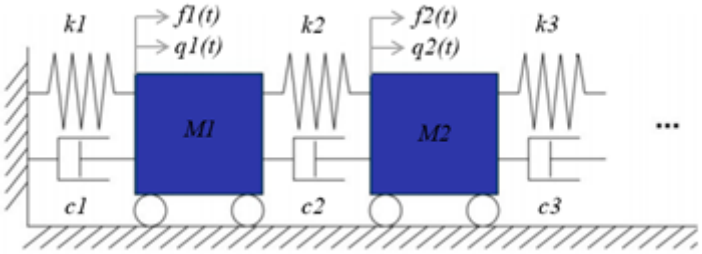

Figure 3.2: *MDOF System*

Assuming that each mass, as shown in the figure, can be subjected to an external force f_i(t), the equation of motion is:

$$M \cdot \ddot{q}(t) + C \cdot \dot{q}(t) + K \cdot q(t) = F(t) = B \cdot f(t) \tag{3.1}$$

where M is the Mass matrix, K the Stiffness matrix and C the Damping matrix, with dimension [n x n]. $\ddot{q}(t)$, $\dot{q}(t)$, $q(t)$ are the vectors of accelerations, velocities and displacements, associated to each SDOF composing the system (with dimension [n x 1]). $F(t)$ is the vector of the exciting forces applied to each SDOF. It can be written as the product of a B matrix, which contains all of the inputs, and a vector $f(t)$, where points of forces application are listed. All functions are defined in the continuous time domain and relate to the same instant t.

The phenomenon of damping and its modelling creates numerous uncertainties. In order to introduce simplifications that allow easy resolution of the problems of dynamic systems without changing their physical meaning, we can refer to a property proposed by Rayleigh according to which proportional damping can be assumed to describe decaying responses and is obtained through a linear relationship (Eq. 3.2) between the properties of mass and stiffness [40]:

$$C = M \cdot \sum_b a_b \cdot [M^{-1} \cdot K^b] \longrightarrow C = \alpha M + \beta K \tag{3.2}$$

The second relation represents the proportional damping property (*Reyleigh damping*) and it is a particular case of a general formula: it is obtained considering the values $b = 0$ and $b = 1$. The problem is presented as a system of coupled second-order differential equations. It can be solved in the time domain using the *Duhamel integral*.

The solution of MDOF system in time domain is dependent on the dynamic responses of the single SDOF components, so it is very complex to present. For this reason, to illustrate the representation of the *Spatial Model*, a SDOF oscillator will be considered. It is described by Eq. 3.3:

$$m\ddot{q}_1(t) + c\dot{q}_1(t) + Kq_1(t) = f_1(t) \tag{3.3}$$

where $\ddot{q}_1(t)$ and $\dot{q}_1(t)$ are the two derivatives (first and second respectively) of $q_1(t)$, which is the response of the oscillator subjected to an arbitrary force $f_1(t)$. Taking the initial conditions of displacement and velocity as null and using the *Duhamel convolution integral*, the solution of the time domain equation is obtained as (Eq. 3.4):

$$q_1(t) = \int_0^t f_1(\tau)h_1(t-\tau)d\tau, \quad t > 0 \tag{3.4}$$

$h_1(t-\tau)$ represents the response of the system in the instant $(t-\tau)$ and caused by a unitary impulse generated in the instant τ. It is defined in Eq. 3.5:

$$h_1(t-\tau) = \frac{1}{m\omega_{1d}} e^{-\omega_1\xi(t-\tau)} \sin\left[\omega_{1d}(t-\tau)\right], \quad t > \tau \tag{3.5}$$

This is the function that defines the dynamic response of a SDOF. It depends on its characteristics of mass m, stiffness k, frequency ω_1 and damping ξ. The following equation (Eq. 3.6) specifies the damped frequency (ω_{1d}):

$$\omega_1 = \sqrt{\frac{k}{m}} \rightarrow \omega_{1d} = \omega_1\sqrt{1-\xi^2} \tag{3.6}$$

In relation to eq. 3.3, the general value of the damping c is connected to the damping coefficient ξ through the following correlation (Eq. 3.7):

$$c = 2\xi m\omega_1 \tag{3.7}$$

To summarise, to solve the problem using Duhamel's integral, it is required to divide the force acting on the system into a sequence of impulsive functions. The system's response will be the sum of each individual impulsive function's response. For the MDOF system described by eq. 3.1, N different coupled second-order differential equations could be written and solved simultaneously to find the solution of the system.

Modal formulation

A viable alternative to the Spatial Model is the *Modal Model*. It consists of converting the system of N coupled second-order differential equations into a system of N decoupled equations. This type of system is solved by considering each SDOF separately. These independent differential equations represent the displacements as a linear combination of N independent vectors (vibration modes φk).

Therefore, considering an undamped system of mass M and stiffness K, as in the previous case, the dynamic behaviour is expressed by the following eq. 3.8:

$$M \cdot \ddot{q}(t) + K \cdot q(t) = 0 \tag{3.8}$$

In Eq. 3.9, we observe the solution of the system described above:

$$q(t) = \varphi_k e^{\lambda_k t} \tag{3.9}$$

It can be noticed that, from a mathematical point of view, its modes of vibration are like those of the system in which the assumption of proportional damping is made.

Applying linear systems theory, the eigenvalues (λ_k^2) and eigenvectors (φ_k) of the generic system (Eq. 3.8) can be obtained from the below equation:

$$\lambda_k^2 M \cdot \varphi_k + K \cdot \varphi_k = 0 \leftrightarrow K \cdot \varphi_k = -\lambda_k^2 M \cdot \varphi_k \tag{3.10}$$

It is proved that the eigenvalues are closely linked to the square of the undamped angular frequencies as follows:

$$\lambda_k = i\omega_k \tag{3.11}$$

Instead, the eigenvectors are closely related to the vibration modes of the structure φ_k, which are arranged in a matrix Φ (*modal matrix*) in which the eigenvectors correspond to the columns of this matrix:

$$\Phi = \begin{bmatrix} \cdots & \varphi_k & \cdots \end{bmatrix}, \quad k = 1, \cdots, N \tag{3.12}$$

Due to the orthogonality property of Φ with respect to the mass and stiffness matrix, the equations of motion of the undamped MDOF system can be decoupled. In this way, the eigenvectors do not depend on external forces and are

independent of each other. Furthermore, by multiplying eq. 3.8 by Φ^T, M and K are transformed into diagonal matrices (Eq. 3.13), named *Modal Mass Matrix* (M_d) and *Modal Stiffness Matrix* (K_d) respectively. m_k and k_k indicating the matrix elements associated with the *k-th* Degree of Freedom (DOF):

$$\Phi^T \cdot M \cdot \Phi = \begin{bmatrix} \ddots & & \\ & m_k & \\ & & \ddots \end{bmatrix} \quad \Phi^T \cdot K \cdot \Phi = \begin{bmatrix} \ddots & & \\ & k_k & \\ & & \ddots \end{bmatrix} \tag{3.13}$$

As in the case of the free response of the simple single degree of freedom oscillator, the undamped angular frequency for one of the SDOFs of the MDOF system can be obtained through the relation:

$$\omega_k = \sqrt{\frac{k_k}{m_k}} \tag{3.14}$$

If we consider the most general case, the case of damped vibration systems, the orthogonality property must also be expanded to the *Damping Matrix (C)* and also assuming a proportional damping distributed in the entire system. This generalisation leads to eq. 3.15:

$$\Phi^T \cdot C \cdot \Phi = \begin{bmatrix} \ddots & & \\ & c_k & \\ & & \ddots \end{bmatrix} = \begin{bmatrix} \ddots & & \\ & 2\xi m_k \omega_k & \\ & & \ddots \end{bmatrix} \tag{3.15}$$

As we can see in the equation above, the *Modal Damping Matrix* (C_d), in the case where damping is considered proportional, is obtained as a linear combination of the *Modal Mass Matrix* (M_d) and *Modal Stiffness Matrix* (K_d).

According to eq. 3.9, the general solution of the free dynamic response of MDOF systems with proportional damping leads to individual equations of the type:

$$\lambda_k^2 + 2\xi_k \omega_k \lambda_k + \omega_k^2 = 0 \tag{3.16}$$

Solving the N expressions of eq. 3.16 of the linear system represented by eq. 3.8, we obtain $n = 2N$ different values of the eigenvalues (λ_k) which are related to the undamped angular frequencies and damping coefficients as follows:

$$\lambda_k, \lambda_k^* = -\xi_k \omega_k \pm i\sqrt{1 - \xi_k^2}\omega_k \tag{3.17}$$

Through these steps, the general solution expressed in eq. 3.1 can be rewritten as a linear combination of the vibration modes in *Modal Space*:

$$q(t) = \sum_{k=1}^{N} \varphi_k \cdot \eta_k(t) \tag{3.18}$$

A system of general linear equations with proportional damping can be turned into a system of independent second-order differential equations by superposition of effects. The solution of this system is expressed by a linear combination of N independent solutions associated with each singular vibration mode:

$$m_k \ddot{\eta}_k(t) + c_k \dot{\eta}_k(t) + k_k \eta_k(t) = f_k(t), \quad k = 1, ..., N \tag{3.19}$$

m_k, k_k and c_k are the modal components of the modal matrices; $\ddot{\eta}_k(t)$ and $\dot{\eta}_k(t)$ are the second and first derivative of the modal coordinate $\eta(t)$; f_k is the modal component of the input excitation associated to $k-th$ DOF and is defined by:

$$f_k(t) = \varphi_k^T \cdot (B \cdot f(t)) \cdot I \tag{3.20}$$

where I is the identity matrix.

Referring to eq. 3.13, the modal matrix (Φ) is used to transform the *Mass Matrix* (M) and *Stiffness matrix* (K) into diagonal matrices. The relationship enabling this transformation is the following:

$$M_d \cdot \ddot{\eta}(t) + K_d \cdot \eta(t) = f_\eta(t) \quad \begin{cases} \eta(t) = \Phi^{-1} \cdot q(t) \\ f_\eta(t) = \Phi^T \cdot B f(t) \cdot I \end{cases} \tag{3.21}$$

The vibration modes are calculated by solving the eigenvalue problem and they can be determined by introducing a scaling factor. Therefore, by scaling the modal mass components with the value $\varphi^T M \varphi$, the *Unit Modal Mass Matrix* is obtained:

$$\ddot{\eta}(t) + \begin{bmatrix} \ddots & & \\ & w_\eta^2 & \\ & & \ddots \end{bmatrix} \eta(t) = \Gamma_\eta(t) \rightarrow \ddot{\eta}(t) + \omega_\eta^2 \dot{\eta}(t) = \Gamma_\eta(t) \tag{3.22}$$

ω_η^2 is the square value of the undamped angular frequency associated to each SDOF and $\Gamma_\eta(t)$ is the *participation coefficient*. This coefficient makes it pos-

sible to identify the modal component associated with each SDOF after normalising the modal mass.

With the introduction of the *Modal Model*, the relations written to obtain the solution of an undamped SDOF system loaded by an arbitrary input with a null initial condition (Eq. 3.3) obtained in the time domain by adopting the Duhamel integral and defined previously in the *Spatial Space*, can be expressed in the *Model Space* as follows:

$$\eta(t) = \int_0^t f_\eta(\tau) h(t-\tau) d\tau, \quad t > 0 \tag{3.23}$$

$$h(t-\tau) = \frac{1}{m_k \omega_{dk}} e^{-\omega_k \xi (t-\tau)} \sin\left[\omega_{dk}(t-\tau)\right], \quad t > \tau \tag{3.24}$$

The function $h(t-\tau)$ defines the impulse response function of an SDOF system in the time domain, according to eq. 3.4 and eq. 3.5. This response defines the output of the system at time t for a unit impulse generated at instant τ. This means that the output response in *Modal Space* can be seen as a sum of input history filters $f_\eta(t)$, where the impulse response function is defined by m_K (mass), ω_k (natural frequency) and ξ_k (damping ratio) associated with the SDOF system as follows:

$$\omega_{dk} = \omega_k \sqrt{1-\xi^2} \qquad \xi_k = \frac{c}{2 m_k \omega_d} \qquad \omega_k = \sqrt{\frac{k_k}{m_k}} \tag{3.25}$$

To conclude this discussion, it can be said that the modal model admits a damping distribution along the structure proportional to the mass and stiffness distributions. This results in a simplified mathematical formulation. However, if some particular structures are considered, for example those of cultural heritage or damaged structures, the damping is not constantly distributed. Hence, this assumption may turn out to be a limited condition and there may be problems in the identification of modal estimates.

3.3.2 Frequency response models

An alternative way to solve the dynamic problem of an MDOF system (Eq. 3.1) is to transfer it from the time domain to the frequency domain. In this way, the second-order differential equations are replaced by simpler algebraic

equations, applying the Fourier transform to all terms in the equation.

3.3.2.1 Frequency response models in Spatial Space

Based on the 1-DOF system (Eq. 3.3), the differential equation, with the introduction of the *Fourier Transform*, is transformed into the following expression:

$$-m\omega^2 Q_1(\omega) + ci_1(\omega) + kQ_1(\omega) = F_1(\omega) \tag{3.26}$$

$Q_1(\omega)$ and $F_1(\omega)$ are the Fourier transforms functions of $q_1(t)$ and $f_1(t)$ respectively. Looking at equation 3.26, it is easy to see how the structural response of the system can be rewritten explicitly:

$$Q_1(\omega) = \frac{F_1(\omega)}{-\omega^2 m + i\omega c + k} = H_1(\omega)_1(\omega) \tag{3.27}$$

In eq. 3.27, $H_1(\omega)$ is the *Frequency Response Function (FRF)* of 1-DOF system and can also be rewritten as follows:

$$H_1(\omega) = \frac{1}{-\omega^2 m + i\omega c + k} = \frac{1/m}{\omega_1^2 - \omega^2 + 2i\xi\omega\omega_1} \tag{3.28}$$

To obtain a more compact form of eq. 3.28 in order to make some features more evident, the numerator and denominator can be divided by the mass m, the natural frequency replaced by the expression $\omega_1 = \sqrt{k/m}$ and the damping by the equality $c = 2\xi m\omega_1$, obtaining:

$$H_1(\omega) = \frac{1/k}{1 + 2i\xi[\frac{\omega_1}{\omega}] - [\frac{\omega_1}{\omega}]^2} \tag{3.29}$$

The expressed FRF, which describes how the input force is transformed into the system's response, is a complex function. It therefore has a real part R and an imaginary part I. Its amplitude is expressed as $\sqrt{R^2 + I^2}$ and its phase as $arctg(I/R)$. From eq. 3.29 and Figure 3.3 some characteristics of the function can be derived:

- the maximum amplitude value of FRF is $\omega = \omega_1 = \sqrt{1 - \xi^2}$ and it represents a good estimation of natural frequency when damping is low;
- FRF tend to be $1/k$ when the excitation is low in relation to the undamped natural frequency; the amplitude is quite constant, and phase is close to zero;

- the response shows a maximum peak when the excitation frequency reaches the natural frequency ($\omega = \omega_1$), and the phase makes a jump from 0° to 180° activating the *resonance phenomenon.*

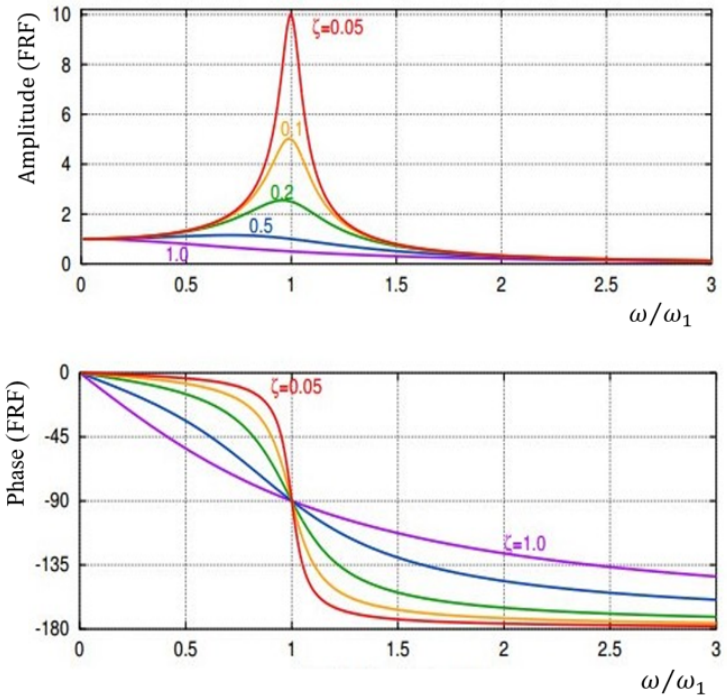

Figure 3.3: *Amplitude and Phase of the FRF of 1-DOF system*

By retracing the steps used for the 1-DOF system and applying the Fourier transform to both members of eq. 3.1, it is possible to express the relationship between the system's response and the input excitation with the following matrix expression:

$$Q_N(\omega) = H(\omega) \cdot F_N(\omega) \tag{3.30}$$

Specifically, the Fourier transform turned each response $q_i(t)$ into the vector $Q_N\omega)$ and each excitation $f_i(t)$ into the vector $F_N(\omega)$. These vectors have dimension [N-by-1] where N is the number of differential equations of the system. H(ω) is a [N-by-N] matrix and it is linked to the characteristics of the structure by the following expression:

$$H(\omega) = [-\omega^2 M + i\omega C + K]^{-1} \tag{3.31}$$

each component $H_{ij}(\omega)$ of the matrix $H(\omega)$ represents the FRF of the system regarding the response at coordinate i subjected to a generic force acting at coordinate j.

3.3.2.2 Frequency response models in Modal Space

With the modal model, as already shown, it is possible to decouple the differential equations describing the dynamic behaviour of the system while preserving the physical meaning between eigenvalues and eigenvectors and between natural frequencies and mode shapes. Thus, transporting the structural response problem of a general MDOF system expressed in modal coordinates into the frequency domain, the solution expressed by eq. 3.30 can be rewritten as follows:

$$Q_{\eta k}(\omega) = H_{\eta k}(\omega) \cdot F_k(\omega) \tag{3.32}$$

Additionally, the elements $H_{\eta k}(\omega)$ of the FRF matrix in the *Modal Domain* can be made explicit according to the following relationship:

$$H_{\eta k}(\omega) = \frac{1}{\omega_k^2 - \omega^2 + 2i\xi_k\omega\omega_k} \tag{3.33}$$

Consequently, the complete FRF matrix can be formulated with generalised coordinates using the vibrational modes of the dynamic system as:

$$H(\omega) = \Phi \cdot H_\eta(\omega) \cdot \Phi^T = \sum_{k=1}^{N} H_{\eta k} \cdot \varphi_k \cdot \varphi_k^T \tag{3.34}$$

H_η is a diagonal matrix consisting of the FRFs calculated in *Modal Space* (normalised with respect to the *modal mass matrix*). Furthermore, the multiplication of this matrix with the *modal matrix* Φ, allows obtaining the $H(\omega)$ relative to each principal mode of the system through the relation:

$$H_{\eta_{i,j}}(\omega) = \sum_{k=1}^{N} \frac{[\varphi_i]_k \cdot [\varphi_j]_k}{\omega_k^2 - \omega^2 + 2i\xi_k\omega\omega_k} \tag{3.35}$$

The construction of the frequency response function matrix through the modal formulation is more powerful as it requires a lower numerical cost in view of the reduced number of mathematical operations. Furthermore, its use in this domain, allows the analysis of the structural response also considering a limited number of vibration modes (e.g. considering only the lower modes that most represent the dynamic behaviour of the studied MDOF system).
In conclusion, based on eq. 3.18 (system response in *modal space*) and eq. 3.33 (relationship in the frequency domain), the output response of the MDOF

system under known excitation forces can be provided by eq. 3.36:

$$Q(\omega) = \sum_{k=1}^{N} \varphi_k \cdot H_{\eta k}(\omega) \cdot F_k(\omega) \tag{3.36}$$

Keeping in mind the time-invariant linear system described in eq. 3.1, it is possible to express the FRF as the ratio of the output data spectrum $Q(\omega)$ to the input force system spectrum $F(\omega)$. This means that the FRF is the Fourier transform of the *Impulse Response Function (IRF)* defined in eq. 3.4 by the Duhamel integral. Ultimately, the FRF of a simple system consisting of an SDOF system excited by various harmonic inputs with a nominal frequency of ω_p can be specified as follows:

$$H(\omega) = \frac{Q(\omega)}{F(\omega)} = \frac{1/k}{1 + 2i\xi(\frac{\omega_p}{\omega_n}) - (\frac{\omega_p}{\omega_n})^2} \tag{3.37}$$

It is evident from eq. 3.37 that the system is in *resonance* (and the phase jumps from 0 to π) when the input excitation ω_p is close to the nominal natural frequency ω_n of the system. The response is purely imaginary and related to the damping forces. The matrix $H_{ij}(\omega)$ can be expressed by means of the relation:

$$H_{ij}(\omega) = \sum_{r=1}^{N} H_{ijr} = \sum_{r=}^{N} \frac{R_{ijr}}{j\omega_p - \lambda_r} + \frac{R^*_{ijr}}{j\omega_p - \lambda^*_r} \tag{3.38}$$

Where λ_r represents the poles of the system (or complex roots of the equations) and which inform about both the damped frequencies (imaginary part) and the damping ratios (real part), and R_{ijr} are the residuals containing the mode shape coefficients. For these two components, the relations apply:

$$\lambda_r = -\xi\omega_n \mp j\omega_n\sqrt{1-\xi^2}, \qquad R_{ijr} = \frac{\varphi_{ir}\varphi_{jr}}{j2\omega_{dr}m_r} \tag{3.39}$$

Eq. 3.38 is called the *modal superposition equation* [41], given that it sums the contribution of the FRFs of each individual SDOF composing the MDOF system. Furthermore, $H_ij(\omega)$ is a symmetric matrix and this implies that it is possible to extrapolate the mode shape associated with a specific frequency by knowing a row or column associated with that frequency.

To conclude this section, it is worth highlighting how the use of FRF (and frequency domain models in general) is appropriate for those cases in which the acting forces can be associated with a stochastic process (such as wind,

traffic loads or waves), thus such as during the development of an AVT, already explained in the previous chapter, but also in the context of continuous dynamic monitoring. This type of topic will be deepened and investigated in more detail in the following paragraphs.

3.3.3 State Space Models

The solution of the classical formulation for *Linear-Time Invariant (LTI) systems* is obtained by separating each differential equation (orthogonality property of the eigenvectors) when the damping is considered proportional. Based on this assumption of proportionality, the modes of a structure with proportional damping are the same as in the undamped structure. The reality is quite different: the distribution of damping and the distribution of mass and stiffness are never proportional, and sometimes localised damping may be present which disables the assumption.
Figure 3.4 shows the steps required to obtain the definition of a *stochastic model*.

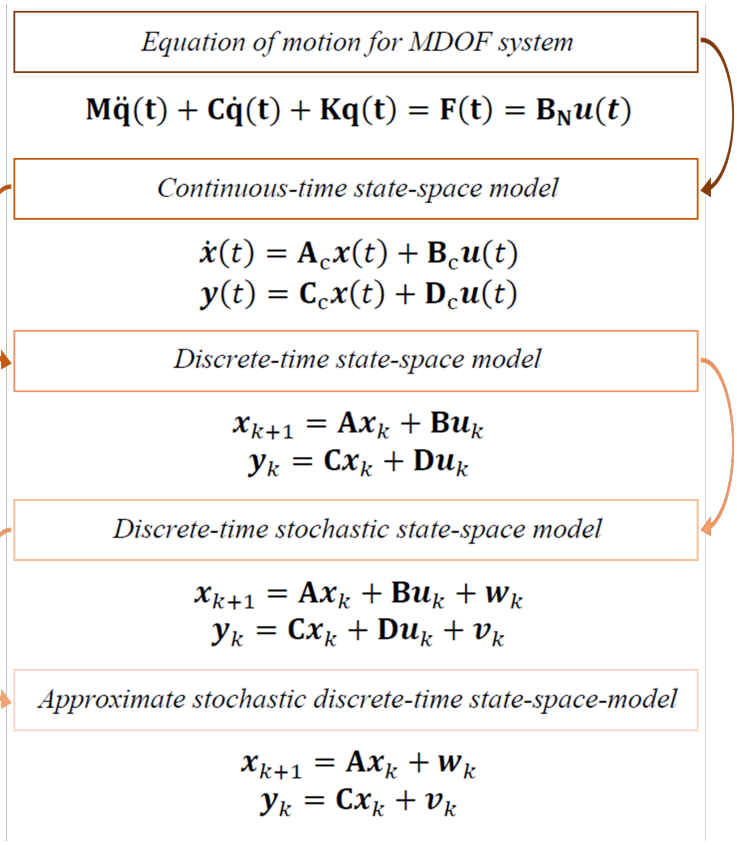

Figure 3.4: *Genesis of the stochastic state-space-model*

This model can be used to solve the problem of identifying modal parameters from experimental data collected under operating conditions: *viscous damping* is introduced and the dynamic problem is reformulated as a linear combination of independent SDOF systems through the use of the *state-space model*. This model is also capable of modelling the noise content of the signals, which, as is well known, is always present in experimental tests.

3.3.3.1 Continuous-time state-space model

Considering an MDOF system characterised by N degrees of freedom, the second-order equation of its motion can be expressed in the state-space formulation as given in eq. 3.40:

$$M \cdot \ddot{q}(t) + C \cdot \dot{q}(t) + K \cdot q(t) = F(t) = B_N \cdot u(t) \tag{3.40}$$

where M, C and K are the mass, damping and stiffness matrices, with dimension [N-by-N]; the vector $q(t)$ is the solution of the differential equation; $F(t)$ is the exciting force vector. This vector is composed of N elements and it can be replaced by a vector $u(t)$, with size $m < N$, since usually not all N degrees of freedom of the system are excited, so the $u(t)$ only takes into account the $m - inputs$ actually applied. This is then multiplied by the B_N [N-by-m] matrix, composed of zeros and ones values, matching the $m - inputs$ with the system's N-DOFs. $F(t)$ and $u(t)$ are considered in continuous time.

The MDOF system consisting of N second-order differential coupled equations, by defining a state vector x(t) of n components, can be converted into an equivalent set of $n = 2N$ first-order differential equations, independent of each other. $x(t)$, consisting of the vector of displacements $q(t)$ and velocities $\dot{q}(t)$, is dependent on the N-DOFs of the structure and defines the P and Q matrices. These are expressed as a combination of the mass, stiffness and damping matrices (Eq. 3.41).

$$x(t) = \begin{bmatrix} q(t) \\ \dot{q}(t) \end{bmatrix}; \quad P = \begin{bmatrix} C & M \\ M & 0 \end{bmatrix}; \quad Q = \begin{bmatrix} K & 0 \\ 0 & -M \end{bmatrix}; \quad F(t) = B_N(t) \cdot u(t) \tag{3.41}$$

The modal matrices P and Q result to be orthogonal (Eq. 3.42)

$$\Psi^T \cdot P \cdot \Psi = \begin{bmatrix} \ddots & & \\ & a_k & \\ & & \ddots \end{bmatrix}; \quad \Psi^T \cdot Q \cdot \Psi = \begin{bmatrix} \ddots & & \\ & b_k & \\ & & \ddots \end{bmatrix} \tag{3.42}$$

Thus, this system of the eq. 3.40 can in turn be expressed, in compact form, through another (equivalent) system composed of first-order differential equations:

$$P \cdot \dot{x}(t) + Q \cdot x(t) = \begin{bmatrix} B_N \\ 0 \end{bmatrix} \cdot u(t) \tag{3.43}$$

Considering $q(t)$ in the generic solution of the classical formulation (Eq. 3.9), the solution of the new formulation, solving the eigenvalue problem [42], can be expressed as:

$$Q \cdot \Psi = -P \cdot \Psi \cdot \Lambda_C \tag{3.44}$$

$$\Lambda_C = \begin{bmatrix} \Lambda & 0 \\ 0 & \Lambda^* \end{bmatrix}, \quad \Psi = \begin{bmatrix} \Theta & \Theta^* \\ \Theta \cdot \Lambda & \Theta^* \cdot \Lambda^* \end{bmatrix} \tag{3.45}$$

Ψ is the eigenvectors matrix and Λ_C is the eigenvalues matrix. The $(*)$ symbol indicates the *complex conjugate*.

Eq. 3.46 expresses the relationships that exist between the elements of the matrices just presented and the modes (ϕ_k and λ_k) that characterise the dynamic behaviour of the structure:

$$\Lambda = \begin{bmatrix} \ddots & & \\ & \lambda_k & \\ & & \ddots \end{bmatrix}; \quad \Theta = \begin{bmatrix} \cdots & \varphi_k & \cdots \end{bmatrix} \text{ with } k = 1...N \tag{3.46}$$

For the orthogonality property, expressed in eq. 3.42, the matrix Θ, containing the vibration modes, does not transform the mass, stiffness and damping matrices.

At this point, considering eq. 3.44, and including the orthogonality condition, the Λ_C matrix is obtained in the following form:

$$\Lambda_C = - \begin{bmatrix} \ddots & & \\ & 1/a_k & \\ & & \ddots \end{bmatrix} \cdot \begin{bmatrix} \ddots & & \\ & b_k & \\ & & \ddots \end{bmatrix} \tag{3.47}$$

The matrix Λ_C is diagonal and the components are obtained from the product of the components of the P and Q (modal and diagonal) matrices.

State equation

Taking eq. 3.40, this can be rewritten, through mathematical treatment, into an equivalent system (first-order differential equations) using the *state-space model* that provides estimates of the modal parameters of structures characterised by general *viscous damping*. For this reason, it is very frequently adopted in civil engineering applications.

Then, eq. 3.44 is considered and both terms are multiplied by the inverse matrix P^{-1}. This transforms the equilibrium equation (Eq. 3.40) into the so-called *state-equation* (Eq. 3.48). In this model, time is assumed to be *continuous* (as denoted by subscripts C):

$$\dot{x}(t) = A_C \cdot x(t) + B_C \cdot u(t) \tag{3.48}$$

Matrices A_C and B_C are represented as follows:

$$\begin{aligned} A_C &= -P^{-1} \cdot Q = \begin{bmatrix} 0 & I \\ -M^{-1}K & -M^{-1}C \end{bmatrix} \\ B_C &= P^{-1} \cdot \begin{bmatrix} B_N \\ 0 \end{bmatrix} = \begin{bmatrix} 0 \\ M^{-1}B_N \end{bmatrix} \end{aligned} \tag{3.49}$$

The matrix A_C is the *state matrix* (with $n = 2N$). It is a square matrix with dimension [n-by-n]. B_C is the *input matrix*, of dimension [n-by-m]. $x(t)$ is the state vector with dimension n.

At this point, with eq. 3.47 in mind, a relationship between the matrix A_C and the matrices Λ_C and Ψ can be defined as follow:

$$\begin{aligned} A_C = -P^{-1} \cdot Q = -\Psi \cdot diag[1/a_k] \cdot \Psi^T \cdot \Psi^T \cdot diag[b_k] \cdot \Psi^{-1} \\ A_C = \Psi \cdot \Lambda_C \cdot \Psi^{-1} \iff A_C \cdot \Psi = \Psi \cdot \Lambda_C \end{aligned} \tag{3.50}$$

Based on the last equality expressed in the previous equation, it is shown that the eigenvalues and eigenvectors of the matrix A_C and those obtained by solving eq. 3.44 are equivalent. From this it can be deduced that all the modal characteristics of the dynamical system can be extracted from the A_C matrix. It is to be noted that the number of elements of the *state vector* $x(t)$, whose

size corresponds to twice-DOFs in the reference system, indicates the number of independent variables describing the state of the system. $x(t)$ in fact contains the displacement and velocity vectors of the dynamic system.

Observation equation

To conclude the *state-space* formulation, a further equation must be defined. This is necessary because in practice it is not possible to measure the structural response for all DOFs, so we consider the measured data only at l-DOFs (where $l < n$). Consequently, the *observation equation*, defined in eq. 3.51, is necessary to correlate the output of the generalised N-DOFs of the system with the directly measured values. Generally, the instrumented points are related to the displacements, velocities and accelerations associated with these points.

$$y(t) = C_a \cdot \ddot{q}(t) + C_v \cdot \dot{q}(t) + C_d \cdot q(t) \tag{3.51}$$

$y(t)$ is the measurement vector of the system with dimension l. C_a is the output location matrix for accelerations, C_v for velocities and C_d for displacements. They have dimension [l-by-N] and are composed of zeros or ones values.

Recalling eq. 3.40 and using the definition of the *state vector* expressed in eq. 3.41, the relationship between the outputs $y(t)$ and the state vector $x(t)$ and the inputs $u(t)$ can be rewritten in the following form:

$$y(t) = C_C \cdot x(t) + D_C \cdot u(t) \tag{3.52}$$

the C_C [l-by-n] and D_C [l-by-m] are the *output matrix* and *direct transmission matrix*,respectively, and they are defined as:

$$\begin{gathered} C_C = \begin{bmatrix} C_d - C_a \cdot M^{-1} \cdot K & C_v - C_a \cdot M^{-1} \cdot C_N \end{bmatrix} \\ D_C = C_a \cdot M^{-1} \cdot B_N \end{gathered} \tag{3.53}$$

From the *state equation* (Eq. 3.48) and the *observation equation* (Eq. 3.53), the *continuous-time deterministic state-space model* of of order N can be defined, which establishes the relationship between the system's response $y(t)$ and the deterministic excitation $u(t)$ and whose order is determined by the state vector

$x(t)$:

$$\begin{aligned} \dot{x}(t) &= A_C \cdot x(t) + B_C \cdot u(t) \\ y(t) &= C_C \cdot x(t) + D_C \cdot u(t) \end{aligned} \tag{3.54}$$

3.3.3.2 Discrete-time state-space model

In the discussion up to now we presented, *continuous time* has been assumed. If thinking of real applications however, specifically civil engineering applications for this work, considering continuous time is an incorrect assumption. In fact, the experimental data, that are collected with the survey campaigns, always have a *discrete* nature: they are analogue signals, recorded by transducers, which are then converted into digital data through special instrumentation, analogue-to-digital (A/D) converters, then stored and processed by computers. For this reason, the state-space model must necessarily be transformed into a *discrete-time state-space model*:

$$\begin{aligned} x_{k+1} &= A \cdot x_k + B \cdot u_k \\ y_k &= C \cdot x_k + D \cdot u_k \end{aligned} \tag{3.55}$$

In this version of the model, the continuous time functions $x(t)$, $y(t)$ and $u(t)$ are replaced by sets of values x_k, y_k and u_k defined in discrete time instant $k\Delta t$ ($k \in \mathbb{N}$). Δt is the adopted sampling interval such that: $x_k = x(k \cdot \Delta t)$.
The continuous-time model matrices A_C, B_C, C_C, D_C can be correlated with their discrete-time matrices A, B, C, D (Eq. 3.56) through the *Zero Order Hold (ZOH)* assumption [43]: time functions connecting two consecutive discrete samples are considered constant.

$$\begin{aligned} A = e^{A_C \Delta t} \quad B = \int_0^{\Delta t} e^{A_C \tau}\, d\tau \cdot B_C \\ C = C_C \qquad D = D_C \end{aligned} \tag{3.56}$$

Considering the discrete-time matrix A, this can be related to the corresponding continuous matrix A_C by performing the McLaurin decomposition:

$$A = e^{A_C \cdot \Delta t} = I + (A_C \cdot \Delta t) + \frac{(A_C \cdot \Delta t)^2}{2!} + \frac{(A_C \cdot \Delta t)^3}{3!} + \cdots \tag{3.57}$$

Furthermore, by referring to eq. 3.50 and substituting the eigenvalues decomposition, it is evident from eq. 3.58 that the eigenvectors of the matrix A and

the matrix A_C are coincident:

$$\begin{gathered} A_C = \Psi \cdot \Lambda_C \cdot \Psi^{-1} \\ A = e^{A_C \cdot \Delta t} = e^{\Psi \cdot \Lambda_C \cdot \Psi^{-1} \cdot \Delta t} = \Psi \cdot e^{A_C \cdot \Delta t} \cdot \Psi^{-1} = \Psi \cdot \Lambda_D \cdot \Psi^{-1} \end{gathered} \tag{3.58}$$

The matrix Λ_D is composed of exactly the eigenvalues of the correlated *state matrix* A as follows:

$$\Lambda_D = \begin{bmatrix} \ddots & & \\ & \mu_k & \\ & & \ddots \end{bmatrix}; \quad \mu_k = e^{\lambda_k \Delta t} \leftrightarrow \lambda_k = \frac{ln(\mu_k)}{\Delta t} \tag{3.59}$$

From the above discussion, it has been shown how the modal parameter of the structure can be easily estimated once a *discrete-time state-space model* has been identified from experimental data: the natural frequencies and modal damping ratio are obtained from the eigenvalues of A using Eq. 3.11. Similarly, it will be shown that the eigenvectors of A also coincide with the eigenvectors of A_C.

3.3.3.3 Stochastic process

Asserting that the input time functions are known, means that the input forces can be expressed in deterministic form. However, as already presented at length, in OMA, the input excitation is unknown and is therefore represented by a stochastic process, which also takes into account the effects of noise in the model.
A stochastic process is defined as a set of n (with $n \to \infty$) *time-dependent random functions* that allow the characterisation of one or more variables, which are also time-dependent. These random functions are designed on the basis of the different realisations of the given variable during the observation process.
In practical applications [44], stochastic processes are defined as:

- *stationary*: the statistical properties of the processes are constant over time;
- *zero mean*: this is because the measured time signals are de-trended before being processed;
- *ergodic*: the statistical properties of measured signals can be calculated by considering the mean values over many realisations at a given instant,

or by using the mean values of a single realisation over time. That is, a stochastic process is called ergodic when statistical averages converge almost everywhere at average times.

From the above, it can be said that a necessary condition for *ergodicity* is therefore *stationarity*. In particular, *ergodicity* of the mean value is obtained when the mean time value and the statistical mean value are coincident.
In the case of *correlation*, ergodicity is verified when the statistical and temporal auto-correlation correspond.
The *autocorrelation function* provides a measure of the similarity of the original signal with its past and future values. When considering the stationarity of the process, the *autocorrelation* is only related to the time-lag and thus provides information on how quickly the process evolves over time.

Given a stochastic process $y(t)$ with n_y components, the *correlation matrix* can be expressed:

$$\sum_{yy}(r) = E[y(t) \cdot y(t+\tau)^T] = \lim_{x\to\infty} \frac{1}{T} \int_{-T/2}^{+T/2} y(t) \cdot y(t+\tau)^T \, dt \tag{3.60}$$

where the square matrix $\Sigma_{yy}(t)$ (with [n_y-by-n_y] dimension) is dependent on the considered $time - lag$ (τ). Its elements on the diagonal are designed $autocorrelations$ or $cross - correlations$.

The *correlation matrix* contains the information of the random data associated with the temporal responses of the system. And this is the reason why in the context of modal analysis, most dynamic identification techniques are applied to correlation functions. Thus, for *discrete-time signals* the correlation function is only defined for $t > 0$, and in the eq. 3.60 the integral is replaced by a sum series, obtaining the equation below:

$$\sum_{yy}(\tau) = E[y_k \cdot y_{k+\tau}^T] = \lim_{n_t\to\infty} \frac{1}{n_t} \sum_{t=0}^{n_t-1} y_k \cdot y_{k+\tau}^T \tag{3.61}$$

where $E[\cdot]$ is the expected value operator, which gives the mean value when the realisation of the stochastic process approaches infinity, and y_k is the value of the time signals $y(t)$ at time $k\Delta t$.
A characteristic feature of the *autocorrelation* function is its natural tendency to zero depending on the irregularity of the time series involved: a higher level

of irregularity corresponds to a faster decay. *Autocorrelation* functions for stationary stochastic processes with zero mean are symmetric functions with a maximum value equal to the standard deviation of the process and centred in the origin ($\tau = 0$).

The $cross - correlation$ function, estimated by limiting the set of acquired samples to a finite number given the impossibility of having an infinite number in practical applications, provides information on the degree of correlation between two different time signals y and x:

$$\Sigma_{yx}(\tau) = E[y_k \cdot x_{k+\tau}^T] = \lim_{n_t \to \infty} \frac{1}{n_t} \sum_{t=0}^{n_t - 1} y_k \cdot x_{k+\tau}^T \tag{3.62}$$

In conclusion, the correlation function describes how an instantaneous observation depends on previous observations. Furthermore, given the zero mean assumption of time signals, in applications of modal analysis the covariance functions and correlation functions are coincident. Therefore, when processing signals, the terms correlation and covariance can be used indiscriminately.

3.3.3.4 Stochastic discrete-time state-space model

When structures are subjected to an unknown excitation, this can be defined through the use of probabilistic concepts and idealised through a stochastic process. Experimentally collected data are affected by noise, which cannot be measured individually and must necessarily be considered in the discrete-time state-space model, which will then include two statistical components. The *stochastic discrete-time state-space model* is expressed as follows:

$$\begin{aligned} x_{k+1} &= Ax_k + Bu_k + w_k \\ y_k &= Cx_k + Du_k + v_k \end{aligned} \tag{3.63}$$

w_k and v_k represent the noise content. Or more precisely, they represent two stochastic processes due to the noise content in the signals. w_k is due to modelling inaccuracies, while v_k is due to measurement noise caused by sensor inaccuracy. Both of these immeasurable vectors are considered as realisations of stochastic processes, so they are assumed to be $zero - mean$, implying the following properties for the covariance matrices, calculated for two arbitrary

time instants p and q:

$$\begin{aligned} E\left(\begin{bmatrix} w_p \\ v_p \end{bmatrix} \begin{bmatrix} w_p^T & v_p^T \end{bmatrix}\right) &= \begin{bmatrix} Q & S \\ R & S^T \end{bmatrix} \\ E\left(\begin{bmatrix} w_p \\ v_p \end{bmatrix} \begin{bmatrix} w_q^T & v_q^T \end{bmatrix}\right) &= 0 \quad p \neq q \end{aligned} \tag{3.64}$$

Each new observation is independent of the previous ones: the correlation matrices of the processes w_k and v_k are assumed to be zero for each non-zero time lag $\tau = q - p \neq 0$. This type of stochastic random process is referred to as a *white noise* process.

In the context of vibration tests and OMA techniques, since the excitation acting on the structure is not measured, the discrete vector U_K is not known. Therefore, a further approximation can be made: the unknown excitation is included in the terms and an *approximate stochastic discrete-time state-space model* is defined:

$$\begin{aligned} x_{k+1} &= Ax_k + w_k \\ y_k &= Cx_k + v_k \end{aligned} \tag{3.65}$$

The terms w_k and v_k are not the same as those introduced in Eq. 3.63, but are slightly different. In this case they represent not only modelling inaccuracies and measured noise but also the effect of unknown inputs. Without this assumption, when the input excitation contains some dominant frequency components, these values will be identified as poles of the state matrix A and will be indistinguishable from the actual natural frequencies of the system.

3.3.4 Auto-spectra and cross-spectra functions

When considering natural phenomena, the correctness of using the hypothesis that the stochastic process of the input excitation has *normal distribution* and *zero mean* value is confirmed. This property is also validated by the *Central Limit Theorem*: the sum of a large number of independent random variables, each with its own independent distribution, tends to a Gaussian distribution. In addition, it can be stated that if the stochastic process is also *stationary* and *ergodic*, the auto-correlation function only depends on the time interval $\tau = t_j - t_i$ and not on the time instants t_i and t_j.

The stochastic process can at this point be defined by a realisation of the process $(x_e(t))$ that depends only on this interval, defining the *auto-correlation*

function as:

$$R_{yy}(\tau) = \lim_{T\to\infty} \frac{1}{T} = \int -T/2^{T/2} x_e(t) \cdot x_e(t+\tau) dt \tag{3.66}$$

As has already been mentioned, the tendency of the auto-correlation function to zero depends on the irregularity of the time series involved: more irregularity, faster decay of the function. For clarity, the auto-correlation functions associated with zero mean stationary stochastic processes are symmetric functions with the maximum value in the origin ($\tau = 0$) and the ordinate is given by the standard deviation of the process.

With the use of the *Fourier Transform*, the function defined in eq. 3.66 can be transposed to the frequency domain, obtaining the *eigenspectrum function*, which quantifies the distribution of the energy content associated with the signal in terms of frequencies:

$$S_{xx}(\omega) = \int_{-\infty}^{+\infty} R_{xx}(\tau) \cdot e^{-i\omega t} dt \tag{3.67}$$

It is underlined that for white noise signals, the energy value is only given by its variance value.

The concepts exposed for the definition of auto-correlation functions (Eq. 3.66) and auto-spectrum functions (Eq. 3.67) can also be adopted to define *cross-correlation* (Eq. 3.68) and *cross-spectrum function* (Eq. 3.69).

$$R_{x_1x_2}(\tau) = \lim_{T\to\infty} \frac{1}{T} \int_{-T/2}^{T/2} x_{1e}(t) \cdot x_{2e}(t+\tau) dt \tag{3.68}$$

$$S_{x_1x_2}(\omega) = \int_{-\infty}^{+\infty} R_{x_1x_2}(\tau) \cdot e^{-i\omega t} dt \tag{3.69}$$

Again, by applying the Fourier Transform to the realisation of the stochastic process, the cross-spectrum function, also called the *cross-spectral density function*, can alternatively be defined as follows:

$$S_{x_1x_2}(\omega) = \lim_{n\to\infty} \frac{1}{n} \sum_{e=1}^{n} \frac{F_{T,e}[x_1(t)]^* \cdot F_{T,e}[x_2(t)]}{T} \tag{3.70}$$

$F_{T,e}[x_1(t)]$ represents the Fourier Transform of the realisation x_e associated

with the process $x_1(t)$ in the interval $[-T/2,\, T/2]$. Considering $x_2 = x_1$, this expression can be used to calculate the automatic spectrum function. It is clarified that auto-spectra are functions with real components given by the product between a complex number and its complex conjugate. Cross-spectrum, on the other hand, are complex functions.

When considering different processes associated with different physical phenomena (maintaining stationarity and ergodicity), it is possible to define a *vector stochastic process*: a *correlation matrix* replaces the scalar function of the auto-correlation. The diagonal elements of the matrix define the auto-correlations, while the extra-diagonal elements are the cross-correlations.
Thus, having defined the vector $y(t)$ that groups the different stochastic stationary processes, the correlation matrix can be defined as follows:

$$R_y(t) = E[y(t) \cdot y(t+\tau)^T] = \lim_{T\to\infty} \frac{1}{T} \int_{-T/2}^{+T/2} y(t) \cdot y(t+\tau)^T dt \tag{3.71}$$

When the objective, as in our case, is to estimate the modal parameters of a system using only the output response, attention must be given to the output spectrum, which obviously depends on the input spectrum and the characteristics of the system itself. Thus, considering a white noise process for the input, their *continuous-time correlation matrix function* is given by:

$$R_y(t) = R_Y \cdot \delta(\tau) \tag{3.72}$$

in which R_y (with $[n_i - by - n_i]$ is a constant matrix and $\delta(r)$ is the *Dirac Delta Function* characterized by the following properties:

$$\begin{gathered} \delta(\tau) = 0 \quad \text{if} \quad t = 0 \\ \delta(\tau) = \quad \text{elsewhere} \\ \textstyle\int_{-\infty}^{+\infty} f(t)\delta(t-a)dt = f(a) \end{gathered} \tag{3.73}$$

Given the property of the function $\delta(t)$ whereby the input spectrum is a constant matrix equal to R_y, the spectrum is 'flat': the energy associated with the input signal is uniformly distributed along the frequency axis. This concept is hereafter explained through the relationship between the output response spectrum S_{yy} and the input spectrum S_{uu} as follows:

$$S_{yy}(\omega) = H(\omega) \cdot S_{uu}(\omega) \cdot H^H(\omega) \tag{3.74}$$

In the case of an input white noise process, the output spectrum of the system only depends on the system transfer function $H(\omega)$ and the constant matrix R_p:

$$S_{yy}(\omega) = H(\omega) \cdot R_p \cdot H^H(\omega) \tag{3.75}$$

Furthermore, again under the assumption of input signals defined by a white noise process and are statistically independent, the *cross-correlation* is zero and the constant matrix becomes a diagonal matrix. Since:

$$H_{i,j}(\omega) = \sum_{k=1}^{N} \frac{[\varphi_i]_k \cdot [\varphi_j]_k}{\omega_k^2 - \omega^2 + 2i\xi_k\omega\omega_k} \tag{3.76}$$

the contribution made by a general $k - mode$ on any element of the output spectrum can be calculated through the expression:

$$S^k_{q_{i,j}}(\omega) = \sum_{k=1}^{N} \frac{[\varphi_i]_k \cdot [\varphi_j]_k}{\omega_k^2 - \omega^2 + 2i\xi_k\omega\omega_k} \cdot R_p \cdot \frac{[\varphi_i]_k \cdot [\varphi_j]_k}{\omega_k^2 - \omega^2 + 2i\xi_k\omega\omega_k} \tag{3.77}$$

Analysing this equation, it is evident how it divides the contribution of each mode for the spectrum system and defines the relationship between the output spectra matrix with the modal properties of the structure. At this point, following [27], it is possible to express the output spectrum as a superposition of the different contributions of the structural modes, taking into account the modal composition of the transfer function:

$$S_{yy}(\omega) = \sum_{k=1}^{N} \frac{\varphi_k \cdot g_k^T}{i\omega - \lambda_k} + \frac{\varphi_k^* \cdot g_k^H}{i\omega - \lambda_k} + \frac{g_k^* \cdot \varphi_k^T}{-i\omega - \lambda_k^*} + \frac{g_k^* \cdot \varphi_k^H}{-i\omega - \lambda_k^*} \tag{3.78}$$

The previous equation defines the output spectral matrix, the structural modes and the vector g_k, the *operational reference vector*, in which the modal participation takes place, depending on all modal parameters, the input position and the input correlation matrix.

The modal decomposition of the output spectrum returns the four different poles (λ_k, $-\lambda_k$, λ_k^*, $-\lambda_k^*$) for each structural mode. To overcome this problem, one can use the *Positive or Half-Spectrum function*, which can be obtained without difficulty from the correlation matrix by restricting the *Discrete Fourier*

Transfer (DFT) function to positive time-lags:

$$S_{yy}^{+}(\omega_j) = \frac{R_{yy}(0)}{2} + \sum_{k=1}^{j} R_{yy}(k\Delta t) e^{-i\omega_j k\Delta t} \tag{3.79}$$

Following the example of [45], the modal decomposition of the *Positive Spectrum* is given by:

$$S_{yy}^{+}(\omega_j) = \sum_{k=1}^{N} \frac{\varphi_k \cdot g_k^T}{i\omega - \lambda_k} + \frac{\varphi_k^* \cdot g_k^H}{i\omega - \lambda_k} \tag{3.80}$$

This equation has the same structure as the FRF or transfer function. Consequently, the models described can be adopted to define the matrix of the positive spectrum.

3.4 Output-only modal identification techniques

As extensively presented above, the identification of the dynamic characteristics of structures can be performed following two different approaches: by relating the output response to the corresponding artificial input excitation also measured (EMA technique), or by analysing only the structural output response and establishing initial hypotheses on the nature of the ambient excitation (OMA technique). In the field of civil engineering, the second approach is the most widely adopted for all the reasons already presented: smaller and less expensive equipment; environmental excitation always available; maintaining the operability of the structure; no damage due to induced excitations; dynamic response under real operating conditions; etc. Taking these assumptions as a basis, methods that aim to identify the modal parameters of a structural system only by the dynamic output response, are known as: ***Output-only modal identification techniques***.

The description of the different identification methods will be presented considering the two categories of *frequency domain methods* (based on spectral estimation of structural response) and *time domain methods* (based on correlations or projections of outgoing responses collected).

For further and more in-depth discussion on the techniques of dynamic identification of civil structures, please refer to [18, 41, 42, 44, 46–51]

In order to introduce the treatment, in most of the output-only modal iden-

tification techniques, the initial phase is represented by the construction of a matrix of data that organizes and contains the information on the output answers of the structure. This matrix is composed of the data from cross-correlations or spectral estimates of the signals recorded. Where all recording channels are used as reference outputs, the matrix is square in size and contains all cross-correlations or cross-spectra between all measured outputs. Otherwise, the matrix can be reduced by adopting only available channels such as the reference ones. This reduction in matrix size enables faster execution and less time-consuming data analysis.

3.4.1 Identification methods in the frequency domain

The main hypothesis in the field of OMA applications for civil structures made regarding the input excitation gives the possibility of representing the structural behaviour through mathematical models that establish a relationship between output spectral matrix and modal parameters.
In the following paragraphs, the main techniques for modal identification in the frequency domain will be proposed: the *Peak Picking method* (the oldest method developed, which is simple to implement and allows for faster analysis during dynamic tests), the *Frequency Domain Decomposition* algorithm and one of its evolution (it is based on the main concept of the Peack Picking method, making improvements to allow for the separation of closely spaced modes and solving the problem of identifying the modal damping ratio).

3.4.1.1 Peak Picking

The first technique presented is the *Base Frequency Domain (BFD)* method, known as the ***Peack Picking (PP)*** method. It is easy to implement and interpret the results, which maintain a clear physical meaning, making it one of the most widely used methods [41, 52, 53].
The PP method allows natural frequencies to be estimated by visual inspection of the magnitude of the power spectrum, plotted on a magnitude vs. frequency diagram. To obtain good results, two initial conditions must be met: the modes must be *slightly damped* and the natural frequencies of the structural modes *well separated*. If this assumption is not satisfied, the method may not provide a reasonable set of modal parameters associated with the resonant modes. To better understand: near each natural frequency value, the dynamic response of the structure is conditioned by the contribution of a resonant mode. Thus, near

natural frequencies, the dynamic behaviour can be approximated to the single contribution of the resonant mode at that frequency (structural response simulated by a 1-DOF oscillator model characterised by the same frequency and damping value of the resonant mode). Given this limitation, the PP method is mainly utilised to extract fast information on dynamic characteristics, thus to provide resonant frequencies and associated modal shapes.

Identification of the natural frequencies

Starting from the FRFs matrix (see Eq. 3.76), the spectral matrix of an MDOF system subjected to random white noise excitation can be estimated. This relationship can be obtained because the spectral function of a white noise excitation is constant and does not depend on other factors:

$$S_q(\omega) = H(\omega) \cdot R_p \cdot H^H(\omega) \tag{3.81}$$

The elements of the FRFs matrix have maximum values at the values of the damped resonance frequencies. When the damping values are low, these correspond to the natural frequencies.

Due to the nature of *white noise* processes, it is clear that it is possible to extract natural frequencies from the analysis of the *auto-spectra function* (or *Power Spectral Density (PSD)* function), defined in the following equation:

$$PSD_i(\omega_k) = \sum_{k=1}^{N} PSD_i(\omega_k) \tag{3.82}$$

To ensure the identification of all natural frequencies during dynamic tests, in [52], a practical implementation of the PP method is proposed in which the use of the *Averaged Normalized Power Spectral Density (ANPSD)* of all measurement points is suggested, i.e. the average of the diagonal elements of the spectrum matrix $S^+_{yy}(\omega)$, as given in the following equation:

$$ANPSD(\omega) = \frac{1}{l}\sum_{i=1}^{l} NPSD_i(\omega) = \frac{1}{l}\sum_{i=1}^{l}\left[\frac{PSD_i(\omega)}{\sum_{i=1}^{N} PSD_i(\omega)}\right] \tag{3.83}$$

l is the number of instrumented DOFs and $NPSD_i$ are the normalised spectra associated with each DOF obtained from Equation 3.82. This strategy has proved to be efficient and has become one of the most important foundations of OMA analysis, as it relates the estimation of modal parameters to the energy

content associated with each DOF of the structure: averaging the elements of the spectrum matrix $S_{yy}^{+}(\omega)$, eliminate the risk of not identifying all resonant frequencies in the case where a reference DOF is present on one of the nodes of a vibration mode (a condition that does not allow mode identification).

Identification of vibration modes

Resuming the relation that describes the FRFs matrix, in modal domain:

$$H(\omega) = \Phi \cdot H_{\eta}(\omega) \cdot \Phi^{T} = \sum_{K=1}^{N} \cdot H_{\eta k} \cdot \phi_k \cdot \phi_k^{T} \tag{3.84}$$

diagonal matrix $H_{\eta}(\omega)$, that depends by the modal parameters, can be defined as follows:

$$H_{\eta}(\omega) = diag\left[\frac{1}{\omega_k^2 - \omega^2 + 2i\xi_k\omega\omega_k}\right] \tag{3.85}$$

Under the necessary assumptions already presented (well-spaced natural frequencies and low damping coefficient values), the diagonal elements of the H_{η} matrix have very high values in proximity of resonance frequencies. This implies that near of a natural frequency ω_k, the k-element of H_{η} can be approximated to the $k-th$ mode contribution at that frequency as:

$$H_{\eta}(\omega_k) = \varphi_k \cdot \frac{1}{\omega_k^2 - \omega_k^2 + 2i\xi_k\omega_k\omega_k} \cdot \varphi_k^{T} = \varphi_k \cdot c_1 \cdot \varphi_k^{T} \tag{3.86}$$

The presented equation shows that the $k-th$ component of the FRFs matrix is a complex scalar value c_1 that depends on the natural frequency ω_k, the damping value ξ_k and the modal form ϕ_k. At this point, by introducing Eq. 3.86 into Eq. 3.81, the spectra can be defined:

$$S_y(\omega_k) = \phi_k \cdot c_1 \cdot \phi_k^{T} \cdot R_u \cdot \phi_k \cdot c_1^{*} \cdot \phi_k^{T} = c_1 \cdot c_1^{*} \cdot \phi_k \cdot c_2 \cdot \phi_k^{T} \tag{3.87}$$

in which $c_2 = \phi_k^{T} \cdot R_u \cdot \phi_k$ is a constant scalar value. Compacting the three coefficients, the relation 3.87 can be re-written as:

$$S_y(\omega_k) = c_3 \cdot \phi_k \cdot \phi_k^{T} \tag{3.88}$$

It is clear from this equation that from a column of the spectral matrix, it is possible to know the mode configuration associated with that specific natural frequency value ω_k, and back. This means that taken a reference DOF, the

element in the ref position of the ref column of the S_y matrix can be calculated as:

$$S_y(\omega_k)_{(ref,ref)} = c \cdot (\phi_{ref})_k \cdot (\phi_{ref})_k^T \tag{3.89}$$

and for other components:

$$S_y(\omega_k)_{(j,ref)} = c \cdot (\phi_j)_k \cdot (\phi_{ref})_k^T \tag{3.90}$$

From the equation 3.89 and 3.90, *pseudo transfer function* can be defined as:

$$T_{(j,ref)} = \frac{S_y(\omega_k)_{(j,ref)}}{S_y(\omega_k)_{(ref,ref)}} = \frac{(\phi_j)_k}{(\phi_{ref})_k} \tag{3.91}$$

T is a complex number and makes it possible to estimate, the components of structural modes at natural frequency ω_k, in instrumented DOFs. This implies that only two reference sensors would be needed to characterise the dynamic behaviour of a structure. Furthermore, it is noted that due to the complex nature of cross-spectra, the transfer functions are complex numbers whose amplitude is dependent on the components of the selected $i-th$ and $ref-th$ modes and the phase is equal to 0°, if $i-th$ and $ref-th$ move in the same direction, or 180°, if $i-th$ and $ref-th$ move in the opposite direction.

3.4.1.2 Frequency Domain Decomposition (FDD)

The motivation for which the ***Frequency Domain Decomposition (FDD)*** method was developed is that it was able to eliminate some limitations present in the PP technique: difficulty in detecting spectrum peaks, separation of close modes and estimation of the modal damping ratio with greater precision (for more details, [18, 42, 47, 49, 50, 52–54], and [19] for an important improvement proposed).

In the analysis of structures excited by environmental inputs, the basic concepts of the FDD method and the extraction of modal parameters from the FRF in the form of *Complex Mode Indication Function (CMIF)* had already been introduced by [55]. The subsequent introduction of the concept of modal domain then improved the identification of the modal parameters of this procedure compared to classical spectral analysis: better evaluation of modal shapes and the possibility of identifying close modes with greater certainty.

In general, the FDD method is a non-parametric method in the frequency domain. It is based on the construction and factoring of *output spectrum matrices* calculated by the *Welch method* [56]. Thus, this method can detect the contribution of different modes in the same frequency.

Considering a vibrating structure, its general response $y(t)$ can be obtained as a superposition of n vibration modes, each with its own modal form ϕ_i, expressed through modal co-ordinates η_i:

$$y(t) = \phi_1 \cdot \eta_1(t) + \phi_2 \cdot \eta_2(t) + ... + \phi_n \cdot \eta_n(t) = [\Phi] \cdot \eta(t) \tag{3.92}$$

Computing the value of the *correlation function* $R^+_{\eta\eta}(\tau)$ in the modal coordinate in the time domain as:

$$R^+_{\eta\eta}(\tau) = E[q(t+\tau) \cdot q(t)^T] = E[\Phi \cdot \eta(t+\tau) \cdot \eta(t)^T \cdot \Phi^T] = [\Phi] \cdot \Sigma^+_{\eta\eta}(t) \cdot [\Phi]^T \tag{3.93}$$

By applying the Fast Fourier Transform (FFT) to Eq. 3.92, the *complete output spectrum matrix* is obtained as:

$$S_{yy}(\omega) = [\Phi] \cdot S_{\eta\eta}(\omega) \cdot [\Phi]^T \tag{3.94}$$

Recalling the orthogonality property of the modal shapes contained in the modal matrix Φ and the assumption of white noise for the input excitation well distributed over the structure, the modal coordinates can be considered uncorrelated. Therefore, the power density spectral matrix $S_{\eta\eta}(\omega)$ is diagonal. With Eq. 3.92 in mind and taking into account what has just been mentioned, the power spectral density matrix can be factorised in terms of SV by performing the *Singular Value Decomposition (SVD)* method.

Singular Value Decomposition

SVD is an algorithm for decomposing a generic matrix $A \in \mathbb{C}^{nxm}$ (with $n>m$) as product of three matrices as follows:

$$A = [U] \cdot [S] \cdot [V]^H \qquad with \qquad S = \begin{bmatrix} S_1 \\ 0 \end{bmatrix} \tag{3.95}$$

where:

- $U \in \mathbb{C}^{nxn}$ is the matrix that contains the right singular vectors of matrix

A; in particular, the columns of U contains the eigenvectors of $A^T A$;

- $V \in \mathbb{C}^{mxm}$ is the matrix that contains the left singular vectors of matrix A; in particular, the columns of V contains the eigenvectors of AA^T;
- $S \in \mathbb{C}^{nxm}$ is a rectangular matrix, from where the diagonal matrix $S_1 \in \mathbb{C}^{nxn}$ can be extracted; into S_1 non-null singular values, defining the rank of matrix A and so the number of linearly non-dependent rows and columns, are positioned in decreasing order.

Applying SVD to the spectrum response matrix in the FDD method produces a sum of different spectral power density functions for each 1-DOF oscillator that has the same frequencies and damping coefficients of the structure modes. The results this procedure provides can be reliable if: the excitation is white noise, the mode shapes are orthogonal and the structure is slightly damped. If these assumptions are not fulfilled, the results is an approximate SVD. However, the results obtained are still more accurate than those provided by traditional techniques.
Before applying the FDD method to estimate the modal parameters, it is necessary to estimate half of the positive spectral matrix, named S_{yy}^+, which is based on the output measurements. Mathematically, the SVD of S_{yy}^+ at each discrete frequency point ω_i is performed and can be formally rewritten for the generic discrete frequency ω as:

$$S_{yy}^+(\omega) = [U(\omega)] \cdot [S_n] \cdot [U(\omega)] \tag{3.96}$$

U is a square matrix of singular vectors. The matrix S_n is diagonal and it is composed of n SVs (where n refers to the instrumented points and the size of the S^+ matrix), in descending order. These SVs coincide with the amplitude of each spectrum, defined for each discrete value of ω, of the SDOF oscillators at the investigated frequency.

Wanting to be more specific, applying the SVD to the S_{yy}^+ matrix, the first singular value contains, in its ordinate, the eigenspectra relative to the dominant mode at that specific frequency. This implies that the dominant mode can be identified by looking at the peaks of the first SV (the others are negligible).
We can distinguish two cases:

I. close modes: the graphical variation of the first SV along the frequency values contains the most important segment of the self-spectrum of all

SDOFs in the proximity of the resonance frequency (necessary to understand the behaviour of the structure)

II. well-separated modes: there are several SVs with significant values equal to the number of modes that are present close to the resonance frequency.

Once the *natural frequency* (resonance peak) is defined, the relative mode shape is obtained by taking the first singular vector u_1 of the U matrix (contributions from other modes provided by the other SVs are negligible). The singular vector is an estimate of the shape of the associated mode:

$$\hat{\phi} = u_1 \tag{3.97}$$

To make more significant the treatment just exposed, the figure 3.5 is proposed. It shows a typical plot of the singular values of the spectral matrix $S_{yy} + (\omega)$ obtained for a simple numerical system. The first SV is much larger than others and the typical "bell-shapes" of the modal peaks associated to the natural frequencies are well defined.

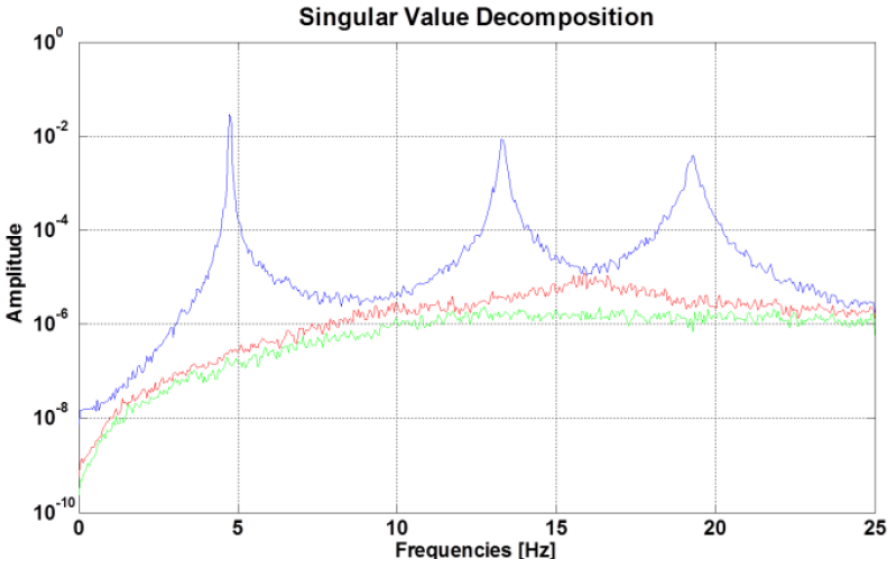

Figure 3.5: *Plot of the first SV lines obtained applying the FDD identification method*

3.4.1.3 Enhanced Frequency Domain Decomposition (EFDD)

The FDD technique has a severe limitation: a high inaccuracy related to damping estimation. Therefore, an improvement has been proposed by develop-

ing the ***Enhanced Frequency Domain Decomposition (EFDD)*** method [49, 57]. In addition to a better estimation of the damping value, the natural frequency and associated modal form can be extracted with less uncertainty. A frequency range is defined in which the peak of the first singular values is dominant.

Operationally, through the use of the correlation between the SV associated with the resonance peak and the SVs associated with other values around that peak, the *modal domain* (Figure 3.6) around the peak is identified, resulting in the definition of the auto-spectral density of the dominant SDOF system in that domain.

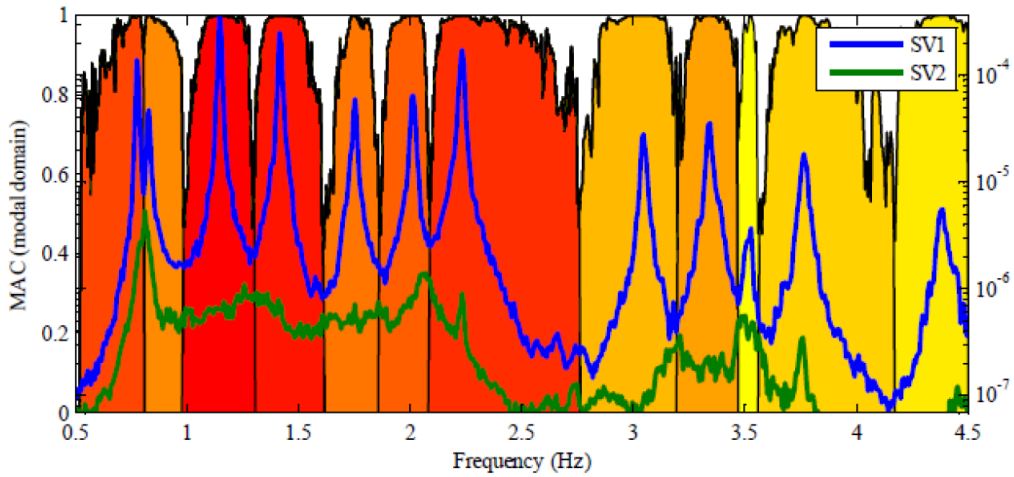

Figure 3.6: *Typical modal domains associated to structural modes [58]*

The Modal Assurance Criterion (MAC) [59, 60] allows the correlation between these vectors to be defined:

$$MAC = \frac{(\phi_1^T \cdot \phi_2)^2}{(\phi_1^T \cdot \phi_1)(\phi_2^T \cdot \phi_2)} \tag{3.98}$$

The MAC is an indicator of consistency between two mode shapes. Its value varies from 0, when two mode shapes are orthogonal, to 1, when the two mode shapes are similar differing only by a scaling factor. If the MAC values calculated between the resonant peak vector and any other around the resonant peak are close to 1, then all such points can be included in the *modal domain*. To define the *modal domain* associated with each resonant frequency, a MAC threshold must be set [49]. Otherwise, singular vectors with a lower degree of correlation (in terms of MAC value) are discarded from the modal domain.

After defining the modal domain for each peak, the mode shape estimation is

performed by averaging all SVs that belong to the same modal domain. Therefore, when similar SVs are selected for a specific mode, the eigen-spectrum segment can be reconverted to the time domain using the *inverse* FFT function. This means that the modal damping ratio of the investigated mode can be extracted from the *auto-correlation* function by applying structural dynamics and considering the structure as a 1-DOF system excited by white noise. This function is proportional to its impulse response, defined as:

$$h(t) = ce^{-\xi_k \omega_k t} \sin(\omega_k t) \tag{3.99}$$

c is a constant and ξ_k and ω_k represent the damping ratio and circular frequency.

Although this procedure is very popular due to its user-friendly approach and its ability to provide useful information with relevant physical meaning, it has some disadvantages, first of all the strong dependence of modal parameters on frequency resolution, which may compromise their correct identification. Furthermore, the occurrence of certain conditions may lead to difficulties in the identification process: low signal-to-noise ratio or the presence of very close modes.

3.4.2 Identification technique in the time domain

After proposing methods in the frequency domain, the most widely used identification method in the *time domain* will be proposed below: ***Stochastic Subspace Identification (SSI) method***. It is a parametric technique in which the modal identification of parameters is performed based on the *discrete-time state-space* representation (see eq. 3.65), and on the identification of the system matrix A, which as extensively demonstrated, contains all the dynamic characteristics of the system under investigation.
In OMA applications, there are two SSI subspace algorithms: *Covariance-driven Stochastic Subspace Identification (SSI-Cov)* [27, 42], based on the construction of the correlation matrix, and *Data-driven Stochastic Subspace Identification (SSI-Data)* [44], based on the projection of the recorded response time series.

3.4.2.1 Covariance-driven Stochastic Subspace Identification (SSI-Cov)

The ***Covariance-driven Stochastic Subspace Identification (SSI-Cov)*** method identifies a *stochastic state-space model* to capture the behaviour of the structure under investigation, starting from the output responses collected on the structure and defining the *correlation matrix* (under the assumption of excitation with *white noise* and *linear time-invariant* properties of the system). To achieve this, the system matrix A, the output matrix C and the model order n are estimated from the output responses [42, 61]. In this case, it is possible to use covariance functions between only a few pre-selected output $references$ (l) instead of all available channels (r). The choice of reference channels depends on the possibility of having redundant information provided by the sensors themselves.

In the case of dynamic tests performed in a "$multi-setup$" configuration, the structural responses in the instrumented DOFs are measured at different times. Some of these DOF, however, must be measured in all setups. Consequently, these become the so-called *reference sensors* (channels). Therefore, for each instant of acquisition k, it is necessary to define: y_k^{ref}, column vector containing the accelerations measured in l reference DOF, and y_k, column vector containing the response measured in all r instrumented DOFs.

The first step consists of defining the *covariance matrix* of the output $y(t)$. In discrete time, the output covariance matrix can be written as reported in eq. 3.100 returning it to the reference channels as expressed in eq. 3.101:

$$R_i = E[y_{k+i} \cdot y_k^T] \tag{3.100}$$

$$R_i = E[y_{k+i} \cdot y_k^{ref^T}] \tag{3.101}$$

Eq. 3.102 represents the *Toeplitz matrix* in which the correlation functions are organized into [$n_0 i$-by-$n_r i$] blocks (n_0 is the number of the selected outputs and n_r corresponds to all channels). These functions are evaluated for positive time-lags varying its value from $l\Delta(t)$ to $(2i-l)\Delta(t)$ represented by $R_1^r ef$ to

R^{ref}_{2i-1}.

$$T^{ref}_{1|i} = \begin{bmatrix} R^{ref}_{i} & R^{ref}_{i-1} & \cdots & R^{ref}_{1} \\ R^{ref}_{i+1} & R^{ref}_{i} & \cdots & R^{ref}_{2} \\ \vdots & \vdots & \ddots & \vdots \\ R^{ref}_{2i-1} & R^{ref}_{2i-2} & \cdots & R^{ref}_{i} \end{bmatrix} \tag{3.102}$$

This Toeplitz matrix can be re-written, using the factorization property, as:

$$T^{ref}_{1|i} = \begin{bmatrix} CA^{i-1}G^{ref} & CA^{i-2}G^{ref} & \cdots & CA^{0}G^{ref} \\ CA^{i}G^{ref} & CA^{i-1}G^{ref} & \cdots & CA^{1}G^{ref} \\ \vdots & \vdots & \ddots & \vdots \\ CA^{2i-2}G^{ref} & CA^{2i-3}G^{ref} & \cdots & CA^{i-1}G^{ref} \end{bmatrix} \tag{3.103}$$

Since the first term of the covariance block R^{ref}_1 contains all information about the system's dynamics, it can be seen from eq. 3.103 that the system information defined by $T^{ref}_{1|i}$ might seem redundant. However, the single block alone is not sufficient to solve the identification problem, so Toeplitz matrix is decomposed into the following matrices:

$$T_i = \begin{bmatrix} C \\ C \cdot A \\ \cdots \\ C \cdot A^{i-1} \end{bmatrix} \cdot [A^{i-1} \cdot G^{ref} \qquad \cdots \qquad A \cdot G^{ref} \qquad G^{ref}] = O_i \cdot \Gamma^{ref}_i \tag{3.104}$$

O_i is the *observability matrix*, consisting of a column of i blocks of dimension [n_0-by-n_r]. Γ^{ref}_i is the *controllability matrix*, consisting of a row of i blocks of dimension [n_r-by-n_r].

Computationally, the factorisation of the Toeplitz matrix can be performed with the SVD algorithm, as shown below:

$$T_i = U \cdot S \cdot V^T = [U_1 \qquad U_2] \cdot \begin{bmatrix} S_1 & 0 \\ 0 & 0 \end{bmatrix} \cdot \begin{bmatrix} V_1^T \\ V_2^T \end{bmatrix} = U_1 \cdot S_1 \cdot V_1^T \tag{3.105}$$

For clarity, the matrices U and V are orthonormal matrices and S is a diagonal matrix composed by positive SVs in descending order.

If eq. 3.104 and eq. 3.105 are related, turns out that the observability and controllability matrices can be obtained by dividing the SVD outputs into two

parts:

$$\begin{aligned} O_i &= U_1 \cdot S_1^{1/2} \\ \Gamma_i &= S_1^{1/2} \cdot V_1^T \end{aligned} \tag{3.106}$$

Considering the structure of the matrices just presented, after extracting them, the identification of the model is performed through the matrices A and C. The latter can be extracted from the first n_0 rows of the observability matrix O_i. The matrix A, on the other hand, is obtained by solving the least squares problem expressed as:

$$\begin{bmatrix} C \\ CA \\ \cdots \\ CA^{i-2} \end{bmatrix} \cdot A = \begin{bmatrix} CA \\ CA^2 \\ \cdots \\ CA^{i-1} \end{bmatrix} \Leftrightarrow \bar{O} \cdot A = \underline{O} \tag{3.107}$$

$$A = \begin{bmatrix} C \\ CA \\ \cdots \\ CA^{i-2} \end{bmatrix}^{\dagger} \cdot \begin{bmatrix} CA \\ CA^2 \\ \cdots \\ CA^{i-1} \end{bmatrix} \Leftrightarrow A = \bar{O}^{\dagger} \cdot \underline{O} \tag{3.108}$$

$$\text{where} \quad \bar{O} = \begin{bmatrix} C \\ CA \\ \cdots \\ CA^{i-2} \end{bmatrix} \quad \text{and} \quad \underline{O} = \begin{bmatrix} CA \\ CA^2 \\ \cdots \\ CA^{i-1} \end{bmatrix} \tag{3.109}$$

$\bar{O}$ contains the first $l \cdot (i-1)$ lines of O_i. $\underline{O}$ contains the last $l \cdot (i-1)$ lines of O_i. $(\bullet)^{\dagger}$ is a symbol that represents the Moore-Penrose pseudo-inverse operational function (used to solve least-squares problems of a system of overdetermined equations by minimising the sum of the squared errors of the individual equations).

Then the modal parameters can be extracted from the A and C matrices by performing the eigenvalue decomposition of the obtained A system matrix as shown here:

$$\lambda_k = \frac{\ln(\mu_k)}{\Delta t} \Rightarrow f_k = \frac{|\lambda_k|}{2\pi}; \qquad \xi_k = -\frac{Re(\lambda_k)}{|\lambda_k|} \tag{3.110}$$

where $|\bullet|$ is the absolute value and $Re(\bullet)$ is the real part value.

Ultimately, the mode shapes ϕ_k are estimated by multiplying the output matrix C and the corresponding eigenvectors ψ_k of the A matrix:

$$V = C\Psi \leftrightarrow \phi_k = C\psi_k \tag{3.111}$$

The matrix A has eigenvectors organised in a [n_0-by-n] dimensional matrix, which contains the columns of the observable components of the mode shapes. Only columns associated with eigenvalues with positive imaginary components are then selected to extract the mode shape. This happens because the solutions of the state-space model are described by complex conjugate couples. Thus, in general, such a model of order n provides $n/2$ possible solutions.

A fundamental step in the whole method is to define a reasonably correct the model order for the state-space. This is not a matter of course. Considerations in regard to this aspect are postponed to the next chapter, in which we aim to present critically and in a sufficiently clear manner, the problems that exist and the possibilities present today to overcome them.

3.4.2.2 Data-driven Stochastic Subspace Identification (SSI-Data)

The second algorithm of the SSI method is the ***Data-driven Stochastic Subspace Identification (SSI-Data)*** [44, 62–64]. Through it, it is possible to estimate the state-space model directly with the acquired response time series. The construction of the covariance matrix of the outputs is avoided, being replaced by the projection of the row space of the "future" outputs into the row space of the "past" outputs after arranging them in the *Hankel matrix*.

To demonstrate the justified use of this method, the main concepts of the *non-stationary Kalman filter* are briefly described. In general, the main steps in the development of this technique can be summarised as follows: initial organisation of the collected responses in the Hankel matrix, subsequent estimation of the observability matrix at two consecutive time instants, and finally extraction of the modal parameters after defining the system matrix A and output matrix C.

Kalman Filter

Only the main concepts relating to the Kalman filter will be presented here, with reference to the implementation of the SSI-Data method, as it is an im-

portant part of the development of this method, but it will be stopped at the surface, as an in-depth discussion would be too complex.
In general, it can be said that the objective of the non-stationary Kalman filter is to provide an optimal estimate of the state vector x_{k+1} using the responses of the outputs contained in the A and C matrices and the statistical properties of the R_0 and G matrices. The estimation of this vector is obtained by applying the expressions of eq. 3.112 recursively considering the observation of the outputs at instant k, the initial state estimate $\hat{x}_0 = 0$ and the initial covariance of the state estimates $P_0 = E[\hat{x}_k \quad \hat{x}_k^T] = 0$

$$\begin{gathered}\hat{x}_{k+1} = A \cdot \hat{x}_k + K_k \cdot (y_k - C \cdot \hat{x}_k) \\ K_k = (G - A \cdot P_k \cdot C^T) \cdot (R_0 - C \cdot P_k \cdot C^T)^{-1} \\ P_{k+1} = A \cdot P \cdot A^T + (G - A \cdot P_k \cdot C^T) \cdot (R_0 - C \cdot P_k \cdot C^T)^{-1} \cdot (G - A \cdot P_k \cdot C^T)^T\end{gathered} \tag{3.112}$$

where K is the *Kalman filter gain matrix* and P is the *Kalman state covariance matrix* [44, 65, 66].

The estimates of the *Kalman filter state vectors* $\hat{x}_i$ can then be arranged to form the of *Kalman filter states sequence* $\hat{X}_i$ as:

$$\hat{X}_i = (\hat{x}_i \quad \hat{x}_i + 1 \quad \cdots \quad \hat{x}_i + N + 1) \quad \in \mathbb{R}^{nxN} \tag{3.113}$$

It is possible to rewrite the sequence as a linear combination of the past output measurements. It is generated by a bank of non-stationary Kalman filters working in parallel on each column of the block Hankel matrix of past outputs Y_p. Consequently, the Kalman filter bank can be determined directly from the output data.

Factorization and Projection matrix

As a first step, the data reduction and smoothing procedures used to divide the experimental signals into "past" and "future" parts are explained. As is known, only *discrete samples* of the time signals y_k ($k = 0, 1, ...N$ with $N \to \infty$) are available in the experimental data. These can be expressed as a matrix of

samples:

$$y_k = [y_m^n] = \begin{bmatrix} y_1^n \\ y_2^n \\ \vdots \\ y_l^n \end{bmatrix} = \begin{bmatrix} y_1^0 & y_1^1 & \cdots & y_1^N \\ y_2^0 & y_2^1 & \cdots & y_2^N \\ \vdots & \vdots & \ddots & \vdots \\ y_l^0 & y_l^1 & \cdots & y_l^N \end{bmatrix} \tag{3.114}$$

where y_m^n refers the n^{th} $(n = 0, 1, 2 \ldots N)$ samples points from the m^{th} $(m = 1, 2 \ldots l)$ available sensor. Once the data are organized in this way, the Hankel matrix can be construct. It is a constant matrix along its anti-diagonal elements and with $[2i$-by-$N]$ dimension. $2i$ defines the number of the block-rows and N is the number of the columns.

Statistically the number of columns should be $N \to \infty$, but in practice this value is chosen in order to use all available data in the projection phase. It is set as $N = j - (2i - 1) \to j - 2i + 1$ where j is the number of all sampling points of the collected response. Nevertheless, since l defines the number of available channels, the size of the Hankel matrix becomes $2ilN$, so the matrix itself can be subdivided into: "past" Y_p and "future" Y_f:

$$H_{0|2i-1} = \frac{1}{\sqrt{N^*}} \left[\begin{array}{c} y_0 \\ y_1 \\ \vdots \\ y_{i-1} \\ \hline y_i \\ y_{i+1} \\ \vdots \\ y_{2i-1} \end{array}\right] = \frac{1}{\sqrt{N^*}} \left[\begin{array}{cccc} y_0 & y_1 & \cdots & y_{N-1} \\ y_1 & y_2 & \cdots & y_N \\ \vdots & \vdots & \ddots & \vdots \\ y_{i-1} & y_i & \cdots & y_{i+N-2} \\ \hline y_i & y_{i+1} & \cdots & y_{i+N-1} \\ y_{i+1} & y_{i+2} & \cdots & y_{i+N} \\ \vdots & \vdots & \ddots & \vdots \\ y_{2i-1} & y_{2i} & \cdots & y_{2i+N-2} \end{array}\right] = \tag{3.115}$$

$$= \left[\frac{Y_{0|i-1}}{Y_{i|2i-1}}\right] = \left[\frac{Y_p}{Y_f}\right]$$

The subscripts of $(0|i-1)$ and $(i|2i-1)$ indicate the first and last block-element in the first column of the H matrix used to define the past and future matrices dimension.

The next step is the division obtained by omitting the first block row from the "future" matrix $Y_{0|2i-1}$ and adding it as the last in the "past" matrix $Y_{0|i}$, as

shown:

$$H_{0|2i-1} = \frac{1}{\sqrt{N^*}} \left[\begin{array}{c} y_0 \\ y_1 \\ \vdots \\ y_i \\ \hline y_{i+1} \\ y_{i+1} \\ \vdots \\ y_{2i-1} \end{array}\right] = \frac{1}{\sqrt{N^*}} \left[\begin{array}{cccc} y_0 & y_1 & \cdots & y_{N-1} \\ y_1 & y_2 & \cdots & y_N \\ \vdots & \vdots & \ddots & \vdots \\ y_i & y_{i+2} & \cdots & y_{i+N-1} \\ \hline y_{i+1} & y_{i+2} & \cdots & y_{i+N} \\ y_{i+2} & y_{i+3} & \cdots & y_{i+N+1} \\ \vdots & \vdots & \ddots & \vdots \\ y_{2i-1} & y_{2i} & \cdots & y_{2i+N-2} \end{array}\right] = \tag{3.116}$$

$$= \left[\frac{Y_{0|i}}{Y_{i+1|2i-1}}\right] = \left[\frac{Y_p^+}{Y_f^-}\right]$$

In this way, the system matrices of the adopted state-space model can be estimated. Once the data are well organised, proceed with the projection of the space of future output rows into the space of past output rows, which is useful because it preserves all the information from the past that is useful for predicting the future:

$$P_i = \left[\frac{Y_{i|2i-1}}{Y_{0|i-1}}\right] = \frac{Y_f}{Y_p} = Y_f Y_p^T (Y_p Y_p^T)^\dagger Y_p \tag{3.117}$$

$Y_{i|2i-1}$ and $Y_{0|i-1}$ are the block matrices containing future and past outputs, respectively.

The notions of projection and covariance are closely related (as shown by the equation above), as both aim to remove noise. The block Toeplitz matrices $Y_f Y_p^T$ and $Y_p Y_p^T$ contain the covariance between the output signals. Furthermore, the projection matrix can be expressed as the product of the extended observability matrix O_i and the sequence of states of the Kalman filter $\hat{X}_i$:

$$P_i = O_i \cdot \hat{X}_i \tag{3.118}$$

This relation is based on the main theorem of the SSI method [44]. It should be underlined that eq. 3.117 is only a definition and that the projection cannot be calculated directly. For practical applications, this is done using the $QR -$

factorisation of the H matrix [42].

$$H_{0|2i-1} = \left[\frac{Y_p}{Y_f}\right] = R \cdot Q^T \tag{3.119}$$

$QR - factorisation$ is in essence a compression of the data: the H matrix, consisting of a very large number of columns, is decomposed and compressed into a smaller triangular R matrix that contains all the information about the system:

$$H_{0|2i-1} = \begin{array}{c} \\ li \\ l \\ l(i-1) \end{array} \begin{array}{c} \begin{array}{ccc} li & l & l(i-1) \end{array} \\ \begin{bmatrix} R_{11} & 0 & 0 \\ R_{21} & R_{22} & 0 \\ R_{31} & R_{32} & R_{33} \end{bmatrix} \end{array} \begin{array}{c} J \\ \begin{bmatrix} Q_1^T \\ Q_2^T \\ Q_3^T \end{bmatrix} \end{array} \begin{array}{c} \\ li \\ l \\ l(i-1) \end{array} \tag{3.120}$$

Substituting the eq. 3.120 in eq. 3.118 makes the projection matrix P_i expressed as follows:

$$P_i = \begin{pmatrix} R_{21} \\ R_{31} \end{pmatrix} \cdot Q_1^T \tag{3.121}$$

Similarity, the subsequent *Projection matrix* P_{i-1} is obtained as:

$$P_{i-1} = \begin{pmatrix} R_{31} & R_{32} \end{pmatrix} \cdot \begin{pmatrix} Q_1^T \\ Q_2^T \end{pmatrix} \tag{3.122}$$

The *factorization property* decrease considerably the computational cost. Therefore, once the projection matrices P_i and P_{i-1} are available, the system matrices and the modal parameters can be easily estimated. Taking up [44], the main theorem of the SSI methods states that the projection P_i can be factorized as:

$$P_i = \begin{bmatrix} C \\ CA \\ \vdots \\ CA^{i-1} \end{bmatrix} \cdot \begin{bmatrix} \hat{x}_i & \hat{x}_{i+1} & \cdots \hat{x}_{i+N+1} \end{bmatrix} = O_i \cdot \hat{X}_i \tag{3.123}$$

and the SVD of the obtained P_i is:

$$P_i = U \cdot S \cdot V^T = \begin{bmatrix} U_1 & U_2 \end{bmatrix} \cdot \begin{bmatrix} S_1 & 0 \\ 0 & 0 \end{bmatrix} \cdot \begin{bmatrix} V_1^T \\ V_2^T \end{bmatrix} = U_1 \cdot S_1 \cdot V_1^T \tag{3.124}$$

where P_i has order n: O_i is a matrix with n columns, X_i is a matrix with n

rows and consequently the number of different non-zero values resulting from its decomposition is also equal to n. This also represents the order of the model and defines the size of the matrix A. Therefore, comparing eq. 3.123 and 3.124, the two matrices can be factored as follows:

$$\begin{aligned} O_i &= U_1 \cdot S_1^{1/2} \\ \dot{X}_i &= O_i^{\dagger} \cdot P_i \end{aligned} \tag{3.125}$$

With the aim of identifying the A and C matrices, a further projection is made by moving a block row down from "past" to "future" outputs of the Hankel matrix:

$$P_{i-1} = \frac{Y_f^-}{Y_p^+} = O_{i-1} \cdot \dot{X}_{i+1} \tag{3.126}$$

And it can be decomposed to the form:

$$P_{i-1} = \begin{bmatrix} C \\ CA \\ \vdots \\ CA^{i-1} \end{bmatrix} \cdot [\hat{x}_i \quad \hat{x}_{i+1} \quad \cdots \hat{x}_{i+N+1}] = O_{i-1} \cdot \hat{X}_{i+1} \tag{3.127}$$

At this point, the Kalman filter state $\hat{X}_{i+1}$ is obtained as:

$$\hat{X}_{i+1} = O_{i-1}^{\dagger} \cdot P_{i-1} \tag{3.128}$$

Using the sequence of state vectors, calculated with only the output data, a system with more equations than unknown variables is obtained. The matrices of the system can be determined from the following overdetermined set of linear equations, obtained by superposition of the state space model for time instants i to $i + N - 1$:

$$\begin{bmatrix} \hat{X}_{i+1} \\ Y_{i|i} \end{bmatrix} = \begin{bmatrix} A \\ C \end{bmatrix} \hat{X}_i + \begin{bmatrix} W_i \\ V_i \end{bmatrix} \tag{3.129}$$

$Y_{i|i}$ is a Hankel matrix with only one block row, instead, W_i and V_i can be treated as the residuals of an optimization problem. Given that the sequences of Kalman states and outputs are known and the residuals are uncorrelated with $\dot{X}_i$, then the set of equations for A and C can be solved by least squares:

$$\begin{bmatrix} A \\ C \end{bmatrix} = \begin{bmatrix} \hat{X}_{i+1} \\ Y_{i|i} \end{bmatrix} \hat{X}_i^{\dagger} \tag{3.130}$$

Based on the outputs, the system order n and the system matrices A and C have been identified, so the identification problem is solved theoretically. Natural frequencies f_k and mode shapes ϕ_k can be obtained in the same way as for SSI-Cov.

Useful variants exist for extracting modal parameters from time series. In the most general formulation of SSI-Data, matrix weighting is performed: two weighting matrices W_1 and W_2 are considered, which are multiplied by the value of the data to be decomposed into singular values.

$$\bar{P}_i = W_1 \cdot P_i \cdot W_2 \tag{3.131}$$

This weighting operation results in a transformation of the co-ordinates of the state vectors, so that similar arrays of patterns are checked, which obviously lead to identical process identification results.

Chapter 4

SHM based on OMA

4.1 Introduction

In the previous chapters, concepts were introduced regarding the use of the SHM strategy based on vibration monitoring and OMA, i.e. the identification of modal parameters from output-only measurements. All that has been described amply demonstrates the usefulness and thus the justified popularity of this approach.
To repeat, SHM is a multidisciplinary process involving:

- repeated or continuous measurement of the response of a structural system through appropriate sensors;
- extraction from the measured data of characteristics representative of the state of health
- analysis of these characteristics to detect novelty or abnormal changes.

The motivations behind the choice of using vibration-based dynamic monitoring are varied. The main ones, already discussed, can be grouped into:

1. natural ageing of existing structures and infrastructure;
2. conservation of cultural heritage;
3. increasing complexity of new constructions, therefore control during construction to ensure optimisation of work;
4. possibility of assessing the health of the structure from the analysis of its dynamic response under operating conditions and with only the presence of environmental excitations.

All these possibilities are of course given by the technological progress that is always in progress, which today allows the installation of low-cost and highly efficient sensors.

In this context, we would like to focus on the usefulness of monitoring the structural response under operating conditions collected and analysed continuously. The implementation of *continuous dynamic monitoring* has had the consequence of stimulating the development of procedures that efficiently process data to control the evolution of modal parameters over time.
Having new and more evolved tools capable of automatically identifying the modal characteristics of a structure is equivalent to having several experts at one's disposal who individually can: check the data during recording, correct and clean them in the most optimal way, process them with the most appropriate identification techniques, and finally read and interpret them in order to act accordingly.

In practical application, continuous monitoring involves the definition of a set of basic modal parameters, which are used as reference characteristics for comparison with the parameters collected subsequently. In this sense, the basic parameters allow a *tracking process* to be set up over time.
The parameter most commonly used as a reference is the *natural frequency*. Although it is a very explicative dynamic characteristic when it comes to changes in structural response, it is subject to the influence of external factors, such as *environmental effects* (temperature, humidity and wind). Therefore, the objective after monitoring operations is to remove environmental and/or operational effects. Various approaches have currently been implemented and applied, which we will briefly discuss below. The ultimate goal of this discussion is the *damage identification*. This is still an evolving field because it is very impregnative.

4.2 Automated OMA algorithms

As anticipated, the diffusion of long-term dynamic monitoring systems for structural health assessment and the implementation of algorithms for damage detection have certainly directed research towards automated modal identification procedures only at the output [9, 67–71]

The most widely used method among those described in the previous chapter is definitely the SSI. This is due to the fact that it can accurately identify even weakly excited and neighbouring modes. It also lends itself particularly well to automation.
Several strategies have been developed for the interpretation of SSI outputs [61] taking into account both the influence of the maximum order of the stochastic model n, and the *time-lag index* (used to define the number of rows of the output block to construct the Toeplitz block matrix in SSI-Cov, or the size of the Hankel matrix of the block in SSI-Data).

4.2.1 Stabilization diagram

The automatization of SSI algorithms involves the interpretation of the so-called ***stabilization diagram***. It was first introduced by [27, 42], and is used in conjunction with any parametric procedure (SSI-Cov and SSI-Data).

Summarising what has already been presented, after defining the state space model, it is possible to extract the modal parameters of the system from the matrices A and C: the eigenvalues of A, μ_k (poles of the discrete-time model of the state space) are related to the λ_k (poles of the continuous-time model). Thus, the natural frequencies (f_k) and modal damping ratios (ξ_k) are obtained from the poles with positive imaginary component, as given in eq. 3.110.
It may be added that the product of the matrix C by the matrix containing the eigenvalues of A returns a matrix where the columns contain the observable components of the mode shapes. Finally, given the presence of the complex conjugate couple, the columns associated with the eigenvalues with positive imaginary part are selected and consequently the state space model of order n provides modal parameters for $n/2$ modes.

In practice, the model that best fits the dynamic response of the structure cannot be identified a priori due to a number of "interferences" that are difficult to control. Therefore the same state-space model matrices derived, and the resulting modal parameters, must also be considered as estimates.
The SVD of the Toeplitz matrix itself does not allow an a priori decision on model order. Furthermore, there are always residual SVDs associated with the highest modes (which theoretically should instead be zero) caused by the

inaccuracy of the measurement process, noise content or the manifestation of non-linear effects. Various practical applications on real structures have also shown that it is not possible to establish even an interval between consecutive singular values that allows reasonable estimates of the model order to represent the correct dynamic behaviour of the system.
To overcome this obstacle, the strategy consists in constructing several models, with increasing orders (within a previously fixed interval in which the maximum is considered to be twice the number of physical modes expected to be found according to the type of structure), and subsequently, the "best" model (and hence model order) is chosen to estimate the correct modal parameters.

It is right to highlight that the use of very high model orders may lead to the identification of *numerical modes* that have no physical meaning (also called *noise* or *spurious modes*), and which are mainly related to the noise content in the collected recordings.
In this context, it is necessary to be able to separate physical and spurious modes in order to not compromise the reliability of the results. The creation and interpretation of the *stabilization diagram* also helps with this.
The figure below shows more clearly what a stabilization diagram looks like.

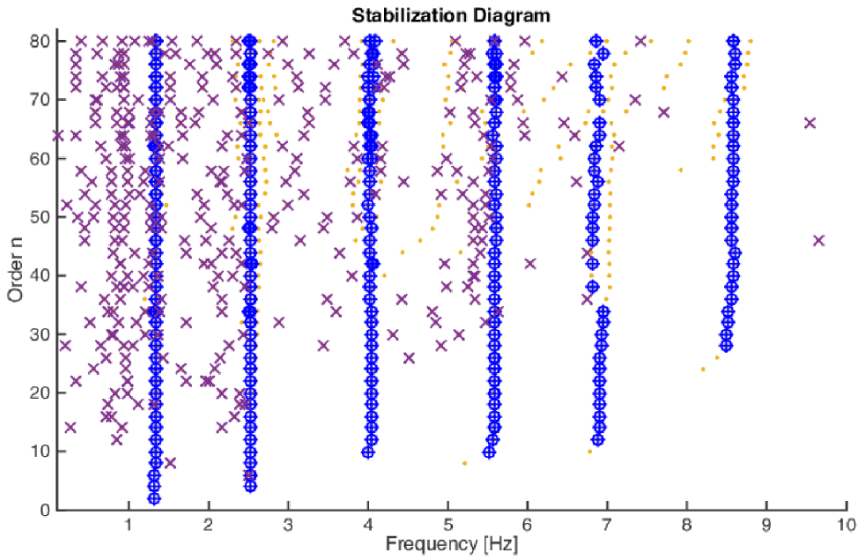

Figure 4.1: *Example of stabilization diagram: stable poles in blue points and unstable poles in purple crosses*

It is essentially a graphical tool in which the modal estimates (natural frequencies) provided by all the models defined for each increasing order are shown, and observation of this diagram makes it possible to identify *stable alignments*.

These alignments consist of the so-called *stable poles*, i.e. those that maintain consistency in terms of modal parameters for each order and thus, in simple terms, always appear.
In contrast, poles that are scattered across the diagram and only appear in certain models are classified as *spurious* and should not be considered when estimating modal parameters.

The most widely used criteria for removing spurious poles from stabilisation diagrams are presented in the following pragraphs.

4.2.2 Single criterion check and Clustering approaches

The separation of physical poles from spurious poles has been discussed extensively in the literature. The ultimate aim is, as mentioned, to obtain a better definition of what are the modes that really represent the behaviour of a structure.
Without going into detail, reference can be made to:

1. *Consistent Mode Indicator*, applicable in the context of input-output tests [72].

2. *Maximum likelihood* in the frequency domain for automation of identification, while estimation of physical modes is based on the uncertainty of such estimates [73].

3. *Component Associated with the modal vector* (modes with high complexity are assimilated to spurious modes) [74].

After removing the spurious poles from the stabilization diagram, the set of modal estimates for the same model must be identified. Manually, the model order that best represents the dynamic characteristics in terms of modal parameters is chosen. It is obvious that this approach is not the best: an expert is needed to correctly identify the right order, the choice of modal parameters to be considered depends on the sensitivity of the operator (e.g. wrongly chosen noise modes) and it is not feasible to implement such a constant interaction as required in the field of continuous monitoring.
Consequently, it is more correct to develop an automated procedure to interpret the data on the stabilization diagram. If the aim is to group poles with the same characteristics, the best approach is to apply ***clustering algorithms***.

Again, numerous application suggestions can be found in the literature, depending on the type of data to be investigated and thus *clustered*.
These have demonstrated the usefulness of clustering procedures in managing the output produced by parametric identification techniques (for estimates in terms of natural frequencies, mode shapes and damping ratios). As proposed in [68], the most widely used strategy is based on clustering stable modes by measuring the "distance" between all pairs of estimated poles. This is possible in practice because stable poles are found clustered in areas of high density. In contrast, spurious modes exhibit greater dispersion. Based on this assumption, a cut-off level, a threshold, is defined that can separate the clusters. Again, as with the order of model n, it is not possible to know the value of the cut-off level a priori, so it is user-defined and closely related to the number of expected modes.

In the case where slender structures are being considered in which the environmental input is therefore capable of producing visible resonance frequencies, a further simplification can be made so as to avoid the manual introduction of many parameters in order to eliminate spurious modes from the diagram. In this case, a quick analysis can be performed to identify the number of main modes expected (corresponding to the peaks of the first singular value) and then define the number of maximum clusters available. Despite the usefulness of this strategy, care must be taken in cases where the structure is instrumented with a limited number of sensors and/or in the case of a low signal-to-noise ratio.

In well-known commercial software used for dynamic tests and OMA analyses, clustering approaches are implemented using these tolerance values in order to control the variability of modal parameters in various models. It is certainly an effective approach and involves a control performed on the variation of natural frequencies, damping ratios and mode shapes. The comparison between the various estimates is performed using the MAC index, already defined in the previous chapter. The disadvantage is obviously related to the necessary interaction of a user who has to set the tolerance values.

4.3 Environmental effects on modal parameters

With the constant development of strategies in the field of SHM, the detection, localisation and automatic evaluation of damage on the structure under investigation has been of increasing interest. In general, it can be said that a damaged structure shows a loss of stiffness. This situation leads to a change that can no longer be recove
red and thus to a permanent change in the dynamic behaviour of the structure. It has already been introduced how normally the control of the possible presence of damage is carried out by monitoring changes in modal parameters (natural frequencies, mode shapes and damping) over time. These characteristics are very sensitive not only to internal changes in the structure, but also to external factors: *environmental and operational conditions* (temperature, humidity, wind, traffic loads, etc.). These influences may hide changes due to actual damage.
Numerous references can be found in the literature in which the effects of external factors on modal parameters are demonstrated:

- *EJ Cross et al.* [75] identify reductions in modal frequencies of 2-3% due to changes in mass and traffic loads;
- *Charles R Farrar et al.* [76] show significant daily fluctuations of the first frequency due to temperature fluctuation (5% change);
- *Bart Peeters and Guido De Roeck* [77] illustrate the same type of variation for the first two natural frequencies of the structure under control.

The first step is the knowledge of the correlations that exist between these factors and the monitored features. The first class of possible algorithms are ***input-output*** models, which reproduce the relationship between external variables and the monitored dynamic characteristics. Main disadvantage: the external factors to be measured must be chosen, and these are not always available or are difficult to interpret.
Other methods are ***output-only*** ones, in which the measurement of the external factor (i.e. the input) is not necessary. In this case, the main approach proposed in the literature is the decomposition of the covariance matrix of dynamic characteristics, which are monitored over a long period with changing external conditions but which are not measured [78–80]. Or there are applications based on the direct decomposition of time series with extracted features or the use of neural networks [81, 82].

4.3.1 Input-output methods

Input-output methods aim to define a *linear regression relationship* between the investigated characteristics and external factors. The latter, as just mentioned, are constantly measured. Depending on how the input variables influence the characteristics, these methods can be divided into two categories:

1. *static regression*: the regression relationship is only defined by means of simultaneously collected data;

2. *dynamic regression*: the regression relation also takes into account the influence of external factors measured at earlier instants of time.

For both categories, different data sets must be used. Once the influence of each factor on the resulting characteristic is understood, the parameters governing the method are considered to be correctly calibrated. The model defined in this way, when the measured external factors (static method) and also the output at previous instants of time (dynamic method) are known, can be used to estimate the controlled characteristics and detect any changes.

Multiple Regression Analysis

Multiple Regression Analysis (MRA) is the simplest statistical technique available and used to analyse the relationship between a single dependent variable and one or more *independent variables* (*predictors*). The aim is to predict the single dependent value using independent variables whose values are known in advance.
The resulting relationship (model) is initially used to investigate the influence of the predictor (input) and the dependent variable (output), subsequently to predict future values of the output when the input is known. Each predictor is weighted by the regression analysis procedure to ensure maximum prediction from the set of independent variables.

A *simple regression* problem is expressed as:

$$y = \theta_0 + \theta_1 x + \varepsilon \tag{4.1}$$

y is the *dependent variable* (output), x is the *predictor* (input), θ_0 is the *intercept* and θ_1 is the *regression coefficient*, which are the parameters of the regression relation. ε is the *prediction error* (or residual), i.e. the difference

between the actual and predicted values of the dependent variable.

If curvilinear effects are to be modelled, transformations of an independent variable can be adopted that add a non-linear component for each additional variable:

$$y = \theta_0 + \theta_1 x + \theta_2 x^2 + \varepsilon \tag{4.2}$$

Meanwhile, when two or more independent variables are used to predict the dependent variable, the problem becomes as *multiple regression*:

$$y = \theta_0 + \theta_1 x_1 + \theta_2 x_2 + \cdots + \theta_n x_n + \varepsilon \tag{4.3}$$

Equations 4.1 and 4.3 reproduce a linear dependence between the predictors and the dependent variable. If two or more independent variables are involved, *multivariate polynomials* can be defined as:

$$y = X\theta + \varepsilon \tag{4.4}$$

where:

- y is a [n-by-1] column vector that contains the n measures (y_k) of the dependent variable (y);
- X is a [n-by-p] matrix connecting n dependent values of the corresponding p selected predictors;
- θ is a [p-by-1] column vector formed by the p parameters weighting the contribution of each independent variable;
- ε is the [n-by-1] column vector of the prediction errors (ε_k) that account for measurement errors of the y element and for the effects of other variables not explicitly considered in the model.

ε has the following properties:

$$\begin{aligned} E[\varepsilon] &= 0 \\ Cov[\varepsilon] = [\varepsilon \cdot \varepsilon^T] &= \sigma_\varepsilon^2 \cdot I \end{aligned} \tag{4.5}$$

$E[\bullet]$ is the expected value operator, and $[\bullet]^T$ means transpose and I represent the *identity matrix* with dimension [n-by-n]. Eq. 4.5 indicates that the mean value of ε is zero, that the errors are independent and also their valiance (σ_ε^2)

is constant.

In order to accurately reproduce the experimental estimates of the dependent variables and simulate their future values, it is necessary to correctly select the input values, independent, and then define the θ_k parameters. These can be estimated using the *Least Squares (LS)* method, minimising the sum of squared errors:

$$\hat{\theta} = (X^T X)^{-1} X^T y \tag{4.6}$$

It is common practice, in the identification of systems, to normalise the input and output data. In this way, the origin of the x and y axes lies in the "centre of gravity" of the data points and the slope of the regression line corresponds to the correlation coefficient [83]. To achieve this, the mean value from each measure x_k and y_k is removed and the results are divided by the standard deviation of the variable:

$$\tilde{x}_k = \frac{x_k - \bar{x}}{\sigma_x} \qquad \tilde{y}_k = \frac{y_k - \bar{y}}{\sigma_y} \tag{4.7}$$

As the LS method minimizes the sum of the squares of the equation errors, a first quality criterion is the value of the *Loss Function (LF)*:

$$LF = \frac{1}{N} \sum_{k=1}^{N} \varepsilon_k^2 \tag{4.8}$$

N is the total number of samples. The prediction errors are obtained as:

$$\varepsilon = y - \hat{y} \tag{4.9}$$

where y and $\hat{y}$ represents the experimental and estimated values of the output variable.

To test the quality of the model, there is another important indicator, the *coefficient of determination* R^2 [84]:

$$R^2 = 1 - \frac{\sum_{k=1}^{N} \hat{\varepsilon_k}^2}{\sum_{k=1}^{N} (y_k - \bar{y})^2} = \frac{\sum_{k=1}^{N} (\hat{y}_k - \bar{y})^2}{\sum_{k=1}^{N} (y_k - \bar{y})^2} \tag{4.10}$$

R^2 is defined by the value of the ratio between two variances. Thus it gives the percentage of the total variation of the experimental output y_k explained by

the predictors. We can distinguish two cases: the selected independent variables have no influence on the output if R^2 tends to zero, the variation of y_k is explained by the predictors if R^2 tends to one.
In the context of SHM, temperatures measured on the structure and the amplitude of excitation (i.e. induced by traffic loads) are usually considered as predictors. This is because they have a significant influence on natural frequency fluctuations.

This just described is the classic static regression model that only establishes a relationship between simultaneously measured data. In the case of applications with common dynamic processes, the use of *dynamic regression* methods is indicated. In fact, they make it possible to take into account the influence of inputs measured at previous instants of time.
A dynamic regression relationship is established between the dependent variable at time k and the values of a single predictor at current time k and at $(p-1)$ previous time instants. Therefore, eq. 4.1 can be rewritten as:

$$y = \theta_0 + \theta_1 x_k + \theta_2 x_{k-1} + \cdots + \theta_p x_{k-(p-1)} + \varepsilon_k \tag{4.11}$$

where X matrix becames:

$$X = \begin{bmatrix} x_1 & \cdots & x_{1-(p-1)} \\ x_2 & \cdots & x_{2-(p-1)} \\ \vdots & \ddots & \vdots \\ x_n & \cdots & x_{n-(p-1)} \end{bmatrix} \tag{4.12}$$

The MRA is the method used in this thesis work to remove the environmental effects on the modal parameters identified during the continuous monitoring.

ARX models

ARX models [62] are a widely used method for estimating output system characteristics from independent variables. They consist of an Auto-Regressive output part and an eXogeneous input part. Given an output variable y_k, an input variable x_k, and an error term ε_k, defined at a general time instant k, the equation representing it is expressed as:

$$y_k + a_1 y_{k-1} + \cdots + a_{n_a} y_{k-n_a} = b_1 x_{k-n_k} + b_2 x_{k-n_k} + \cdots + b_{n_b} x_{k-n_k-n_b+1} + \varepsilon_k \tag{4.13}$$

This equation can be generalised to the case of multiple inputs by replacing b_k and x_k with the corresponding row and column vectors.
It can be seen from eq. 4.13 that ARX models are characterised by three orders: autoregressive order n_a (number of past measures of the dependent variable considered), exogenous order n_b (number of previous model inputs considered) and pure time lag between input and output n_k. The first two, determine the number of model parameters: a_i (i=1, ..., n_a), b_j (j=1, ..., n_b). This shows how static regression models are a particular class of ARX models, setting $n_a = 0$, $n_b = 1$, $n_k = 0$ and defining it as ARX010:

$$y_k = b_1 x_k + \varepsilon_k \tag{4.14}$$

that can be rewritten as:

$$a(q)y_k = b(q)x_k + \varepsilon_k \tag{4.15}$$

A new relation is introduced: $q^{-1}y_k = y_{k-1}$.
$a(q)$ and $b(q)$ are two polynomials:

$$\begin{aligned} a(q) &= 1 + a_1 q^{-1} + \cdots + a_{n_a} q^{-n_a} \\ b(q) &= b_1 q^{-n_k} + b_2 q^{-n_k-1} + \cdots + b_{n_b} q^{-n_k-n_b\mp 1} \end{aligned} \tag{4.16}$$

Eq. 4.14 can be transformed to obtain he general expression typically used to define linear input-output models:

$$y_k = H(q,\theta)x_k + W(q,\theta)\varepsilon_k \tag{4.17}$$

θ is the vector that groups the modal parameters. H and W are the transfer function and the noise model. They can be expressed relating eq. 4.15 and eq. 4.17:

$$\begin{aligned} \theta^T &= (a_1 \cdots a_{n_a} \quad b_1 \cdots b_{n_b}) \\ H(q,\theta) &= \frac{b(q)}{a(q)} \qquad W(q,\theta) = \frac{1}{a(q)} \end{aligned} \tag{4.18}$$

Also the parameters of ARX models can be estimated by applying a LS method.

$$y_k = \phi^T \theta + \varepsilon_k \tag{4.19}$$

where ϕ^T is a row vector grouping the past measures of dependent variables and predictors.

Considering N measured values of output and input variable, eq. 4.19 can be rewrites for each of N samples. In conclusion, the ARX can be represented by the same matrix equation derived for the multiple regression analysis by introducing the following vectors:

$$y = \begin{pmatrix} y_1 \\ y_2 \\ \vdots \\ y_N \end{pmatrix} \in \mathbb{R}^N \qquad X = \begin{pmatrix} \phi_1^T \\ \phi_2^T \\ \vdots \\ \phi_N^T \end{pmatrix} \in \mathbb{R}^{Nx(n_a+n_b)} \qquad \varepsilon = \begin{bmatrix} \varepsilon_1 \\ \varepsilon_2 \\ \vdots \\ \varepsilon_N \end{bmatrix} \in \mathbb{R}^N \quad (4.20)$$

The estimates $\hat{\theta}$ of the model parameters are obtained by solving the considered system of equations using the LS method.

4.3.2 Output-only methods

As anticipated, it is not always possible to control and measure external factors that substantially influence modal parameters. Moreover, if continuous dynamic monitoring is considered, these factors must also be measured continuously and this may not always be feasible. Output-only models manage to bypass this problem: knowledge of them is not required.
Two classes of *output-only methods* are described below, although they are not the methods actually used in the development of the thesis work. In this case, the removal of environmental effects on the monitored modal parameters is done by decomposing a covariance or correlation matrix of the temporal variation of structural characteristics over a reference time period (*training period*). The former proposed is the *Principal Component Analysis (PCA)* method, while the latter is the *Factor Analysis (FA)* method.

Principal Component Analysis

Principal Component Analysis (PCA), used over the years by numerous researchers and applied to many real-world cases, also proposing various extensions [7, 61, 79, 80, 84–88], is a multivariate statistical tool that performs a *linear transformation* of data. This takes place from an original coordinate system, in which the data are defined, into a new, less dimensional coordinate

system. This is a method that is useful when it is necessary to reduce the size of the problem: a set of correlated variables is replaced by a smaller set of independent variables, the *Principal Component (PC)s*. Practically, the aim is to find an *orthonormal matrix* T, of dimension [n-by-n] and where $T^T = T^{-1}$ that allows the coordinate transformation as:

$$x = T \cdot y \tag{4.21}$$

y is the vector of n original variables, x is the vector composed by n variables that are independent and T is the transformation matrix that applies a rotation of the original coordinate system.
The transformation allowed by T means that in the set of *PCs* (x) all variables are independent of each other, the covariance matrix of x is diagonal and of full rank, and their variance is arranged in a decreasing manner from x_1 to x_n (this means that the first *PC* is more relevant in explaining the variability of the initial data-set, while the last *PC* are minor variances and can also be ignored).
Eq. 4.21 can therefore be rewritten as:

$$y = T^T \cdot x \tag{4.22}$$

If each variable is ZOH, the covariance matrix Σ_{yy} of y coincides with the correlation matrix of y and can be linked to the diagonal covariance matrix Σ_{xx} of x as follows:

$$\Sigma_{yy} = E[y \cdot y^T] = E[T^T x \cdot x^T T] = T^T \cdot \Sigma_{xx} \cdot T \tag{4.23}$$

The SVD of Σ_{yy} provides the relation:

$$\Sigma_{yy} = U \cdot \Lambda \cdot U^T \tag{4.24}$$

Λ is a diagonal matrix and its components are the elements λ_i, arranged in descending order, corresponding to the eigenvalues of the covariance matrix Σ_{yy}. U, on the other hand, is an orthonormal matrix and its columns correspond to the eigenvector of the covariance matrix Σ_{yy} (reminder: each $j-th$ column is eigenvector corresponding to the $j-th$ eigenvalue of the covariance matrix Σ_{yy}).

Thus, eq. 4.24 can be used to obtain the matrix ($T = U^T$) and the variance

of the component of x from the elements of the diagonal of Λ. Furthermore, since the SVD provides the SV in descending order, the first element of Λ and the variance of X_1 are coincident.

Since the aim of the PCA technique is to reduce the size of the initial problem, only the first p (of the total n) eigenvalues collected in Λ are considered, which are relevant to explain the variance of the original components of y, the matrix Λ can be divided into:

- $\Lambda_1 = diag(\lambda_1, \lambda_2, \cdots, \lambda_p \rightarrow$ diagonal matrix composed of the first p singular values;
- $\Lambda_2 = diag(\lambda_{p+1}, \lambda_{p+2}, \cdots, \lambda_n \rightarrow$ diagonal matrix with the remaining singular values, not relevant.

The choice of p (which should be selected by looking for a gap in the diagram of eigenvalues) is based on the definition of the ratio I:

$$I = \frac{\sum_{i=1}^{p} \lambda_i}{\sum_{i=1}^{n} \lambda_i} \tag{4.25}$$

I defines the percentage of the variability of the original variables y explained by the first p components of x. Then, once the threshold I is set, the value of p can be identified and the set of PCs x_j can be obtained, applying eq. 4.21, through the $\hat{T}$ matrix. This is a reduced T matrix because it is constructed only from the first p columns of U (remembering $T = UT^T$).

Although it can be asserted that, at this point, the problem has been reduced in size, when it comes to structural health monitoring, a further step is performed: the selected $\hat{x}$ components are remapped to the original y space. To do this, the selected PCs are re-transformed into the original co-ordinate system, using the $\hat{T}$ matrix, as follows:

$$\hat{y} = \hat{T}^T \cdot \hat{x} = \hat{T}^T \cdot \hat{T} \cdot y \tag{4.26}$$

If the re-mapped values are removed from the original variables as:

$$\varepsilon = y - \hat{y} \tag{4.27}$$

the obtained *residual features* ε will not be affected by the factors modeled by

the PC. In order to demonstrate the detection of structural anomalies during the normal behaviour of the structure, which could justify the occurrence of damage, post-processing of these new features can be performed.

Principal Component Analysis

Factor Analysis (FA) [84] is also a multivariate statistical tool. It explains the covariance relationship between many variables in terms of a few random quantities, the factors. It can be seen as an extension of PCA (both are based on the decomposition of the covariance matrix), but FA is based on a more elaborate model in which the factors are unobservable.
As already shown, the estimation of observed features (usually natural frequencies) can be defined as:

$$y = f(f_1, f_2, f_3, f_4, \cdots) + \varepsilon \tag{4.28}$$

where:

- y is the vector of n components (extracted natural frequencies);
- f is a function that depends on environmental/operational factors where the various f_i are the specific external factors that are considered (e.g. f_1 temperature, f_2 humidity, f_3 wind, ...);
- ε is a vector that quantifies the influence of these anomalous events on each component of y.

The function f can be decomposed into two mappings:

$$f(f_1, f_2, f_3, f_4, \cdots) = L[NL(f_1, f_2, f_3, f_4, \cdots)] \tag{4.29}$$

a first mapping, which could be non-linear (NL), transforms the p environmental/operational factors into a set of unobservable factors (x) (using e.g. a regression analysis) that are then related to the n estimated, observable characteristics (natural frequencies) by a linear mapping. The relationship can be expressed as:

$$y = L \cdot x + \varepsilon \tag{4.30}$$

L is a [n-by-p] matrix whose elements are designed *factor loadings*, the components of x are the *common factors* and the components of ε are the *specific factors*. It should be highlighted that eq. 4.30 is similar to that used for multi-

variate linear regression, but here the components of x are not measured. The following properties are also assumed for the factorial model:

$$E[y] = E[x] = E[\varepsilon] = 0 \quad E[x \cdot x^T] = I \quad E[\varepsilon \cdot x^T] = 0 \quad E[\varepsilon \cdot \varepsilon^T] = \Psi \tag{4.31}$$

where

$$\Psi = \begin{bmatrix} \psi_1 & 0 & \cdots & 0 \\ 0 & \psi_2 & \cdots & 0 \\ \vdots & \vdots & \ddots & \vdots \\ 0 & 0 & \cdots & \psi_n \end{bmatrix} \tag{4.32}$$

and through these, for the covariance matrix of the observations is the equation:

$$\begin{aligned} \Sigma &= [y \cdot y^T] \\ &= E[(L \cdot x + \varepsilon) \cdot (L \cdot x + \varepsilon)^T] \\ &= E[L \cdot x \cdot x^T \cdot L + L \cdot x \cdot \varepsilon^T + \varepsilon \cdot x^T \cdot L^T + \varepsilon \cdot \varepsilon^T] \\ &= L \cdot E[x \cdot x^T] \cdot L^T + E[\varepsilon \cdot \varepsilon^T] \Leftrightarrow \Sigma = L \cdot L^T + \Psi \end{aligned} \tag{4.33}$$

To define the L matrices, which fit a set of n observations of y, two algorithms are possible: the principal factor method and the maximum likelihood method. Please refer to [84] for further details.

Having established the L and Ψ matrices, common factor estimates (x) (*factor scores*) can be performed with different formulations [84]. The difference lies in the minimisation of the specific factors.
Consider a simple least-squares procedure:

$$\hat{x} = (L \cdot L^T)^{-1} \cdot \hat{L}^T \cdot y = (S_1)^{-1/2} \cdot U_1^T \cdot y \tag{4.34}$$

The resolution (in which the squared errors ε_i^2 are weighted by the inverse of their variances $1/\Psi_i$) gives the following factor scores:

$$\hat{x} = (\hat{L}^T \cdot \hat{\Psi}^{-1} \cdot \hat{L})^{-1} \cdot \hat{L}^T \cdot \hat{\Psi}^{-1} \cdot y \tag{4.35}$$

As mentioned at the beginning, the aim of FA is to identify variables x that are *insensitive* to environmental/operational conditions. Since they are insensitive, they can be used as reference characteristics to perform the subsequent damage detection.

4.4 Detection of structural anomalies

In the field of SHM based on OMA applications, by applying the models presented in the previous paragraphs, it is possible to eliminate environmental and operational effects on modal parameter estimates. Therefore, it can be said that the presence of *anomalies* and *damage* on the structure can be detected by studying the evolution of its characteristics over time without worrying about environmental influence.
To detect the damage, it is possible to explore the trend of the modal parameters in terms of:

1. prediction error ε_k between the experimental estimates and the predicted values of the modal frequencies (after removing external factors);

2. purified experimental frequencies, calculated as:

$$\hat{f}_I = \bar{f}_I + \varepsilon_{ik} \tag{4.36}$$

   where $\bar{f}_i$ is the mean value of the original $i-th$ frequency during the reference period.

4.4.1 Control Charts

The most widely used strategy for damage control is the use of the ***control chart*** [61, 85, 89]. This is a statistical tool and is essentially a graph within which it is easy to recognise the trend of data over time and in which upper and lower *limits* are marked, in which data are defined as *safe*.
Their first possible use sees them involved in monitoring of the stability of a sample of observations, in other words, it is checked if the *control limits* extracted from several available observations are respected.
Another approach sees them involved in defining a *safe control region* to check the quality of future observations. It starts with a *training period*, an interval of time in which it is assumed that the process is under control, meaning that the structure is undamaged. From this period, the control limits are calculated and consequently the control region is defined. At this point, a check is made to determine if each new observation, obtained from the analysis of a collected data set, is within this *safety region*. If an observation is found to be outside the control limits, it means that the structure is exhibiting unusual behaviour that depends on a structural anomaly (e.g. damage).

Considering the technique of permanent monitoring, it is easy to see how this approach is particularly appropriate to be implemented in the system.
The $\bar{X} - chart$ is one of the most frequently used control diagrams: by using three horizontal lines defined to control each new observation. These lines are:

- the *Centre Line (CL)*, positioned at the sample mean and defined by all observations ($\bar{\bar{x}}$): $CL = \bar{\bar{x}}$
- the *upper Control Limit (UCL)*, obtained by adding three times the sample standard deviation σ to the mean value $\bar{\bar{x}}$: $UCL = \bar{\bar{x}} + 3\sigma$
- the *Lower Control Limit (LCL)*, obtained by subtracting three times the sample standard deviation σ from the mean value $\bar{\bar{x}}$: $LCL = \bar{\bar{x}} - 3\sigma$

UCL and LCL define the limits of the safety region. σ can be calculated as the standard deviation of the sample divided by $\sqrt{m}$, where m is the size of the sub-samples into which the total sample is divided.
Additionally, in the case of an SHM approach in which observations are obtained from the analysis of structural responses, it is possible to say that x_k refers to the generic observation of a one-dimensional feature at time t_k, after the removal of operational and environmental effects. This feature can be referred to as the *Newness Index (NI)*, as suggested by [90]. It is defined from the prediction error (ε) and using the Euclidean norm expressed in eq. 4.37 or the Mahalanobis norm defined in eq. 4.38:

$$NI_k^E = ||\varepsilon_k|| \tag{4.37}$$

$$NI_k^M = \sqrt{\varepsilon_k^T \left(\sum_{yy} \right)^{-1} \cdot \varepsilon_k} \tag{4.38}$$

Σ_{yy} is the covariance matrix of y, that is the measured characteristic, and the indices (Euclid's and Mahalanobis') are assumed to be normally distributed.
Where more than one characteristic is to be monitored, *multivariate control charts* can be used. After the definition of a safety region as explained above, after the training period, future observations can be checked:

I. continuously running the check for each new observation;

II. by running the check only when a set of new observations is available.

One type of multivariate control chart is the *Shewhart T*. This is characterised by the equation:

$$T^2 = \frac{n}{n+1}(x - \bar{\bar{x}})^T S^{-1}(x - \bar{\bar{x}}) \tag{4.39}$$

$T^2 - statistic$ is the parameter obtained when extracting each new observation x, which is a vector with p components. n is the number of observations collected during the reference period. $\bar{\bar{x}}$, process mean, and S, covariance matrix, are both calculated from the observations available during the reference period.
The LCL is set equal to zero, while the UCL is defined as:

$$UCL = \frac{(n-1)\,p}{n-p} F(\gamma) \tag{4.40}$$

In eq. 4.40, $F(\gamma)$ denotes the percentage point γ of the distribution F with p and $(n-p)$ DOF. When instead future observations are controlled using subgroups with r observations of x, the value of the $T^2 - statistic$ is calculated as:

$$T^2 = r(\bar{x} - \bar{\bar{x}})^T S^{-1}(\bar{x} - \bar{\bar{x}}) \tag{4.41}$$

where $\bar{x}$ is the subgroup mean, $\bar{\bar{x}}$ and S the same as defined above. LCL always set equal to zero while UCL changes, as expressed below:

$$UCL = \frac{p\,(m+1)\,(r-1)}{mr - m - p + 1} F(\gamma) \tag{4.42}$$

p represents the variable size (components of each individual observation of x), m is the number of subgroups collected during the reference period and $F(\gamma)$ denotes the percentage point γ of the distribution of F with p and $(mr - m - p + 1)$ degrees of freedom.

4.4.2 Subspace-based damage detection

Other methods for structural damage detection are *subspace-based* and are those used in the present work [32, 91, 92]. As mentioned in the previous section, it is the practice, from the vibration data measured with the monitoring system, to perform damage detection by detecting the changes in modal parameters between the reference state and the current, possibly damaged state. Natural frequencies, which are rather reliably identifiable parameters, are mainly used for comparison. However, extensive pre-processing and data processing

may be required. Consequently, eliminating the phase of identifying the structure in the damaged state and using other techniques (e.g. *outlier analysis* for damage detection [90]; *Kalman filter* innovations [79, 93]) could be advantageous.
In the case study that will be proposed in the following chapters, a ***subspace-based fault detection residual*** is used, in which the estimation of modal parameters in the possibly damaged state is avoided. Nevertheless, it must be said that most work assumes that the excitation properties of the environment, which in the case of AVT as we already know are not measured, remain constant for both the measurement in the reference condition and in the possibly damaged condition. Needless to say, this condition is difficult to satisfy. Therefore, in case the covariance of the excitation changes, such failure detection methods are modified by making them more robust [33].

Vibration-based damage detection methods have developed very rapidly in recent decades. An introduction to vibration-based damage detection can be found in [36]. For a broader overview of damage identification methods and strategies, see [24, 90, 94].

Going into the merits of the damage detection technique proposed here, a *subspace-based residual function* and a *statistical hypothesis test* ($\chi^2 - test$) built on it is used to compare the reference state model with the current, possibly damaged state model in order to detect the damage, avoiding the estimation of modal parameters. In this way, measured vibration data are used directly, which could therefore be influenced by changes in the covariance of the excitation. To overcome this problem, even though it increases the computational burden, the method can be corrected by recalculating the residual covariance for each data set tested.

According to the known background on statistical subspace-based fault detection, the use of *state-space representation* for structural monitoring based on only vibrations corresponds to the monitoring of *discrete-time model eigenstructure*, according to the relationships already seen in the previous chapter:

$$\begin{aligned} x_{k+1} &= Ax_k + w_k \\ y_k &= Cx_k + v_k \end{aligned} \tag{4.43}$$

Where:

- the states $x_k \in \mathbb{R}^n$;
- the outputs $y_k \in \mathbb{R}^r$;
- the state transition matrix $A \in \mathbb{R}^{nxm}$;
- the observation matrix $C \in \mathbb{R}^{rxn}$;
- n in the system order;
- r in the number of sensors;
- w_k is the measurement noise;
- v_k is the excitation and it is an unmeasured Gaussian white noise sequence with zero mean and constant covariance matrix Q: $E(v_k v_k^T) \stackrel{\text{def}}{=} Q\delta(k-k')$. E is the expectation operator.

The set of eigenvalues and mode shapes (λ, ϕ) of the system in previous equation is obtained from:

$$det\,(A - \lambda_i I) = 0, \qquad A\phi_i = \lambda_i \phi_i, \qquad \varphi_i = C\phi_i \tag{4.44}$$

This expression and this eigenstructure is considered as system parameter $\theta \in \mathbb{C}^{(r+1)n}$ with:

$$\theta \stackrel{\text{def}}{=} \begin{bmatrix} \Lambda \\ vec(\Theta) \end{bmatrix} \tag{4.45}$$

Where:

- λ_i and ϕ_i are the eigenvalues and eigenvectors of A and φ_i the corresponding mode shapes;
- $\Lambda = [\lambda_1,\ ...\,\lambda_n]^T$ is vector containing all eigenvalues;
- $\Phi = [\varphi_1,\ ...\ , \varphi_n]$ is a matrix in which the columns are the mode shapes;
- vec represents the vectorization operator.

4.4.2.1 Subspace-based residual vector

The *residual function*, proposed in [32, 91], for detecting any changes in the eigenstructure θ from y_k measurements without effectively performing parameter identification in the possibly damaged state, is associated with a *covariance-driven subspace identification algorithm*. It is considered the cross-covariance between the states and the outputs G, the theoretic covariances of the outputs R_i and the block theoretical Hankel matrix $H_{p+1,q}$:

$$G = \mathbf{E}(x_k + {}_1y_k^T) \tag{4.46}$$

$$R_i = \mathbf{E}(y_k y_{k-i}^T) = CA^{i-1}G \tag{4.47}$$

$$H_{p+1,q} \stackrel{\text{def}}{=} \begin{bmatrix} R_1 & R_2 & \cdots & R_q \\ R_2 & R_3 & \cdots & R_{q+1} \\ \vdots & \vdots & \ddots & \vdots \\ R_{p+1} & R_{p+2} & \cdots & R_{p+q} \end{bmatrix} \stackrel{\text{def}}{=} Hank(R_i) \tag{4.48}$$

The latter, through the factorization property, can be expressed in the observability and controllability matrices:

$$\begin{gathered} H_{p+1,q} = O_{p+1}C_q \\ \text{where} \qquad O_{p+1} = \begin{bmatrix} C \\ CA \\ \vdots \\ CA^p \end{bmatrix} \qquad C_q = [G \; AG \; \cdots \; A^{q-1}G] \end{gathered} \tag{4.49}$$

From the observability matrix O_{p+1}, the matrices C and A can be recovered [95] and thus the system parameter θ.
As is well known, damage to the system causes changes in A and C and thus in the Hankel matrix (eq. 4.48) via properties in eq. 4.49. This change can be detected with a statistical test, as mentioned at the beginning of this section.

Starting from the measured data $(y_k)_{k=1,..,N}$, a consistent estimate of $\hat{H}_{p+1,q}$ can be made from the empirical covariances of the output and can be written:

$$\hat{R}_i = \frac{1}{N}\sum_{k=1}^{N} y_k y_{k-i}^T \qquad \hat{H}_{p+1,q} = Hank(\hat{R}_i) \tag{4.50}$$

$\hat{H}_{p+1,q}^{ref}$ is defined as the *averaged Hankel matrix* in the reference state and

through its SVD we also calculate its left null space $S = \hat{U}_0$:

$$\hat{H}^{ref}_{p+1,q} = [\hat{U}_1 \quad \hat{U}_0] \begin{bmatrix} \hat{\Delta}_1 & 0 \\ 0 & \hat{\Delta}_0 \end{bmatrix} \begin{bmatrix} \hat{V}_1^T \\ \hat{V}_0^T \end{bmatrix} \tag{4.51}$$

where Δ_1 is of size [n-by-n] and the SVs in $\hat{\Delta}_0$ are very small and tend to zero for $N \to \infty$.
The characteristic property of the reference state is expressed as:

$$S^T \hat{H}_{p+1,q} \approx 0 \tag{4.52}$$

In a damage state, this product differs from 0. Thus, to determine whether or not the measured data fall within the domain of the reference state, a ***residual vector*** is calculated as:

$$\zeta = \sqrt{N} vec(S^T \hat{H}_{p+1,q}) \tag{4.53}$$

To determine how the value of ζ is different from zero, the $\chi^2 - test$ (statistical test) is used, expressed as:

$$\chi^2_\zeta = \zeta^T \Sigma_\zeta^{-1} \zeta \tag{4.54}$$

$\Sigma_\zeta = cov(\zeta)$ is the *empirical residual covariance*, calculated using different measures of the reference state.

Whether or not damage occurs depends on the comparison of the χ^2-test value with a *threshold*. This threshold can be obtained from the same χ^2 values of measurements corresponding to the reference state. In this way, the collected data is processed more efficiently and directly [96].

After the aforementioned, it must be underlined, as mentioned at the beginning, that it is necessary to take into account the possibility that the excitation properties of the environment, which are not measured in the case of AVT, change. That is to say, the condition whereby the excitation remains constant is difficult to achieve if it refers to two different moments of data acquisition (to reiterate the definitions already introduced, this means the reference state and the current state, following the first, hypothetically damaged one). A variation in the excitation properties implies a variation of the Hankel matrix, hence of the residual vector.

Thus, a variant of this approach [33] has been introduced that is *robust* to significant variations in the excitation levels of the environment. This extension refers to the relationship between the *Hankel matrix* in eq. 4.48 and the matrix of its *principal singular left vectors* U_1 (Eq. 4.51). These share the same left null space S. Therefore, in a similar way to eq. 4.52, another characteristic property of the reference state can be written as:

$$S^T \hat{U}_1 \approx 0 \tag{4.55}$$

Unlike the Hankel matrix in eq. 4.48, the matrix of singular vectors U_1 does not depend on the characteristics of the ambient excitation since it is a matrix with orthonormal columns. From this, a second residual vector can be defined, which is considered robust to changes in the excitation and is defined as:

$$\xi = \sqrt{N} vec(S^T \hat{U}_1) \tag{4.56}$$

For a more in-depth discussion of this topic, which was the basis for the implementation of the algorithm used to assess the damage to the structure being worked on, please refer to: [33].

In anticipation of the treatment proposed in chapter 6, the problem of assessing the health of the structure was not addressed in order to identify and quantify a specific damage, but to have, in real time, an *alert* on a possible change in dynamic behaviour. Such an approach was considered significant when considering the possibility of implementing it on a considerable number of structures, given the importance, now well known, of preserving Italy's cultural heritage.

Chapter 5

Dynamic monitoring in practice: tool and process

5.1 The workflow

In the previous paragraphs there has been much talk about what monitoring means a structure. However, realizing a proper monitoring system implies knowledge of structures, but also of other sectors (for example, knowledge of materials, types of damage detection, sensors, data management and intelligent processing). Moreover, although each monitoring system can be characterized by different specific details, in figure 5.1, are reported the components that are typically present in each of them.

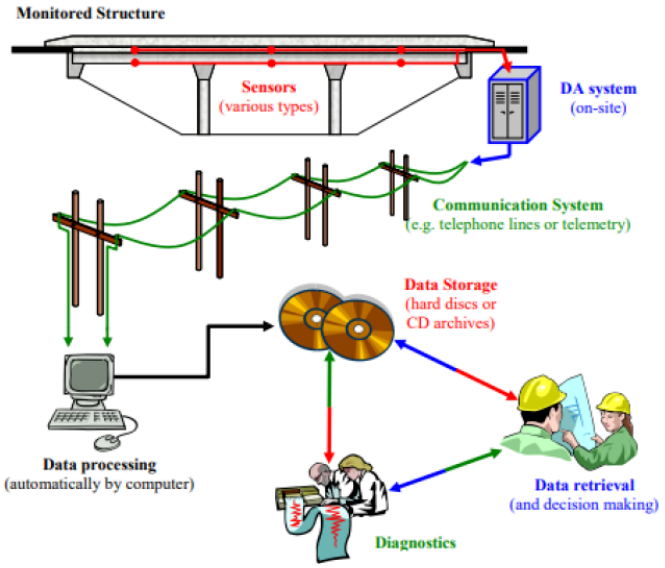

Figure 5.1: *Visual scheme of a typical SHM system [97]*

The variety of techniques that SHM provides are specifically designed to analyse a particular phenomenon. Whether short-term or continuous, static or dynamic monitoring, the system involves some instrumentation, sensors, data acquisition devices, a data processing system and finally a storage unit.
A fundamental step to start the process in the best way is the careful selection of the necessary instrumentation. Having high quality measurements means setting the stage for successful modal identification.
The function of any sensor is the conversion of a physical quantity into an electrical quantity (typically voltage). The electrical signal is then transferred to the data acquisition hardware for digitisation. Data processing, for which various techniques are available, involves a pre-processing phase, in which an initial check of the data is made by eliminating noise, and finally the actual data analysis phase with the extraction of the relevant parameters.

5.2 Instrumentation

As mentioned above, for meaningful monitoring to be guaranteed, the type of sensors to be used must be chosen appropriately. Currently, the sensors used in civil engineering are capable of measuring, among other things, stress, deformations, environmental parameters such as temperature and humidity, or even accelerations. For a single monitoring system, it is possible to consider using different types of sensors in order to acquire multiple signals simultaneously. The number of sensors to be used, as well as their position within the structure, is a fundamental point of structural monitoring, and is an ever-evolving issue. An error of judgement at this stage could compromise the performance of the system itself. In fact, each type has different characteristics (accuracy, reliability, power requirements and signal transmission limits) and it must be said that the best choice must fall on the best possible instrumentation. But better performance and features mean higher costs. Considering structural monitoring, the measured motion is usually very small and low frequency. Therefore, the sensitivity characteristic of the sensor must be high.
Once the target and the quantities to be measured have been set, the system must be designed, considering the cabling of sensors, conduits, junction boxes and all other accessories required to accommodate the SHM system on site.
Another feature of sensors that is sometimes underestimated is the simplicity of installation. Inadequate installation could affect the performance of the in-

dividual sensor and the entire monitoring system.
At present, the cabled solution is still the best for a continuous monitoring system, because it eliminates the problem of power consumption. Nevertheless, it is fair to mention that over the last decade, there has been a lot of effort in the development of wireless sensor networks. Several solutions are now available that certainly offer interesting advantages (e.g. cost reduction, because the system generally involves fewer components, and reduced installation time).
Let us now look at some types of sensors, without going into too much detail. Although several types of sensors are available for measuring the dynamic response of civil structures, we will focus mainly on piezoelectric accelerometers, which are the ones used to develop the thesis work.
Other types are, for example, force-balance accelerometers or electromagnetic (seismograph, geophone), fibre-optic (spectrometric, interferometric), displacement transducers, thermocouples, etc.

5.2.1 Accelerometers sensors

The choice of sensors is usually based on a number of considerations:

- the expected amplitude of the movement to be measured;
- the type of structure under investigation (e.g. masonry, reinforced concrete, steel, etc.);
- the available budget.

In general, accelerometers (Figure 5.2) are devices through which accelerations induced by natural vibrations or external forcing can be measured. They consist of a test mass that is held in suspension by an elastic element. In the presence of an acceleration, this mass moves from its rest position by a certain amount that is proportional to the measured acceleration. By converting the change in position into a suitable electrical signal, these devices ensure that information about the measured physical quantity is obtained. By means of one or two integrations, it is then possible to determine the velocity and displacement, if necessary.
The sensors presented here and used for short-term and long-term monitoring campaigns are *piezoelectric accelerometers* and *MEMS accelerometers*, respectively.

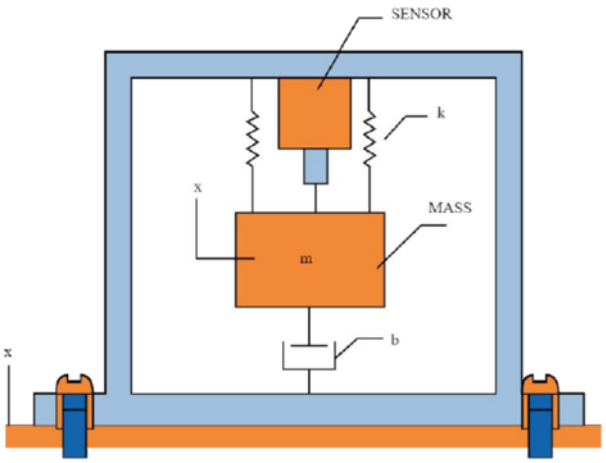

Figure 5.2: *Accelerometric sensors scheme*

Piezoelectric accelerometers

Piezoelectric accelerometers are small, lightweight devices consisting of a piezoelectric crystal and a mass attached to a support base.

If they are subjected to a general external mechanical stress (e.g. an acceleration), the inertia force associated with the mass causes the crystal to deform. By exploiting the capacity of the crystals, they are able to generate an electrical signal proportional to the acting pressure. This is transmitted to a signal conditioner which reads it in terms of voltage. This conditioner can be remote, as in *charge-mode* sensors, or embedded, as in *Integrated Electronics Piezo-Electric (IEPE)* sensors. Compared to the first mentioned, IEPEs offer a number of advantages: simplified operation, lower cost, resolution not affected by cable type and length. They are currently the most widely used in the piezoelectric category.

Figure 5.3: *Piezoelectric accelerometers: IEPE KS48C*

Among the advantages of piezoelectric accelerometers, the main one is that they are able to measure accelerations even without a power supply. However, since the crystal only generates an electrical signal when the stress does not persist, piezoelectric accelerometers cannot measure quasi-static accelerations. In fact, if, for example, there is a compression in such devices that persists over time, such that it is considered static (signal freezes until it dissipates), no output signal is produced.

To choose the most appropriate sensor according to the application, reference should be made to:

- *Sensitivity*: smallest detectable change in the measurement. As already mentioned, high sensitivity accelerometers are required due to the small amplitude of movement and the limited frequency range present in typical structures to be investigated. This is defined by the possibility of amplifying the signal before digitising it ("gain"of the sensor, e.g. 10 V/g). This is because electrical noise limits the smallest detectable signal, so a high gain should be preferred to minimise its effects.

- *Dynamic Range (DR)*: normally expressed in dB, this is the ratio between the largest and smallest measurable signal:

$$DR = 10 \cdot log\left(\frac{V_{max,s}}{V_{n,s}}\right)^2 \tag{5.1}$$

  $V_{max,s}$ represents the maximum voltage signal and $V_{n,s}$ represents the sensor noise background. A suitable dynamic range is approximately 120-140 dB, as it fits well with the average 24-bit resolution that most digitisers have.

- *Resolution*: represents the smallest variation of the physical input quantity perceived in the sensor output. In other words, it indicates the maximum and minimum physical values that the sensor can achieve. It is usually expressed in absolute terms or as a percentage of full scale.

- *Linearity*: tendency in the conversion between input and output measurement. Idally, the sensor should behave linearly, but a deviation component is always present. This must be as limited as possible. It is expressed by the percentage of non-linearity (for high performance accelerometers it should be less than 1%).

MEMS accelerometers

Micro Electro Mechanical Systems (MEMS) represent a technology of devices or systems with small dimensions that combine miniaturised mechanical and electromechanical components realised through microfabrication techniques. Typically, the size of such devices ranges from one micrometre to one millimetre. Their development is due to the rapid evolution of micromachining over the last decade.

In the field of structural monitoring, such sensors are used to measure various physical parameters such as acceleration, inclination and temperature.

They can be manufactured using different technologies (modified silicon fabrication, moulding and plating, electric discharge machining and other innovative technologies. electrical discharge, etc.).

Their small size allows them to be placed in areas inaccessible to traditional sensors.

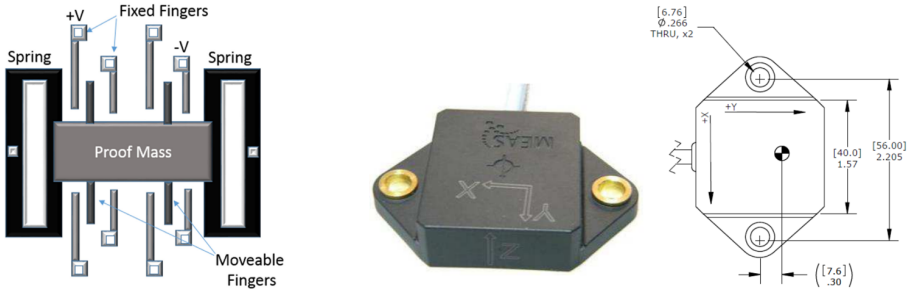

Figure 5.4: *MEMS accelerometers: model 4030*

This type of sensor consists of a moving mass, connected to moveable fingers (creating an electronic system equivalent to the elastic mass system of piezoelectric technology). When the mass moves, the displacement is measured through the change in differential capacitance recorded between three electrodes, two of which are fixed and one moving.

In the case of non-excitation, the moving electrode remains fixed in an intermediate position between the other two zero differential output components). When an acceleration occurs, the mass moves by inertia, changing the distance of the moving electrodes from the fixed electrodes. In this case, the output capacity is converted to acceleration.

For this type of accelerometers, the triaxial version is common. It is considered reliable, as demonstrated in the literature [98, 99], even when configured in arrays [100].

5.3 Data acquisition hardware

The system that allows the acquisition of raw data from the various sensors arranged on the structure is generally located near the monitoring site. In the *Data-Acquisition (DAQ)* system, signal demodulation, conditioning and storage of the measured data are conducted before being transferred for analysis. As mentioned, the sensors can be connected with the acquisition system via a cabled or wireless connection. The former is certainly the most cost-effective solution, but it can be affected by electromagnetic phenomena that can lead to measurement errors. It is possible to try to bypass this problem, or at least reduce it, by using differential signalling techniques and suitably shielded cables. It sounds obvious, but it is right to emphasise that in order to guarantee correct data acquisition, cables must not be damaged or broken. Despite the higher cost and slower data transfer, it is sometimes necessary to resort to a wireless connection. This is the case of very large facilities, where the required cable extension is prohibitive.

The analogue-to-digital A/D converter is a device whose function is to transform a continuous signal recorded by sensors into digital sequences that represent the signal in terms of amplitude. Currently, it is possible to find dedicated solutions (Figure 5.5 (a)), in which the equipment is ready-to-use and includes acquisition software, and customisable solutions (Figure 5.5 (b)), based on programmable hardware (usually adopted by experienced users).

a) b)

Figure 5.5: *Types of A/D converter: dedicated solution (a) and customisable solution (b)*

Conversion is based on the discretisation of time (sampling) and signal amplitude (quantisation). For the choice of the most appropriate instrument, reference must be made to:

- *resolution*: number of bits that the converter can use to represent the signal;
- *noise level*: number of bits that noise occupies for a null input (for good quality 24-bit digitisers, only the last two bits are typically corrupted by noise);
- *dynamic range*: expressed in dB and defined as the ratio between the largest and smallest value that the ADC can acquire without significant distortion;
- sampling frequency (f_s): number of samples acquired per second (the investigable frequency range is defined as the maximum frequency of the ADC). In civil applications, the interesting range can be considered to be between 0 and 100Hz, so a maximum sampling frequency of 200Hz may be satisfactory.

5.4 Data communication

Once the data has been acquired by the DAQ system, it must be transferred through a system consisting of telephone lines or the Internet. Thus doing so, it will be possible to process and analyse the data appropriately.
Typically, data are processed and analysed at a different location, away from the structure being monitored. This not only allows the work to be monitored remotely, but above all eliminates or at least reduces the need to travel to the site in the future. Finally, it should be added that, although rarely chosen, it is possible to provide for the physical transfer of data by means of mobile DAQ units or hard drives. It is clear that this solution does not enjoy the advantages of the techniques described above and implies an extension of time for the entire process.

5.5 Signal processing

Good signal quality is essential for satisfactory analysis. To achieve this, it is necessary to set up the instrumentation correctly before starting with the acquisition of recordings.

Briefly, the first setting required before starting the measurement is the definition of a correct value for the sampling frequency, already introduced in the previous paragraph, based on the structure to be investigated. Having noted the frequency range of interest, Nyquist's Theorem states that:

$$f_s > 2 \cdot fM \tag{5.2}$$

where f_s is the sampling frequency and fM is the maximum frequency in the sampled signal, and:

$$f_N = f_S/2 \tag{5.3}$$

is the so-called Nyquist frequency, i.e. the maximum frequency contained in the signal that can be sampled without error.

It should be noted that the same signal can be sampled in different ways (Figure 5.6 (a)) . If you increase the resolution on the amplitude axis, for example by using a better converter, the system reproduces the signal more faithfully, but you must also increase the resolution on the time axis. It makes no sense to have a signal with high amplitude resolution but undersampled in the time domain.
If the sampling rate is too low, aliasing occurs (Figure 5.6 (b)). If $f_s < 2f_N$ the higher frequencies contained in the analogue signal will assume a false identity by appearing as lower frequencies. The waveform after digitisation will be "false". Since the erroneous aliasing effect cannot be corrected after conversion, A/D converters are usually equipped with an anti-aliasing filter.

From a good instrumentation set-up phase, it is then easy to ensure that the acquired data is processed correctly before the identification methods are applied. The data processing and analysis phases certainly represent the operational part of the entire monitoring process.
The signal is cleaned through filtering and decimation.
Filtering is useful for removing unwanted frequency components from signals.

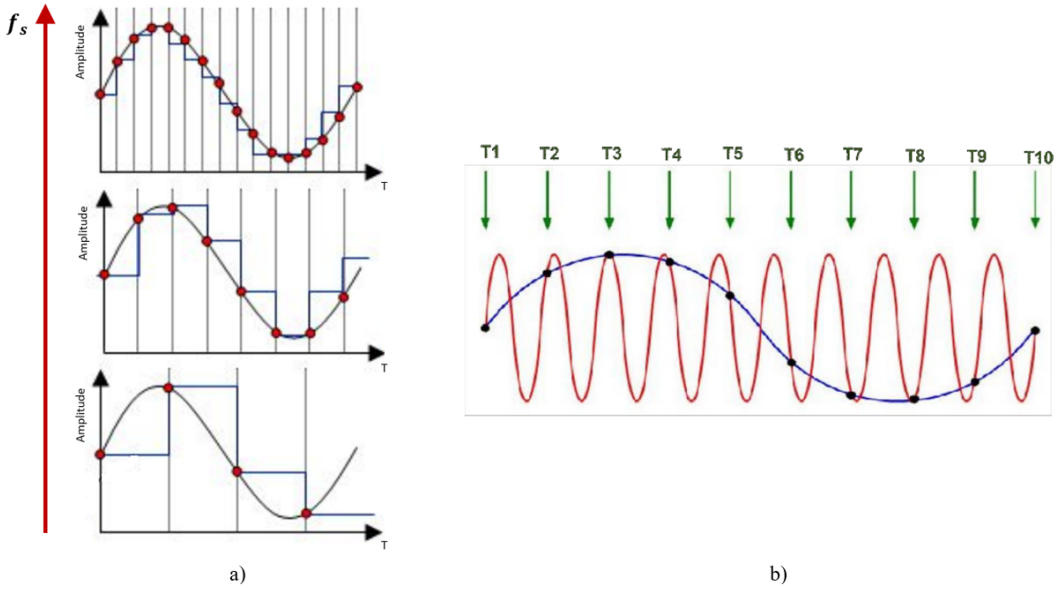

Figure 5.6: *Different sampling of the same signal (a); Aliasing: original signal in red, aliased signal in blue (b)*

The filters that can be used are: low-pass filters (exclude all frequencies above a certain threshold), high-pass filters (remove frequencies below a set value), band-stop (exclude frequencies defined in the band, in the range, defined in the filter) and band-pass (opposite to the previous one, they remove frequencies outside the range defined in the filter).
Decimation is necessary when signals are acquired with a sampling frequency above the interval of interest for analysis. The acquired signals are then re-sampled at a lower sampling frequency. The result of these operations is the removal of redundant or unwanted information in order to ensure, as mentioned, a correct subsequent diagnosis.

5.6 Storage and diagnosis

After the processing steps, the data must be stored in such a way that it can be re-used at a later date. In order to avoid data corruption problems, attention must be paid to this phase.
In the case of continuous monitoring, the amount of data to be stored can also be very large, so problems related to lack of memory must be avoided. In order to reduce the amount of data stored, only data from the processing phase should be retained, eliminating the raw data, but this eliminates any possibility

of analysing the data again in the future.

Once the data has been collected and processed, it is necessary to interpret it. The aim is to acquire information that can be used to correctly assess the dynamic behaviour of the structure.

After all this procedure, it is necessary to store the data. Having to return to the same data to process it again, in order to arrive at a different solution, is something that often happens.

Chapter 6

The case study: OMA identification and Damage Detection

6.1 San Francesco Church

In the previous chapters, the potential, processes and theoretical basis of what is SHM have been presented. Improving knowledge of the mechanical properties of structures, assessing their state of health and identifying damage are, as already mentioned, deeply actual topics, especially considering the high vulnerability of the Italian historical heritage.

This chapter presents the outcome of the work carried out on these issues: definition of an automated procedure to continuously analyse the data of approximately one year of dynamic monitoring, tracing the main structural modes and taking into account the influence of environmental factors on them, and direct processing of the time histories to obtain information on variations in the dynamic behaviour of the structure and thus presume the occurrence of damage.

The structure on which the work focused is the Church of San Francesco in Sarnano.
Sarnano, in the province of Macerata (Marche, Italy) (Figure 6.1), rises at the base of the Sibillini Mountains, overlooked to the west by the northernmost peaks of the chain. The village is situated on a hill (Figure 6.2) to the right of

the Tennacola stream, on a tongue of land enclosed between the latter and its affluent, the Rio Terro. The territory, predominantly hilly, extends eastwards between valleys, woods and cultivated fields. To the north, the hills slope down into the ancient lake plain of Pian di Pieca (San Ginesio).
Sarnano's climate is sub-Apennine: in winter, when there are cold spells from the north-east, its position with the Sibillini Mountains behind it favours abundant snowfall. The summer is hot and dry, although heat storms are frequent. It is located at 539 m a.s.l., covers an area of about 63.17 km^2 and has just over 3,000 residents.

Figure 6.1: *Location of the Sarnano municipality*

Figure 6.2: *Aerial view of the Sarnano municipality*

6.1.1 Historical survey

The Church of San Francesco (Figure 6.3), adjacent to the town hall, is dedicated to the Assisian friar in memory of his permanence in the town between 1214 and 1216.

Figure 6.3: *Church of San Francesco, Sarnano, Marche, Italy*

The present church, together with the buildings used as Municipal Offices, constituted the ancient Franciscan convent of Sarnano that originated from the Franciscan friars of Roccabruna, a hill to the north of the historical centre. In 1327, the friars who occupied this convent, decided for greater security, considering the thefts, to move within the walls of the Municipality of Sarnano.
In 1332 the new convent with the church within the municipal walls was to be complete.
During the 14^{th} century, the Franciscan convent was favoured by numerous bequests aimed at completing the building. The convent was built on a very important street on the main road leading to the square. In 1578, the convent was expanded, and the complex belonged to the Friars Minor until the Napoleonic suppression.
In 1818 the church and convent passed to the Philippine congregation.
In the years 1822-1833, the church was renovated, as attested by the inscription

on the lintel of the portal bearing the date 1832. The project for this intervention was entrusted to architect Ignazio Cantalamessa (according to historians). The interventions certainly concerned the façade, which was rebuilt in the Neoclassical style, and the elevation of the church, easily recognisable by the discontinuity between the overlapping wall equipment on the north-east side (Figure 6.4). This period also saw the construction of the oratory, later the sacristy, next to the church entrance.

Figure 6.4: *Church of San Francesco, Sarnano: North-East side*

In the 16^th century, funds were allocated by Cardinal Costanzo Torri for the reconstruction of the building complex. However, likely, only a renovation was carried out with perhaps some extensions.
In 1862, the Municipal Council of Sarnano decided to proceed with the purchase of the entire convent to make it the municipal seat, which became such in 1872, but the church remained state property.
Over the following centuries, until today, the complex has remained subdivided as mentioned.

6.1.2 Geometrical and material survey

The building is rectangular in shape with a single nave and semi-circular apse. The belfry with a square plan is placed next to it. The sacristy is instead placed on the same side but next to the entrance (Figure 6.5).

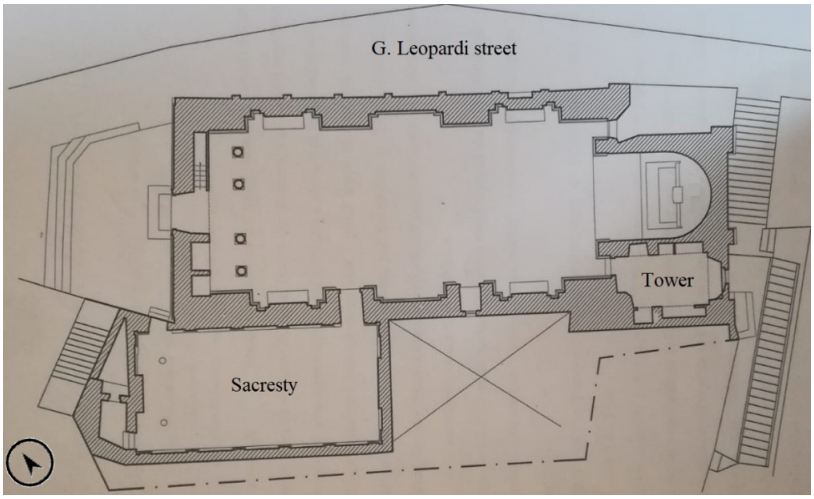

Figure 6.5: *Chruch of San Francesco, Sarnano: ground floor plan*

The entire complex is built of solid brick in the exterior parts, like all the buildings in the old town. The facade has a large semi-circular window, and the portal is in sandstone and limestone (Figure 6.6 (a)). The tower is also made entirely of brick with sandstone mouldings in the belfry (Figure 6.6 (b)). It consists of three floors (ground floor, first floor and belfry) separated by wooden mezzanines.

Figure 6.6: *Church of San Francesco, Sarnano: facade (a) and tower (b)*

The interior from 1830 was completely reformed according to the dictates of neoclassical architecture. Soft and monochromatic colours. It is bordered by a giant perimeter order of paired Ionic columns supporting a continuous cornice (Figure 6.7). The counter facade is occupied by the organ and the nave is covered by a barrel vault in camorcanna. The attic is not accessible, and the roof is double pitched with a tile covering. The window openings have sandstone lintels.

Figure 6.7: *Church of San Francesco, Sarnano: interior*

Geometrically, the church measures about 24x12 metres and the facade is about 13 metres high, taking the height of the portal floor as the base. The sacristy measures approximately 12.5x6.5 metres. The apse is at an elevation of +0.50 metres above the floor of the nave.
The tower measures approximately 4.5x3 metres internally. It rises approximately 30 metres at its highest point (at the back).

6.1.3 Interventions and damage survey

After the 1979 earthquake, the church was quite badly damaged, and plans were made to repair the damage.
After the 1997 earthquake, a project was prepared to improve the seismic response, but the project was not funded. As a result, the church lacked seismic protection (such as metal curbs or tie bars and chains).
Ordinary and extraordinary maintenance works were proposed in 2014: new painting and new pavement; seismic improvement of the sacristy; reopening of

the two external windows on the facade overlooking the public street (via G. Leopardi); seismic improvement of the tower through internal works; restoration of the tower's external masonry and mouldings, including the roof; seismic improvement of the roof of the nave and sacristy and works connected to both the wooden structures and the camorcanna; closure of the semi-circular window and restoration of the spur. Of the various interventions mentioned here, those related to the seismic behaviour of the building (such as the laying of chains or angle brackets) are not actually reflected in the field. This hypothesis is also confirmed by the parish priest, who has been working at the Church of St Francis for many years.

After the 2016 earthquake, the Church was certainly damaged to a good measure. It was closed to the public for a while, but then inspections did not reveal any particularly serious structural damage. The main injuries were concentrated on the camorcanna vault. Both in the centre and at the points where it connects with the facade (Figure 6.8 (a)) and the wall delimiting the apse (Figure 6.8 (b)). These injuries are still visible because they have not been repaired .

a) b)

Figure 6.8: *Camorcanna vault damage survey: in the middle and with the facade (a) and with the wall delimiting the apse (b)*

Concerning the bell tower, there is no particular information, and at the time of the inspection (May 2021) for the installation of the long-term monitoring system, no significant damage was visually found. However, it was the subject of a safety intervention in 2018: a metal truss structure was inserted inside, connected to the outer walls by threaded bars (Figure 6.9). It was not possible to know if there were any particularly visible injuries at the time of the first post-earthquake inspection. No technical and design drawings were found regarding the safety intervention carried out. Engineers from the technical of-

fice informed that, although the intervention is of limited duration, there are still no plans for the intervention. In general, the structure is visibly in poor condition (Figure 6.10).

Figure 6.9: *Tower safety intervention (2018)*

Figure 6.10: *Tower masonry conditions*

6.2 Short-term monitoring

As mentioned in the previous paragraph, short-term monitoring campaigns were conducted on the structure. In particular, after the earthquake event that involved Central Italy in 2016, two AVTs were carried out, respectively in 11^{th} July 2017, before the safety intervention, and in 12^{th} June 2018, immediately after the intervention was carried out.
The two campaigns will be presented in detail below with the results obtained.

6.2.1 Instrumentation and sensors layouts

In both short-term monitoring, in 2017 and 2018, the following instrumentation was used:

- Piezoelectric sensors (IEPE) KS48C and KB12VD with voltage sensitivity of 1V/g and 10V/g, rispectively, and measuring range of ±6g (calibration certificates issued approx. 40 days prior to testing).

Figure 6.11: *Piezoelectric sensors: KS48C (a) and KB12VD (b)*

- Signal conditioner M32-M28.
- Dynamic Data System 8-channel acquisition unit DaTa500, with 24 bit resolution.

Figure 6.12: *Dynamic Data System acquisition unit DaTa500*

The accelerometers were installed in 4 couples (to measure the X and the Y axes) and made integral to the supporting structure with the use of bi-component resin or by metal anchors to guarantee the perfect adhesion of the sensor with the contact surface.
The figure below show the sensors layouts during the two short-term monitoring.

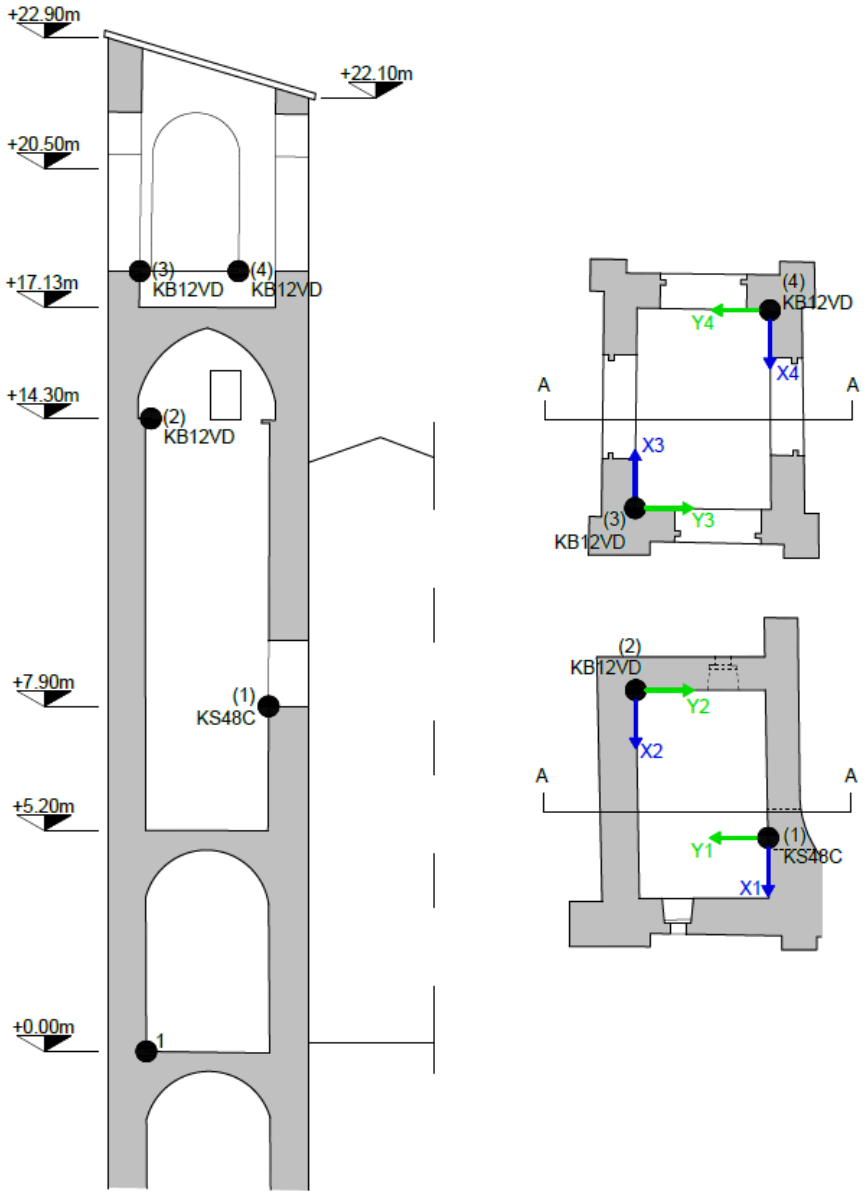

Figure 6.13: *Short-term monitoring sensors layouts*

In both 2017 and 2018, three acquisitions were made at different times, leaving the sensors in the same position during the tests, with a sampling rate of 200Hz. The first acquisition was 60 minutes, the second and third 40 minutes.

6.2.2 Results

Each time history is appropriately processed and a text document is exported for each channel regarding the acquired accelerations. Once all time histories had been acquired, the data was processed in the following way:

- application of 0.5Hz - 50Hz band-pass filter in order to eliminate frequencies that are not of interest for building characterisation;
- elimination of time sequences with the presence of anomalous peaks;
- decimation of the data in order to reduce the sampling frequency from 200Hz to 50Hz, and then to 12.5Hz.

The data is then processed through identification software capable of extracting the dynamic parameters of the structure, eigenfrequencies, modal shapes and damping ratio.The identification software operates through the SSI algorithm in the time domain, performing an estimation of the FRF of the system from which the modal parameters are extracted. The figure 6.14 shows the stabilization diagram obtain for the two acquisition campaigns.

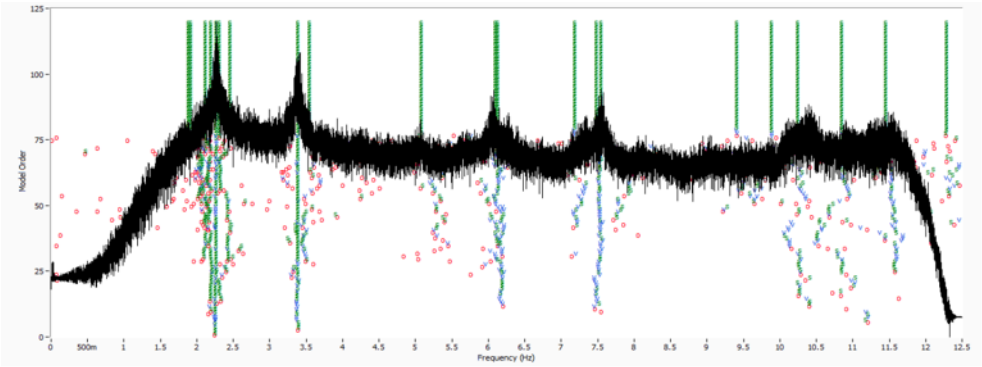

a)

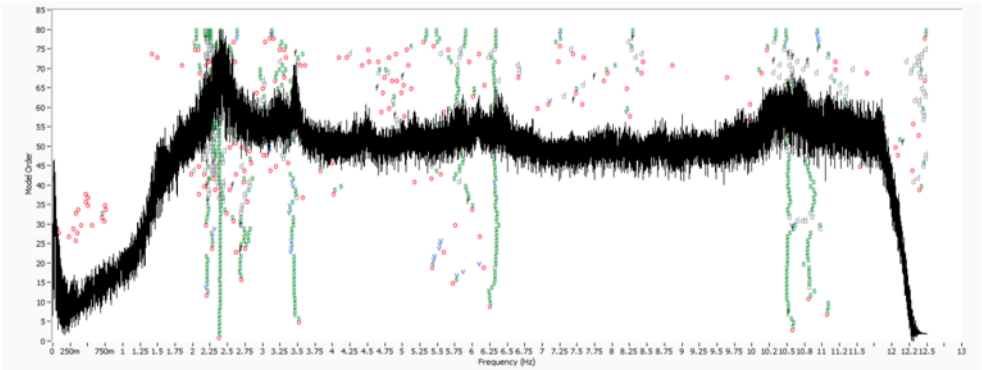

b)

Figure 6.14: *Stabilization diagrams of short-term monitoring: 2017 (a) and 2018 (b)*

From the analysis of the measurements, a clear frequency content of the signals was found. The table 6.1 shows frequencies and damping ratios identified during the two environmental tests studied.

Table 6.1: *Comparison of the modal frequencies and damping ratios of 2017 and 2018 short-term monitoring*

Mode	f_{2017} (Hz)	f_{2018} (Hz)	ξ_{2017} (%)	ξ_{2018} (%)	$\lvert\Delta f\rvert$(%)
1	2.268	2.283	0.705	1.513	0.657
2	3.386	3.465	0.917	1.172	2.279
3	6.127	6.334	1.631	2.612	3.268

In addition, in the identification software, an Experimental Model (EM) was created to schematically represent the structure under examination. This model does not contain any information on the materials and boundary conditions, but allows for the detection of how each monitored point moves at each of its own frequencies.

The following assumptions were made when plotting the modal shapes:

- rigid behaviour in the plane of the various decks;
- modal shapes referring only to the x- and y-axes (plane);
- points at the base of the building that were not monitored were assumed to have zero displacement (embedded at the base).

In figure 6.15 the results in terms of modal shapes associated with the identified frequencies are also shown.

From the results shown, it can be stated that the safety intervention implemented in the tower did not significantly alter the dynamic behaviour of the building. In fact, the increase in frequencies is very small: the first frequency has remained almost unchanged, the subsequent frequencies show a greater increase but in any case not particularly noteworthy. If we look at the modal shapes, they too are not altered.

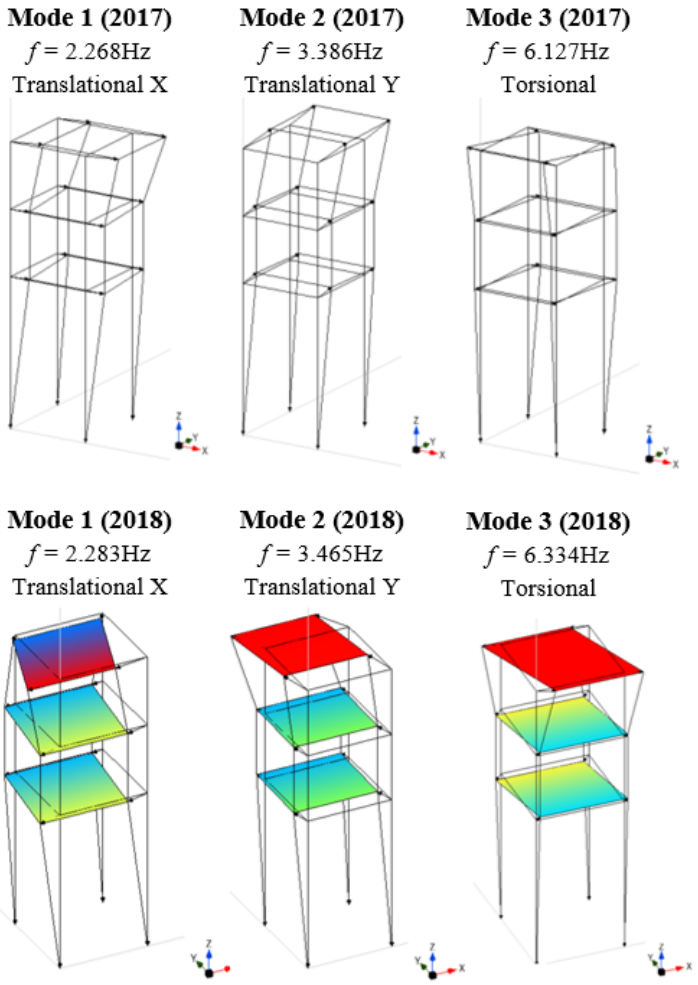

Figure 6.15: *Comparison of modal modal shapes of 2017 and 2018 short-term monitoring*

6.3 Finite Element Model - FEM

The information obtained from the geometric and material survey of the structure was used to construct a preliminary FEM of the complex (church and bell tower). The software used to achieve this was Diana©. This model, in the context of the SHM [101, 102], can be used to conduct an initial modal analysis to get an idea of the range of frequencies to be considered as significant during the identification process. In addition, it may be useful to carry out a preliminary assessment of the most suitable points in which to position the sensors of the monitoring system.

Having already taken the indications provided in the survey campaigns conducted in 2017 and 2018 as a basis, we relied on the results of these for the

necessary assessments regarding the design of the continuous monitoring system.

In any case, the model shown here can be a useful tool, after careful calibration, for further analysis and evaluation. These may be necessary to determine particular criticalities and perhaps design interventions aimed at the seismic improvement of the entire structure, given the total lack of these.

The construction of the geometry was followed by the assignment of material parameters according to the values proposed by the Italian code [103, 104] (Figure 6.16). Then the constraints and finally the loads due to the horizontals were imposed.

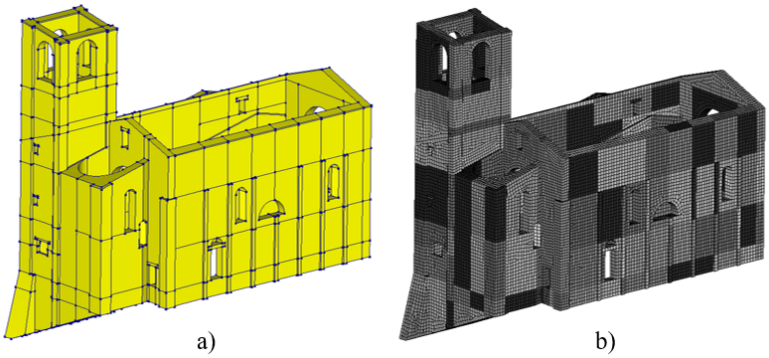

Figure 6.16: *Church of San Francesco, Sarnano: numerical model (a) and discretized numerical model (b)*

The figure 6.17 shows the results obtained after modal analysis.

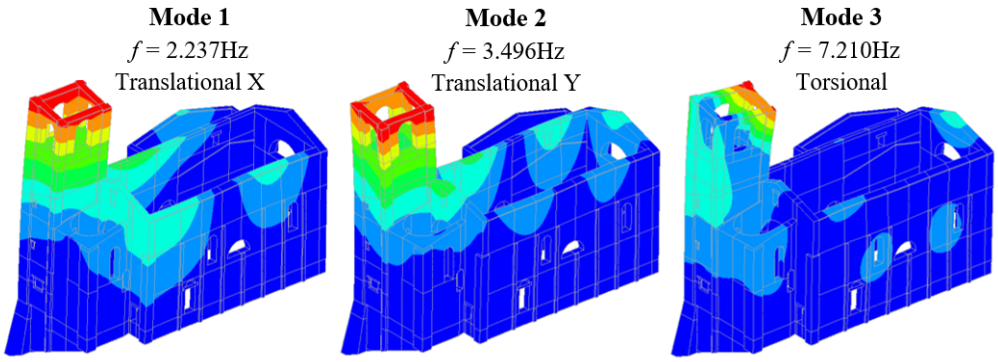

Figure 6.17: *Frequencies and mode shapes resulting from modal analysis over non calibrated FE model*

These presented are the identified natural modes and frequencies that most affect the bell tower. Compared to the values obtained in the short-term cam-

paigns, the frequencies are higher. This indicates that higher parameters were included than in reality. The mode shapes seem to reflect the trend seen previously.

6.4 Long-term monitoring

The continuous monitoring process started in June 2021. Given the objective of setting up a "sustainable" monitoring campaign, as mentioned in the abstract and especially in the introduction to this thesis work, it was decided to use MEMS accelerometers. These, compared to piezoelectric ones, are less expensive and therefore suitable for the purpose. We would like to emphasise once again that their reliability is proven by numerous reports in the literature [98–100]. Once the instrumentation was installed, a short acquisition was carried out at the start of the entire process. This was necessary to assess the health of the tower at that time. Thanks to the presence of the 2017 and 2018 data, it was possible to make a comparison. As will be seen, there are no substantial variations in terms of frequencies and modal shapes.

6.4.1 Instrumentation and sensors layouts

The continuous monitoring system consists of four MEMS triaxial capacitive accelerometers (at the end of this subsection, the parameters of the sensors used are presented). The Z-axis channel was switched off, storing only X- and Y-axis data, as it was not considered particularly significant and reduced the amount of data to be processed. The accelerometers were mechanically fixed to the structure to make them integral. The first sensor (number 1) was placed in a corner at the base of the tower. At the same corner, but in the belfry, the fourth sensor (number 28) was fixed. The remaining two (number 10 and number 26) were positioned at intermediate heights, opposite to those already mentioned (Figure 6.18).
All accelerometers are linked in a chain, ensuring the synchronisation of measurements and connected to the Dynamic Data System 8-channel acquisition unit DaTa500 (24-bit resolution), the same one used for the short-term campaigns.

The system is set to acquire a time history of 20 minutes every hour. The sam-

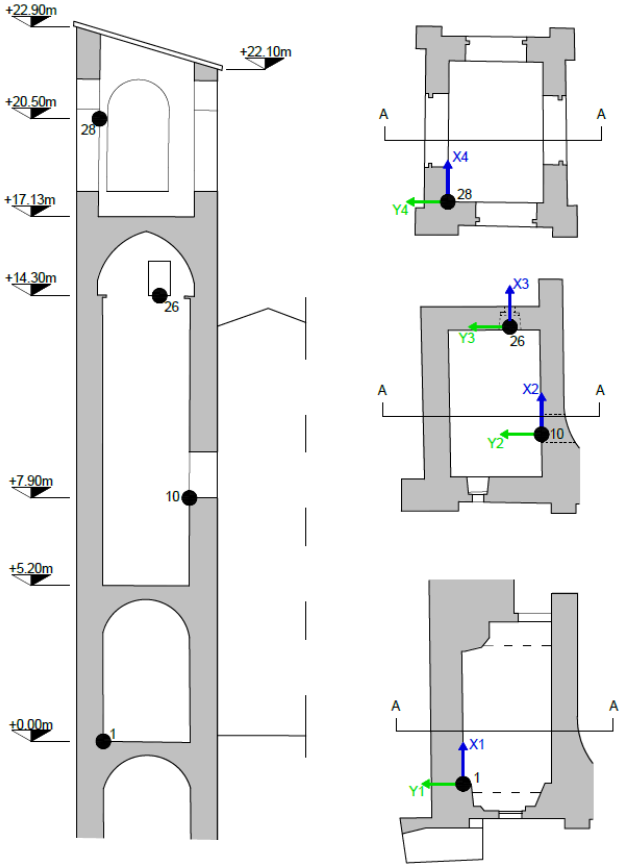

Figure 6.18: *Long-term monitoring sensors layouts*

pling rate is 200Hz. At the end of the continuous, the process enters trigger mode: if events occur, the system starts recording. In this case, a sampling rate of 1000Hz and a pre-trigger and post-trigger duration of 60 seconds are set.The data is then stored in a physical unit located on site, on the ground floor of the tower. Thanks to the Internet, they are uploaded online and can therefore be viewed and analysed remotely.
Environmental data (outside temperature, outside relative humidity and wind speed) were collected through a weather station located near the structure. All data can be retrieved and downloaded from the Italian Civil Protection website: http://app.protezionecivile.marche.it/sol/login.sol?lang=it.

Figure 6.19 shows the dynamic, electrical and physical parameters of the MEMS accelerometers used, while figure 6.20 shows an example of the acquired time signals.

DYNAMIC	
Range (g)	±2
Sensitivity (mV/g)	1000
Frequency Response (Hz)	0-200
Frequency Response (Hz)	0-600
Transverse Sensitivity (%)	<3
Non-Linearity (%FSO)	±0.5
Shock Limit (g)	2000
Residual Noise (µV rms)	600
Spectral Noise (µg/√Hz rms)	42
Self Test Output Change (mV)	X = +210 ±90 Y = -210 ±90 Z = -340 ±190

ELECTRICAL	
Zero Acceleration Output (V)	2.5 ±0.1
Excitation Voltage (Vdc)	5 to 30
Excitation Current (mA)	4
Full Scale Output Voltage (Vdc)	±2
Ground Isolation	Isolated from mounting surface

ENVIRONMENTAL	
Thermal Zero Shift (%FSO)	±4
Thermal Sensitivity Shift (%)	±5
Operating Temperature	-40 to +85°C (-40 to +185°F)
Humidity	Epoxy Sealed, IP65

PHYSICAL	
Housing Material	Nylon 6-6, 30% GF Molded Housing, Brass Inserts at Mounting Holes
Cable	6 x 0.14mm Conductors PVC Insulated, Braided Shield, PVC Jacket
Weight (grams)	50
Mounting	2x 1/4inch or M6 Metric Screws
Mounting Torque	18 lb-in (2.0 N-m)

Figure 6.19: *MEMS sensor parameters (model 4030)*

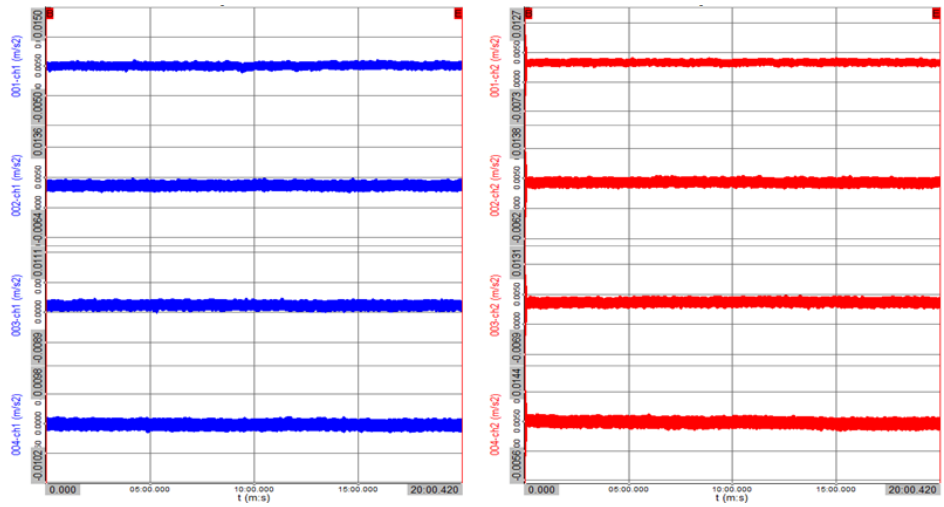

Figure 6.20: *Example of the acquired time signals with MEMS accelerometers*

6.4.2 Automatic identification process

The work started with the implementation of the algorithm for the automatic identification of the acquired data. In the following sections, the procedure will be shown with the results obtained.
After a presentation of the set workflow, the preliminary results, given by the short-term acquisition performed before the start of the continuous process, will be shown so that they can be set as targets for the automatic procedure. Then the results of the modal tracking will be shown even after the elimination of environmental factors.

6.4.2.1 The method

The implementation of the programme began considering the large amount of data it would have to process. Using various modules and toolboxes for processing, signal analysis and system identification, it was possible to handle all acceleration time series and thus extract the modal characteristics of the structure (natural frequencies f, mode shapes φ and damping ratios ξ). The data were saved in a specific file format according to the acquisition software, then converted to text files and loaded into the program. At this point, a specific script organises the data channels, sorting the columns of the file and, if necessary, adjusting the orientation of the axes.

In addition to the time histories, the program was set up to be able to return an experimental model (Figure 6.21). To do this, a file was imported containing the various geometric information such as the position of the nodes (in blue) and their connections and boundary conditions. The model thus obtained shows the structure under investigation schematically, but allows to visualise the mode shapes graphically. The acquisition points, i.e. where the sensors are attached, are highlighted in green.

Subsequently, after setting up all the characteristics for data analysis, the program starts analysing the acquisition files one by one. A general schematization of the procedure is presented in figure 6.22.

The methodology implemented was based on that proposed by *Ceravolo et al.* in [105]. It is possible to distinguish two stages:

I. after pre-processing operations, an initial analysis via the SSI-Cov method

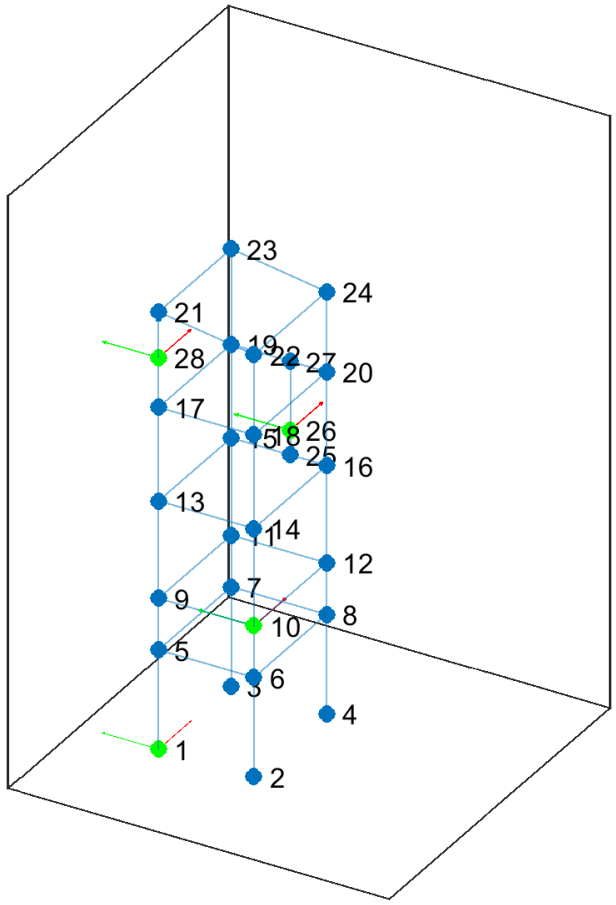

Figure 6.21: *Experimental model with highlighted reference nodes (in green)*

is applied to each data file; then the modal parameters for the different model orders are calculated and spurious poles are eliminated through two validation criteria;

II. the previously obtained parameter sets are subjected to *k-means* clustering analysis; through this, the most coherent modes and their corresponding parameters are identified.

Finally, the modal characteristics are correlated with the collected environmental data and their influence is removed by applying MRA.

6.4.2.2 Preliminary dynamic identification

This section shows the results obtained from the processing of the preliminary monitoring recordings.

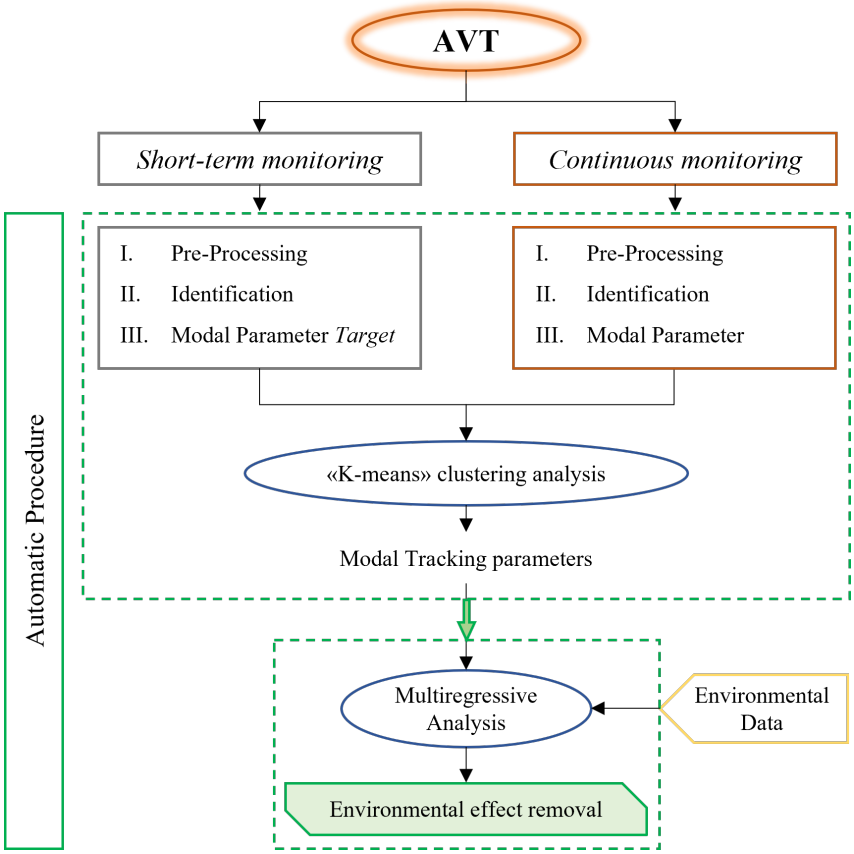

Figure 6.22: *Workflow of the automatic identification process*

The data were initially pre-processed by applying a filter to eliminate frequencies not of interest and a decimation. Given the structural type to be investigated, the frequency range of interest was set between 0 and 12.5Hz
At the end of this initial cleaning, the data is subjected to:

1. first identification process: automatic EFDD identification, in the frequency domain, so as to make the most significant modes evident;

2. second identification process: identification with the SSI-Cov method, then in the time domain, implemented with the same automatic algorithm that will be used for the modal tracking process of the continuous monitoring data.

Modal parameters (subsequent targets of the k-means clustering analysis) are chosen through an iterative comparison procedure: each j^{th} modal frequency and mode shape found in the time domain is compared with the i^{th} modal frequency and mode shape found in the frequency domain. The procedure

ends then the objective function expressed as [105] is minimised:

$$\delta_{i,j} = \left| \frac{f^i_{EFDD} - f^j_{SSI}}{f^i_{EFDD}} \right| + (1 - MAC_{i,j}) \tag{6.1}$$

Table 6.2 shows the results obtained for the first three modes.

Mode	$f(Hz)$	*Shape*
1	2.284	Translational X
2	3.383	Translational Y
3	6.087	Torsional

Table 6.2: *Modal frequencies of the tower identified from preliminary monitoring data*

In figure 6.23, the corresponding mode shapes are shown graphically. As also written in the table, the first mode is translational along the X-axis (based on the set axis orientation), the second translational along Y, and the third torsional. Recalling the figure 6.15, which showed the frequencies and modal shapes identified in 2017 and 2018, it can be said that the tower does not appear to have changed significantly.

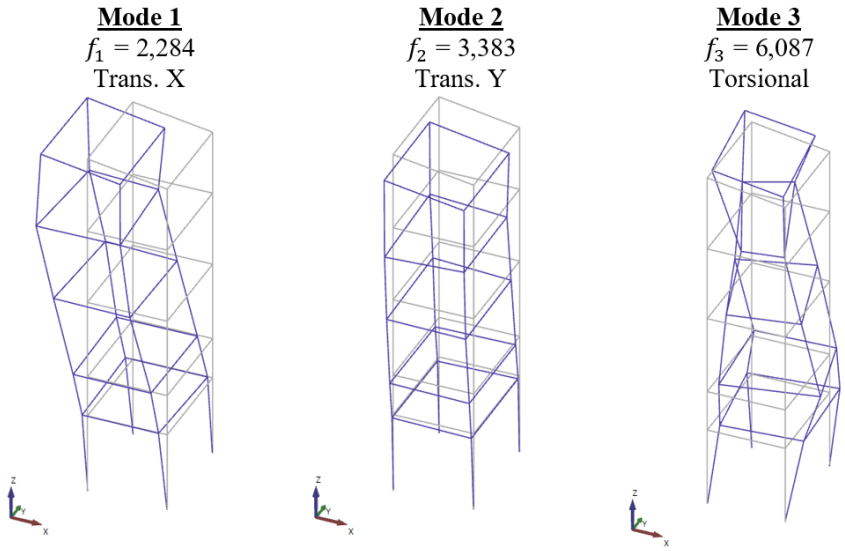

Figure 6.23: *Target frequencies and mode shapes*

6.4.2.3 Automatic modal parameters identification

Pre-processing data

At this point, having imported the continuous monitoring acquisitions and organised them, the process begins with a subroutine that takes care of the pre-processing operations:

- *filtering*: two digital filters are created (with the "designfilt" function), a high-pass filter between 0 and 0.5Hz, to remove disturbing factors for frequencies that are too low, and a low-pass Finite Input Response (FIR) filter based on the "Kaiser" window to remove unwanted frequency components that are too high;
- *decimation*: this is performed to remove all frequencies outside the range of interest, so from 200Hz (sampling frequency set for the continuous period) it goes to a maximum of 12.5Hz. Finally, a final filtering is performed to remove any noise due to resampling.

Stable poles identification

The pre-processed data thus individually introduced into the subroutine implementing the SSI-Cov method [42]. Recalling the discussion proposed in chapter 3, a state-space model is constructed through this method. The general equation of motion of the second order (Eq. 3.40) is converted into a system consisting of the state equation and the observation equation (Eq. 3.65).
The system contains the matrices A and C from which the modal parameters can be extracted. The eigenvalues μ_k of A are the poles of the discrete-time model of the state space, correlated with those of the continuous-time model, λ_k; among these poles, those with positive imaginary components are used to obtain the natural frequencies, f_k and modal damping ratios, ξ_k, via eq. 3.110.

As already mentioned in practical applications, it is not possible to know a priori the order of the model that best describes the dynamic behaviour of the structure to be investigated. Therefore the order is overestimated, considering the maximum value to be at least twice the number of expected physical modes, and the responses are calculated for each increasing order increment. The procedure can involve a high computational burden, so the solutions are calculated between the minimum and maximum order with a step size of five orders [105].

Recalling the discussion again in chapter 3 and chapter 4, considering high model orders can also result in the identification of solutions relating only to numerical modes, which are spurious and have no physical meaning. Such modes must be excluded, and to do so in a suitable manner, the stabilisation diagram is used (Paragraph 4.2.1).
The interpretation of the stabilisation diagram lends itself to being handled by clustering procedures [68, 106]. Through these, poles that maintain coherence on the stabilisation diagram in terms of natural frequency, mode shape and modal damping are recognised and are therefore stable (they almost always appear for the various model orders and manifest vertical alignment).

Elimination of spurious poles
The removal of spurious poles is crucial for accurate results, and thus adequate identification of physical modes. The presence of spurious modes can be due to various aspects, such as low Signal-to-Noise Ratio (SNR) of sensors or over-estimation of model order, as mentioned above.
Several considerations can be made in this regard. The first concerns the damping ratios. If we consider that the structure, when monitored, is in an operating condition, it is slightly damped and its behaviour is assumed to be stable. This necessarily implies that the damping ratio of a structural, physical mode is positive [107]. Furthermore, it can be stated that if highly damped modes (>10%) are identified, these are not realistic results due to the signal noise content [106].
In conclusion to this consideration, a first way to eliminate unstable poles is to set a *threshold* for the damping ratio: poles associated with a negative or high damping ratio are discarded.

Having removed most of the spurious poles, it is necessary to identify the set of modal estimates for the same model. To do this, a check is performed by imposing tolerance values on the variability of modal parameters for increasing

orders of the state-space model.

$$\delta_f = \left| \frac{f_{i,n} - f_{j,n+\Delta n}}{f_{i,n}} \right| \cdot 100 \leq \varepsilon_f$$

$$\xi_f = \left| \frac{\xi_{i,n} - \xi_{j,n+\Delta n}}{\xi_{i,n}} \right| \cdot 100 \leq \varepsilon_\xi \tag{6.2}$$

$$MAC(\varphi_{i,n}, \varphi_{j,n+\Delta n}) = \frac{|\varphi_{i,n} * \varphi_{j,n+\Delta n}|^2}{||\varphi_{i,n}||_2^2 ||\varphi_{j,n+\Delta n}||_2^2} \geq \varepsilon_{MAC}$$

Disadvantage of this strategy: strong human interaction is required during the analysis to adjust these tolerance values. In this case, in order to consider the poles associated with consecutive model orders as stable, the minimisation of a two-term objective function is required, which takes into account both the variation of frequencies and mode shapes [68, 105]:

$$\delta_{i,j} = \left| \frac{f^i_{target} - f^j_{continuous}}{f^i_{target}} \right| + (1 - MAC_{i,j}) \tag{6.3}$$

Figure 6.24 shows the stabilisation diagram reconstructed using the data obtained from the techniques just described. From the SVDs of the SSI-Cov method, the alignments corresponding to the stable modes were obtained.

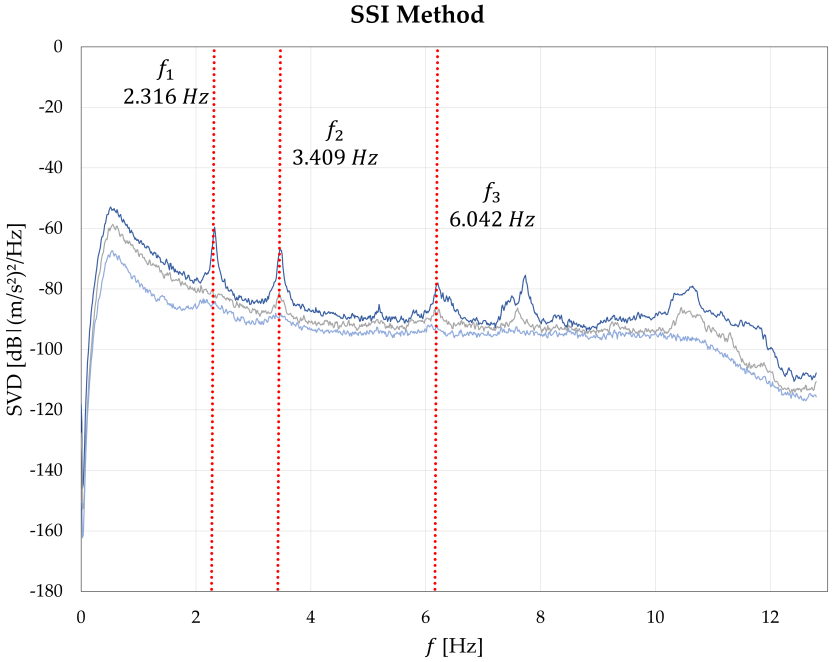

Figure 6.24: *Stabilization diagram*

Once these validation procedures are completed, the matrices containing all candidate modal parameters for each model order are subjected to the clustering process as described in the next section.

6.4.2.4 The "k-means" clustering analysis

All modal features associated with the extracted stable poles for the different model orders are grouped into a matrix, which undergoes *"k-means" clustering* [68, 108]. This is a partitioning method in which a k-means function groups the data into k mutually exclusive clusters. It then returns a value identifying the cluster for each observation (the observation and corresponding data are treated as an object occupying a space). The function attempts to organise partitions in such a way as to minimise the distances between elements of the same cluster and maximise those between different clusters. The requirements are: a distance metric and the definition of a number of clusters to be constructed. This type of clustering operates on actual observations, creating only a single cluster level, rather than a multi-level hierarchy.

Distances are calculated automatically via the Euclidean distance metric. The number of k partitions, on the other hand, is chosen as a multiple of the number of target parameters in order to separate the different parameters. Mode shapes and damping ratios are expressed through the average values of the partition elements and the corresponding standard deviation.

Once the groups are formed, the values are compared with the characteristics of the target modes by applying eq. 6.3, and those that minimise it are selected as plotted frequencies.

6.4.2.5 Preliminary results

At the end of this process, the script returns the modal frequency traces for the first three modes before removing the influence of environmental parameters (Figure 6.25). The gaps visible in the image are caused by malfunctions in the system that caused a temporary interruption.

For a bit of detail, zooming in on the results, we can better see how the frequencies fluctuate over the week and on the same day in the figure 6.26.

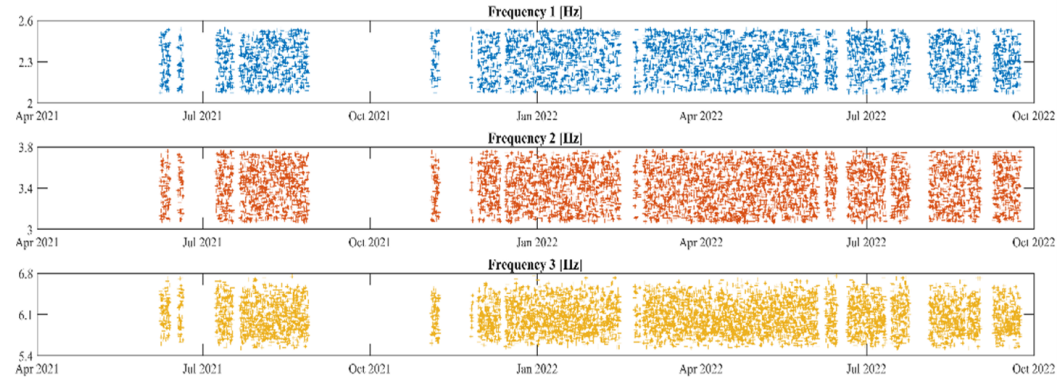

Figure 6.25: *Modal tracking of the frequencies associated to the first three modes*

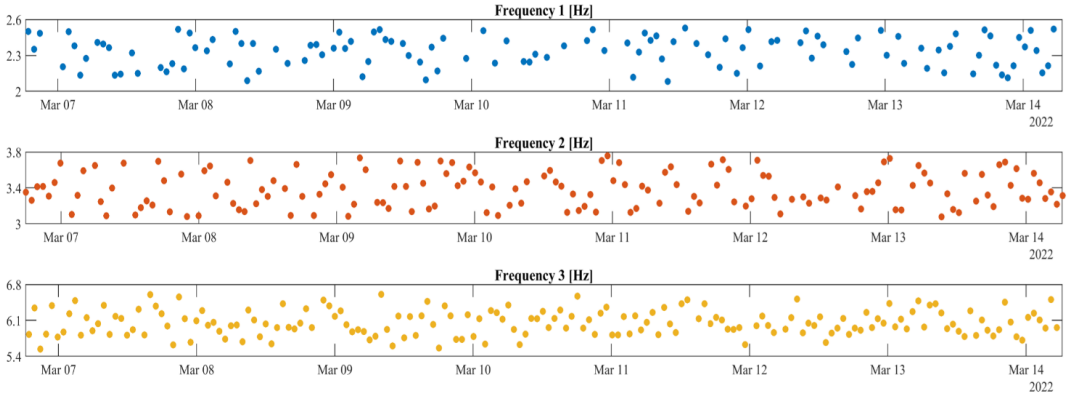

Figure 6.26: *Focus on one-week modal tracking of frequencies*

The table 6.3 shows the target values of the frequencies and the average values after cluster analysis. The percentage difference values show that there is a good match (a value is considered acceptable when it is $<5\%$). The largest difference is seen on the first frequency.

Mode	$f_T(Hz)$	$\bar{f}(Hz)$	$\lvert\Delta f\rvert(\%)$
1	2.284	2.316	1.401
2	3.383	3.409	0.769
3	6.087	6.042	0.739

Table 6.3: *Average values for tracked modal frequencies without environmental effects removal ($\bar{f}$) and comparison ($\lvert\Delta f\rvert$) with the correspondent target values (f_T)*

6.4.3 Environmental effects

As has already been discussed extensively, in order to develop a successful damage detection process, it is essential to identify modal characteristics that are closely linked to the structure alone. In the case of continuous monitoring, there are external influences due to environmental factors (temperature, humidity and wind) that make the task difficult. In many discussions in the literature, it is evident how these agents can also lead to significant variability [75–78, 81, 89]. Good modal tracking must be cleaned of these effects.
The first fundamental step is a thorough knowledge of the factors influencing the structure and how these are related, and to what extent, to the modal parameters [75]. Correlation can be performed with input-output [78, 79, 81, 82] or output-only models [80, 85–88]. To resume this topic, please refer to paragraph 4.3 in chapter 4. The application of such models makes it possible to recognise the occurrence of changes in structural behaviour (damage) by comparing predicted data with data from the processing of real measured data.

In the application proposed here, MRA was used. This is a technique for assessing the dependence between a variable and one or more independent factors, the predictors. For applications in the context of civil engineering-related SHM, the variables are the modal parameters, while the predictors are the environmental factors.
Once the correlation between these is established, the outcome of the variable can be predicted in response to the values assumed by the predictors.
The environmental parameters chosen as predictors in this work are external temperature $[C]$, external relative humidity [%] and average wind speed $[m/s]$. Figure 6.27 shows the results obtained for the frequencies. Figure 6.28 instead presents the results for the damping ratios. In this case, as can be seen, the dependence of damping on frequency was also taken into account during the correlation process, so the regression was performed using four parameters as predictors.
A certain constant trend can be observed in both frequencies and damping ratios.

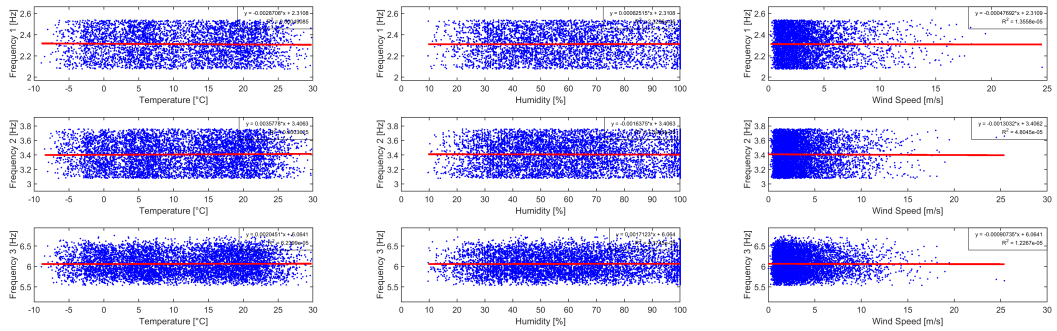

Figure 6.27: *Correlation of frequencies with environmental data*

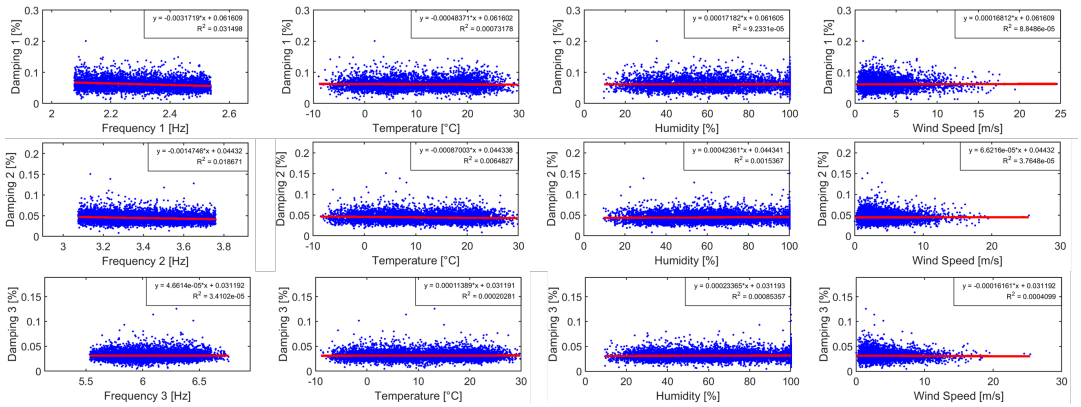

Figure 6.28: *Correlation of damping with frequencies and environmental data*

6.4.4 Final monitoring results

The autoregressive model (MRA) is then applied to the data.
The training phase has, as we have said, the objective of establishing the dependencies necessary to make a prediction of the modal output parameters. This phase is carried out on 80% of the data from the first year (July 2021 - July 2022, inclusive) of monitoring, while the remaining 20% is used as validation. The prediction is then processed on the remaining data (August 2022 - September 2022, inclusive).

Table 6.4 shows the average values of the predicted frequencies plotted, together with the target frequencies, and the previous average values without the removal of environmental factors. Their comparison certainly shows an improvement in the percentage difference, but very minimal.
In the figure 6.29, the modal tracking of frequencies is shown graphically. The predictions (in black) are superimposed on the original identified frequencies.

Mode	$f_T(Hz)$	$\bar{f}_p(Hz)$	$\lvert\Delta f_{t,p}\rvert(\%)$	$\bar{f}(Hz)$	$\lvert\Delta f_p\rvert(\%)$
1	2.284	2.306	0.963	2.316	0.434
2	3.383	3.407	0.709	3.409	0.059
3	6.087	6.071	0.263	6.042	0.478

Table 6.4: *Average values for predicted modal frequencies ($\bar{f}_p$) and comparison ($\lvert\Delta f_{t,p}$) with the correspondent target values (f_T); average values for previous tracked modal frequencies ($\bar{f}$) and comparison ($\lvert\Delta f_p\rvert$) with the correspondent predicted values*

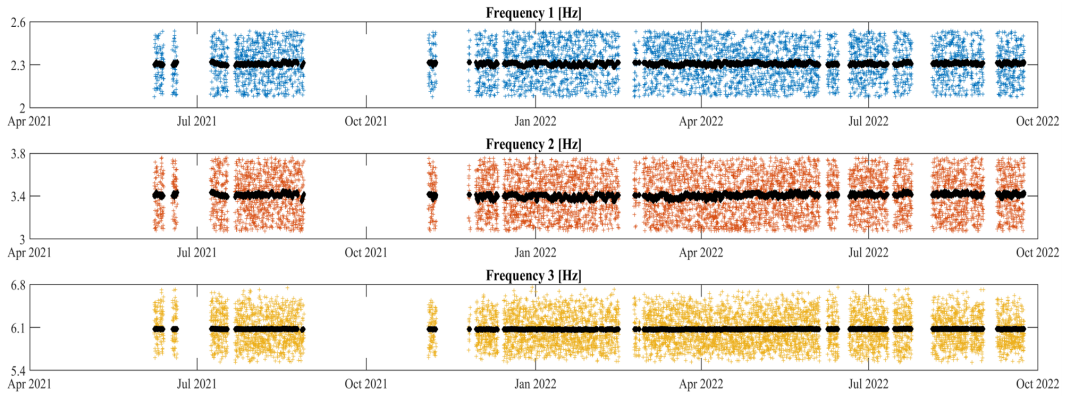

Figure 6.29: *Modal tracking of frequencies (in black) after removal of environmental effects*

6.5 Damage detection

As mentioned, it is the practice, from the vibration data measured with the monitoring system, to perform damage detection by detecting changes in modal parameters between the reference state and the current, possibly damaged state. Natural frequencies, which are rather reliably identifiable parameters, are mainly used for comparison. However, extensive pre-processing and data processing may be required. Exactly as demonstrated by the entire discussion above. Indeed, to arrive at a prediction of modal parameter values that can be compared with target values, the process was quite laborious. Thus, in practice, a lot of time certainly elapsed between the acquisition of the recordings and the check for the presence of a possible anomaly. Consequently, the elimination of the structure identification phase and subsequent modal tracking could be advantageous.

In this work, to achieve the goal of having an almost instantaneous response, an alarm, regarding changes in the dynamic behaviour of the structure, a subspace-based fault detection residual was implemented.

This damage detection technique (Paragraph 4.4) uses a subspace-based residual function and a statistical hypothesis test ($\chi^2 - test$) built on it. This test allows comparison of the reference state model with the current, possibly damaged, state model in order to detect the damage, avoiding the estimation of modal parameters. Measured vibration data are used directly and as they may be affected by changes in the covariance of the excitation, the method is corrected to be robust.

The results of the implementation of this procedure are shown in figure 6.30:

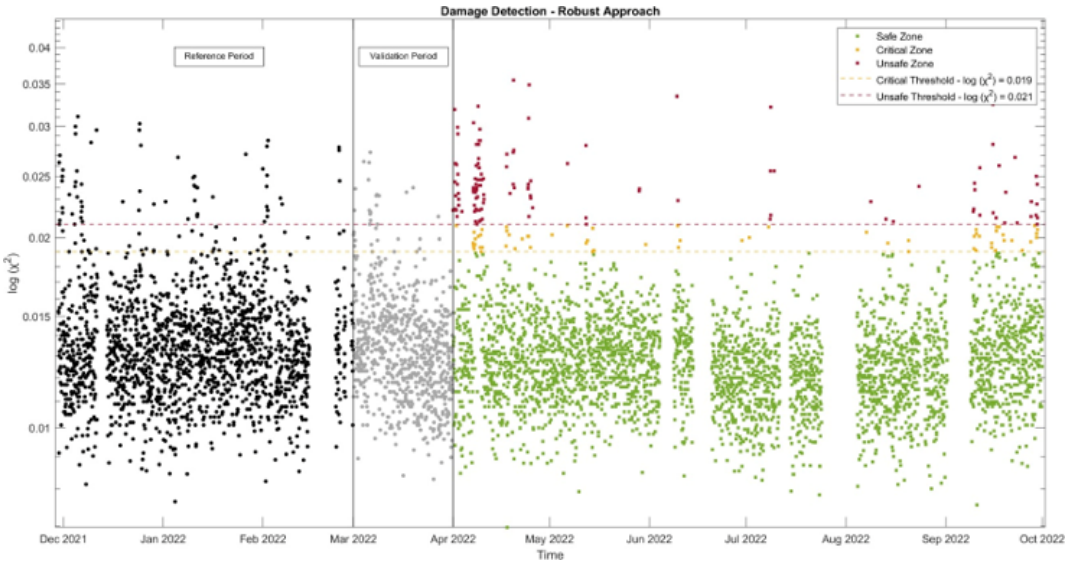

Figure 6.30: *Diagram of the tower damage identification*

Again, empty gaps between the results indicate temporary breaks in the system. Furthermore, the records obtained between July 2021 and December 2021 were excluded from the analysis, because the gap that was present (August 2021 - November 2021) was too large to falsify the results.

The first step was the choice of the *reference period* (black dots) in which to consider the structure "undamaged". Based on this period of just over three months (December 2021 to the beginning of March 2022), the implemented procedure "trained" itself and calculated a threshold based on the mean and variance of the χ^2 values of the measurements. The reference period itself and thus the threshold were then subsequently validated through a one-month *validation period* (grey dots). Thus, the remaining period is identified as the *inspection period* (green dots).

A fundamental condition for all measurements of the inspection period to be considered healthy is that the extracted χ^2 value remains below the calculated threshold. From the threshold value, corresponding to the red line, a second, lower threshold (yellow line) was chosen. Thus, in addition to defining an unsafe zone, above the red line, a critical zone was also identified. This means that between the yellow line (corresponding to 95% of the calculated threshold) and the red line we are in a situation where the dynamic behaviour of the structure has changed to the point of risking damage.

In order to interpret the diagram correctly, some clarifications must be made. The points displayed on the diagram "graphically represent" the behaviour of the tower. To be clearer, these points indicate the possible presence of damage because the dynamic behaviour of the structure has changed. So if we focus especially on the red points, which are those that return an alarm because the calculated χ^2 value is above the threshold, these tell us that there has been an unknown vibration that has temporarily modified the behaviour of the structure.

To explain further, let us consider the actual acquisitions corresponding to some of the red dots displayed on the diagram (Figure 6.31).

- 9-10/04/2022: unknown vibrations were recorded. They do not seem to correspond to any recorded earthquake (using the database provided by the Istituto Nazionale di Geofisica e Vulcanologia - INGV), in fact there are several around the same day and in the following days. There was probably a condition, external or internal to the structure, that produced these vibrations.
- 20/07/2022: recorded earthquake sequence with epicentre in Crete.
- 22/09/2022: earthquake recorded with epicentre in Folignano (in the province of Ascoli Piceno, Marche).

The fact that after an unexpected excitation, the χ^2 values extracted from the measurements fall back into the green zone clearly indicates that the change in dynamic behaviour was not permanent. It is therefore assumed that there was no real damage that caused an irreparable change in the dynamics, otherwise we would have expected all points to be concentrated in the unsafe zone.

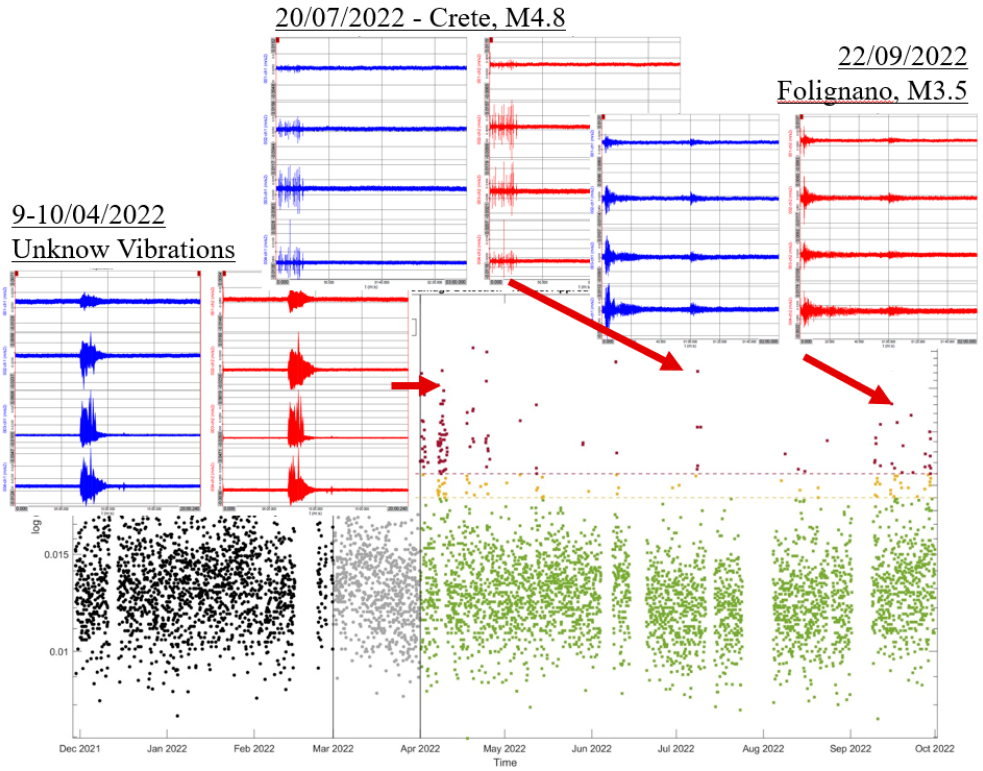

Figure 6.31: *Diagram of the tower damage identification: details*

It should be emphasised that not all earthquakes or vibrations in general have the same impact on the dynamic behaviour of the structure, so we tried to implement an intelligent selection of alarms in the algorithm, so that the red dots indicate vibrations that could really be significant and therefore potentially dangerous.

Chapter 7

Conclusion

Reviewing all the work carried out and proposed here, the discussion was opened with a wide-ranging introduction in which we highlighted all the advantages, but also the disadvantages and criticalities, that a process such as SHM can bring if correctly, but above all widely, used.
In fact, the issue of the conservation of buildings, especially historic ones, is now widespread and of common interest.
However, we would like to focus attention on the question of its actual use, both with regard to the topic just outlined and for its application on strategic structures, infrastructures, or even simple homes for civil use.
Because of the great benefits it could bring, it is still considered to be underexploited. It is obvious that in order to fully utilise it, it must also be possible for less expert users to correctly interpret the results.

The OMA allows an identification of the structure under operating conditions, without having to interrupt the operability of the structure in any way. This is very significant when considering an infrastructure such as a bridge, or a strategic structure such as a hospital.

The Italian territory, like many other countries in Europe, must deal with a high seismic hazard and with the now periodic succession of events of considerable magnitude. Acting as a consequence of a seismic sequence is certainly more expensive, involves very long timescales for the design and execution of the necessary interventions, and therefore foresees a long period of inactivity of the structure, if it is considered unfit for use or unsafe for the protection of people's lives.

In such a scenario, being able to have constant and continuous information on the variations in the dynamic behaviour of a structure, makes it possible to have information that can be used to implement the necessary maintenance in a preventive manner. In this way: the use of the structure remains unaltered; preventive interventions can be implemented that can support the structure in the event of an earthquake occurring; linked to this last reason, it is easier to conserve historical structures while respecting their original layout; and last but not least, safety for people is improved.

On the basis of all these considerations, the work that has been carried out will hopefully help, together with that of many other researchers, to aid the diffusion of SHM in continuous use.

The work steps can be summarised as follows:

- implementation of an automated procedure for the identification and modal tracking of the parameters of a continuously monitored structure. This procedure produced good results, especially considering that even after the removal of environmental effects, the results in terms of natural frequencies remained almost unchanged. As much as this procedure can help in the handling and processing of a large amount of data, such as that from continuous monitoring, it is still a lengthy process. Therefore, as already mentioned, the time between recordings and expected results is not very short. Consequently, the identification of the resulting damage is not immediate. To meet this need, the focus shifted to the second step of the work, namely:

- implementation of a damage detection technique that eliminates the entire record processing phase and uses the collected time series directly for analysis. In this way, satisfactory results were obtained in terms of timing, but above all in the interpretation of the results. The alarm that the program sends out at the moment of a possible dangerous situation is easy for everyone to read. It is obvious that in order to verify the actual significance of this alarm, the intervention of experts sensitive to the subject is necessary.

In conclusion, the procedure for identifying possible damage states can still be significantly improved. In fact, the program's ability to select vibrations that

may actually be harmful to the structure should be even more refined, and it would be interesting to be able to add to the procedure the possibility of precisely identifying the location of damage, should this be necessary.
With reference to what has just been said, a further development of the work presented here is based on the use of the numerical model through which, after calibration, it would be possible to generate damage scenarios.

Bibliography

[1] Francesco Clementi, Angela Ferrante, Ersilia Giordano, Frédéric Dubois, and Stefano Lenci. Damage assessment of ancient masonry churches stroked by the central italy earthquakes of 2016 by the non-smooth contact dynamics method. *Bulletin of Earthquake Engineering*, 18(2):455–486, 2020. https://doi.org/10.1007/s10518-019-00613-4.

[2] Sergio Lagomarsino and Stefano Podestà. Damage and vulnerability assessment of churches after the 2002 molise, italy, earthquake. *Earthquake Spectra*, 20 (1_suppl):271–283, 2004. https://doi.org/10.1193/1.1767161.

[3] Maurizio Acito, Massimiliano Bocciarelli, Claudio Chesi, and Gabriele Milani. Collapse of the clock tower in finale emilia after the may 2012 emilia romagna earthquake sequence: Numerical insight. *Engineering Structures*, 72:70–91, 2014. https://doi.org/10.1016/j.engstruct.2014.04.026.

[4] Michele Betti and Andrea Vignoli. Numerical assessment of the static and seismic behaviour of the basilica of santa maria all'impruneta (italy). *Construction and Building Materials*, 25(12):4308–4324, 2011. https://doi.org/10.1016/j.conbuildmat.2010.12.028.

[5] Giuseppe Brandonisio, Giuseppe Lucibello, Elena Mele, and Antonello De Luca. Damage and performance evaluation of masonry churches in the 2009 l'aquila earthquake. *Engineering Failure Analysis*, 34:693–714, 2013. https://doi.org/10.1016/j.engfailanal.2013.01.021.

[6] Charles R Farrar and Keith Worden. An introduction to structural health monitoring. *Philosophical Transactions of the Royal Society A: Mathematical, Physical and Engineering Sciences*, 365(1851):303–315, 2007. doi:10.1098/rsta.2006.1928.

[7] Carmelo Gentile, Marco Guidobaldi, and Antonella Saisi. One-year dynamic monitoring of a historic tower: damage detection under changing environment. *Meccanica*, 51(11):2873–2889, 2016. https://doi.org/10.1007/s11012-016-0482-3.

[8] Keith Worden and Janice M Dulieu-Barton. An overview of intelligent fault detection in systems and structures. *Structural Health Monitoring*, 3(1):85–98, 2004. doi:10.1177/1475921704041866.

[9] Antonella Saisi, Carmelo Gentile, and Marco Guidobaldi. Post-earthquake continuous dynamic monitoring of the gabbia tower in mantua, italy. *Construction and Building Materials*, 81:101–112, 2015. https://doi.org/10.1016/j.conbuildmat.2015.02.010.

[10] Giovanni Castellazzi, Antonio Maria D'Altri, Stefano de Miranda, Andrea Chiozzi, and Antonio Tralli. Numerical insights on the seismic behavior of a non-isolated historical masonry tower. *Bulletin of Earthquake Engineering*, 16(2):933–961, 2018. https://doi.org/10.1007/s10518-017-0231-6.

[11] Alessandro Cabboi, Carmelo Gentile, and Antonella Saisi. From continuous vibration monitoring to fem-based damage assessment: Application on a stone-masonry tower. *Construction and Building Materials*, 156:252–265, 2017. https://doi.org/10.1016/j.conbuildmat.2017.08.160.

[12] Gianni Bartoli, Michele Betti, Luciano Galano, and Giacomo Zini. Numerical insights on the seismic risk of confined masonry towers. *Engineering Structures*, 180:713–727, 2019. https://doi.org/10.1016/j.engstruct.2018.10.001.

[13] Vanni Nicoletti, Davide Arezzo, Sandro Carbonari, and Fabrizio Gara. Expeditious methodology for the estimation of infill masonry wall stiffness through in-situ dynamic tests. *Construction and Building Materials*, 262:120807, 2020. https://doi.org/10.1016/j.conbuildmat.2020.120807.

[14] Dora Foti, Vincenzo Gattulli, and Francesco Potenza. Output-only identification and model updating by dynamic testing in unfavorable conditions of a seismically damaged building. *Computer-Aided Civil and Infrastructure Engineering*, 29(9):659–675, 2014. doi:10.1111/mice.12071.

[15] Carmelo Gentile and A Saisi. Ambient vibration testing of historic masonry towers for structural identification and damage assessment. *Construction and building materials*, 21(6):1311–1321, 2007. https://doi.org/10.1016/j.conbuildmat.2006.01.007.

[16] Filippo Ubertini, Carmelo Gentile, and Annibale Luigi Materazzi. Automated modal identification in operational conditions and its application to bridges. *Engineering Structures*, 46:264–278, 2013. https://doi.org/10.1016/j.engstruct.2012.07.031.

[17] Francesca Bianconi, Georgios Panagiotis Salachoris, Francesco Clementi, and Stefano Lenci. A genetic algorithm procedure for the automatic updating of fem based on ambient vibration tests. *Sensors*, 20(11):3315, 2020. https://doi.org/10.3390/s20113315.

[18] Filipe Magalhães and Álvaro Cunha. Explaining operational modal analysis with data from an arch bridge. *Mechanical systems and signal processing*, 25 (5):1431–1450, 2011. https://doi.org/10.1016/j.ymssp.2010.08.001.

[19] Rune Brincker and Lingmi Zhang. Frequency domain decomposition revisited. In *Proc. 3rd Int. Operational Modal Analysis Conf.(IOMAC'09)*, pages 615–626, 2009.

[20] Anders Rytter. Vibrational based inspection of civil engineering structures. 1993.

[21] MM Abdel Wahab and Guido De Roeck. Damage detection in bridges using modal curvatures: application to a real damage scenario. *Journal of Sound and vibration*, 226(2):217–235, 1999. https://doi.org/10.1006/jsvi.1999.2295.

[22] RD Adams, JE Flitcroft, D Short, and D Walton. *Vibration testing as a non-destructive test tool for composite materials*. ASTM International, 1975.

[23] Scott W Doebling, Charles R Farrar, Michael B Prime, and Daniel W Shevitz. Damage identification and health monitoring of structural and mechanical systems from changes in their vibration characteristics: a literature review. 1996. https://doi.org/10.2172/249299.

[24] Scott W Doebling, Charles R Farrar, Michael B Prime, et al. A summary review of vibration-based damage identification methods. *Shock and vibration digest*, 30(2):91–105, 1998.

[25] Ersilia Giordano, Nuno Mendes, Maria Giovanna Masciotta, Francesco Clementi, Neda Haji Sadeghi, Rui André Silva, and Daniel V Oliveira. Expeditious damage index for arched structures based on dynamic identification testing. *Construction and Building Materials*, 265:120236, 2020. https://doi.org/10.1016/j.conbuildmat.2020.120236.

[26] Bart Peeters and Guido De Roeck. Stochastic system identification for operational modal analysis: a review. *J. Dyn. Sys., Meas., Control*, 123(4):659–667, 2001. https://doi.org/10.1115/1.1410370.

[27] Bart Peeters. System identification and damage detection in civil engeneering. 2000.

[28] John E Mottershead and MI Friswell. Model updating in structural dynamics: a survey. *Journal of sound and vibration*, 167(2):347–375, 1993. https://doi.org/10.1006/jsvi.1993.1340.

[29] Sheng-En Fang and Ricardo Perera. Power mode shapes for early damage detection in linear structures. *Journal of Sound and Vibration*, 324(1-2):40–56, 2009. https://doi.org/10.1016/j.jsv.2009.02.002.

[30] YJ Yan, Li Cheng, ZY Wu, and LH Yam. Development in vibration-based structural damage detection technique. *Mechanical systems and signal processing*, 21(5):2198–2211, 2007. https://doi.org/10.1016/j.ymssp.2006.10.002.

[31] Enrique García-Macías and Filippo Ubertini. Seismic interferometry for earthquake-induced damage identification in historic masonry towers. *Mechanical Systems and Signal Processing*, 132:380–404, 2019. https://doi.org/10.1016/j.ymssp.2019.06.037.

[32] Michele Basseville, Maher Abdelghani, and Albert Benveniste. Subspace-based fault detection algorithms for vibration monitoring. *Automatica*, 36(1):101–109, 2000. https://doi.org/10.1016/S0005-1098(99)00093-X.

[33] Michael Döhler, Laurent Mevel, and Falk Hille. Subspace-based damage detection under changes in the ambient excitation statistics. *Mechanical Systems and Signal Processing*, 45(1):207–224, 2014. https://doi.org/10.1016/j.ymssp.2013.10.023.

[34] James MW Brownjohn. Structural health monitoring of civil infrastructure. *Philosophical Transactions of the Royal Society A: Mathematical, Physical and Engineering Sciences*, 365(1851):589–622, 2007.

[35] Fu-Kuo Chang, Johannes FC Markmiller, Jinkyu Yang, and Yujun Kim. Structural health monitoring. *System health management: with aerospace applications*, pages 419–428, 2011. https://doi.org/10.1002/9781119994053.ch26.

[36] Charles R Farrar, Scott W Doebling, and David A Nix. Vibration–based structural damage identification. *Philosophical Transactions of the Royal Society of London. Series A: Mathematical, Physical and Engineering Sciences*, 359 (1778):131–149, 2001. https://doi.org/10.1098/rsta.2000.0717.

[37] F Necati Çatbaş, Tracy Kijewski-Correa, and A Emin Aktan. Structural identification of constructed systems: approaches, methods, and technologies for effective practice of st-id. American Society of Civil Engineers, 2013. https://doi.org/10.1061/9780784411971.

[38] Giovanni Fabbrocino, Carlo Rainieri, and GM Verderame. L'analisi dinamica sperimentale e il monitoraggio delle strutture esistenti. *Controllo e monitoraggio di edifici in Calcestruzzo Armato: il caso-studio di Punta Perotti Giornata di Studio ENEA*, 2007.

[39] Carlo Rainieri, Giovanni Fabbrocino, Edoardo Cosenza, and Gaetano Manfredi. Implementation of oma procedures using labview: theory and application. In *2nd international operational modal analysis conference*, volume 30, pages 1–13. Denmark Copenhagen, 2007.

[40] R.W. Clough and J. Penzien. *Dynamics of structures*. Computers Structures, Inc., Berkley, CA USA, 2003.

[41] Julius S Bendat and Allan G Piersol. Engineering applications of correlation and spectral analysis. *New York*, 1980.

[42] Bart Peeters and Guido De Roeck. Reference-based stochastic subspace identification for output-only modal analysis. *Mechanical systems and signal processing*, 13(6):855–878, 1999. https://doi.org/10.1006/mssp.1999.1249.

[43] Haluk Elci, Richard W Longman, Minh Phan, Jer-Nan Juang, and Roberto Ugoletti. Discrete frequency based learning control for precision motion control. In *Proceedings of IEEE International Conference on Systems, Man and Cybernetics*, volume 3, pages 2767–2773. IEEE, 1994. https://doi.org/10.1109/ICSMC.1994.400292.

[44] Peter Van Overschee and Bart De Moor. Continuous-time frequency domain subspace system identification. *Signal Processing*, 52(2):179–194, 1996. https://doi.org/10.1016/0165-1684(96)00052-7.

[45] P. Verboven, P. Guillaume, B. Cauberghe, S. Vanlanduit, and E. Parloo. Modal parameter estimation from input–output fourier data using frequency-domain maximum likelihood identification. *J. Sound Vib.*, 276:957–979, 2004. https://doi.org/10.1016/j.jsv.2003.08.044.

[46] Jer-Nan Juang and Richard S Pappa. An eigensystem realization algorithm for modal parameter identification and model reduction. *Journal of guidance, control, and dynamics*, 8(5):620–627, 1985. https://doi.org/10.2514/3.20031.

[47] A Cunha, A Cabboi, F Magalhães, and C Gentile. Automated modal identification and tracking: Application to an iron arch bridge. 2017. https://doi.org/10.1002/stc.1854.

[48] Patrick Guillaume, Luc Hermans, and Herman Van Der Auweraer. Maximum likelihood identification of modal parameters from operational data. In *IMAC-PROCEEDINGS OF THE 17TH INTERNATIONAL MODAL ANALYSIS CONFERENCE, VOLS I AND II*, volume 3727, pages 1887–1893. Society of Photo-optical Instrumentation Engineers, 1999.

[49] Rune Brincker, Lingmi Zhang, and Palle Andersen. Modal identification of output-only systems using frequency domain decomposition. *Smart materials and structures*, 10(3):441, 2001. https://doi.org/10.1088/0964-1726/10/3/303.

[50] Christof Devriendt and Patrick Guillaume. Identification of modal parameters from transmissibility measurements. *Journal of Sound and Vibration*, 314(1-2): 343–356, 2008. https://doi.org/10.1016/j.jsv.2007.12.022.

[51] Bart Peeters, Herman Van der Auweraer, Patrick Guillaume, and Jan Leuridan. The polymax frequency-domain method: a new standard for modal parameter estimation? *Shock and Vibration*, 11(3-4):395–409, 2004.

[52] Andreas Felber and Reto Cantieni. Advances in ambient vibration testing: Ganter bridge, switzerland. *Structural Engineering International*, 6(3):187–190, 1996. https://doi.org/10.2749/101686696780495671.

[53] SF Stiemer and AJ Felber. Object-oriented approach to ambient vibration measurement analysis. *Journal of computing in civil engineering*, 7(4):420–438, 1993. https://doi.org/10.1061/(ASCE)0887-3801(1993)7:4(420).

[54] Rune Brincker and Lingmi Zhang. Modal identification from ambient responses using frequency domain decomposition. In *Proc. 18th Int. Modal Anal. Conf. San Antonio, TX, Febr., San Antonio, Texas*, page 625–630, 2000.

[55] CY Shih, YG Tsuei, RJ Allemang, and DL Brown. Complex mode indication function and its applications to spatial domain parameter estimation. *Mechanical systems and signal processing*, 2(4):367–377, 1988. https://doi.org/10.1016/0888-3270(88)90060-X.

[56] Peter Welch. The use of fast fourier transform for the estimation of power spectra: a method based on time averaging over short, modified periodograms. *IEEE Transactions on audio and electroacoustics*, 15(2):70–73, 1967. https://doi.org/10.1109/TAU.1967.1161901.

[57] Rune Brincker, Carlos E Ventura, and Palle Andersen. Damping estimation by frequency domain decomposition. In *Proceedings of IMAC 19: A Conference on Structural Dynamics: februar 5-8, 2001, Hyatt Orlando, Kissimmee, Florida, 2001*, pages 698–703. Society for Experimental Mechanics, 2001.

[58] Filipe Magalhães, Álvaro Cunha, Elsa Caetano, and Rune Brincker. Damping estimation using free decays and ambient vibration tests. *Mechanical Systems and Signal Processing*, 24(5):1274–1290, 2010. https://doi.org/10.1016/j.ymssp.2009.02.011.

[59] R. J. Allemang and D. L. Brown. A correlation coefficient for modal testing. In *Proc. 1st Int. Modal Anal. Conf.*, 1983.

[60] Miroslav Pastor, Michal Binda, and Tomáš Harčarik. Modal assurance criterion. *Procedia Engineering*, 48:543–548, 2012. https://doi.org/10.1016/j.proeng.2012.09.551.

[61] Filipe Magalhães, Álvaro Cunha, and Elsa Caetano. Dynamic monitoring of a long span arch bridge. *Engineering Structures*, 30(11):3034–3044, 2008. https://doi.org/10.1016/j.engstruct.2008.04.020.

[62] Lennart Ljung. System identification. In *Signal analysis and prediction*, pages 163–173. Springer, 1998. https://doi.org/10.1007/978-1-4612-1768-811.

[63] Edwin Reynders and Guido De Roeck. System identification and operational modal analysis with macec enhanced. In *2nd International Operational Modal Analysis Conference*, pages 325–331, 2007.

[64] Artemis modal. 2018.

[65] Farhat Fnaiech and Lennart Ljung. Recursive identification of bilinear systems. *International journal of control*, 45(2):453–470, 1987. https://doi.org/10.1080/00207178708933743.

[66] Jer-Nan Juang. *Applied system identification*. Prentice-Hall, Inc., 1994.

[67] Palle Andersen, Rune Brincker, Maurice Goursat, and Laurent Mevel. Automated modal parameter estimation for operational modal analysis of large systems. In *Proceedings of the 2nd international operational modal analysis conference*, pages 299–308, 2007.

[68] Filipe Magalhaes, Alvaro Cunha, and Elsa Caetano. Online automatic identification of the modal parameters of a long span arch bridge. *Mechanical Systems and Signal Processing*, 23(2):316–329, 2009. https://doi.org/10.1016/j.ymssp.2008.05.003.

[69] Bart Peeters, G Couvreur, O Razinkov, C Kündig, Herman Van Der Auweraer, and Guido De Roeck. Continuous monitoring of the øresund bridge: system and data analysis. *Structures and Infrastructure Engineering*, 5(5):395–405, 2009.

[70] Carmelo Gentile and Antonella Saisi. Continuous dynamic monitoring of a centenary iron bridge for structural modification assessment. *Frontiers of Structural and Civil Engineering*, 9(1):26–41, 2015. https://doi.org/10.1007/s11709-014-0284-4.

[71] Filippo Ubertini, Gabriele Comanducci, and Nicola Cavalagli. Vibration-based structural health monitoring of a historic bell-tower using output-only measurements and multivariate statistical analysis. *Structural Health Monitoring*, 15 (4):438–457, 2016.

[72] Richard S Pappa, George H James III, and David C Zimmerman. Autonomous modal identification of the space shuttle tail rudder. *Journal of Spacecraft and Rockets*, 35(2):163–169, 1998.

[73] Peter Verboven, Eli Parloo, Patrick Guillaume, and Marc Van Overmeire. Autonomous modal parameter estimation based on a statistical frequency domain maximum likelihood approach. In *Proceedings, International Modal Analysis Conference (IMAC)*, page 15111517, 2001.

[74] Peter Verboven, Eli Parloo, Patrick Guillaume, and Marc Van Overmeire. Autonomous structural health monitoring—part i: modal parameter estimation and tracking. *Mechanical Systems and Signal Processing*, 16(4):637–657, 2002. doi:10.1006/mssp.1492.

[75] EJ Cross, KY Koo, JMW Brownjohn, and K Worden. Long-term monitoring and data analysis of the tamar bridge. *Mechanical Systems and Signal Processing*, 35(1-2):16–34, 2013. https://doi.org/10.1016/j.ymssp.2012.08.026.

[76] Charles R Farrar, Scott W Doebling, Phillip J Cornwell, and Erik G Straser. Variability of modal parameters measured on the alamosa canyon bridge. Technical report, Los Alamos National Lab.(LANL), Los Alamos, NM (United States), 1996. https://doi.org/10.1006/jsvi.1997.0977.

[77] Bart Peeters and Guido De Roeck. One-year monitoring of the z24-bridge: environmental effects versus damage events. *Earthquake engineering & structural dynamics*, 30(2):149–171, 2001. https://doi.org/10.1002/1096-9845(200102)30:2<149::AID-EQE1>3.0.CO;2-Z.

[78] Jyrki Kullaa. Eliminating environmental or operational influences in structural health monitoring using the missing data analysis. *Journal of Intelligent Material Systems and Structures*, 20(11):1381–1390, 2009. https://doi.org/10.1177/1045389X08096050.

[79] A-M Yan, Gaëtan Kerschen, Pascal De Boe, and J-C Golinval. Structural damage diagnosis under varying environmental conditions—part i: a linear analysis. *Mechanical Systems and Signal Processing*, 19(4):847–864, 2005. https://doi.org/10.1016/j.ymssp.2004.12.002.

[80] Arnaud Deraemaeker, Edwin Reynders, Guido De Roeck, and Jyrki Kullaa. Vibration-based structural health monitoring using output-only measurements under changing environment. *Mechanical systems and signal processing*, 22(1): 34–56, 2008. https://doi.org/10.1016/j.ymssp.2007.07.004.

[81] Hoon Sohn, Keith Worden, and Charles R Farrar. Statistical damage classification under changing environmental and operational conditions. *Journal of intelligent material systems and structures*, 13(9):561–574, 2002. https://doi.org/10.1106/104538902030904.

[82] Steve Vanlanduit, Peter Verboven, Patrick Guillaume, and Joannes Schoukens. An automatic frequency domain modal parameter estimation algorithm. *Journal of Sound and Vibration*, 265(3):647–661, 2003. https://doi.org/10.1016/S0022-460X(02)01461-X.

[83] David E Newland. Harmonic wavelet analysis. *Proceedings of the Royal Society of London. Series A: Mathematical and Physical Sciences*, 443(1917):203–225, 1993. https://doi.org/10.1098/rspa.1993.0140.

[84] Richard A Johnson, Dean W Wichern, et al. Applied multivariate statistical analysis. *New Jersey*, 405, 1992.

[85] Jyrki Kullaa. Damage detection of the z24 bridge using control charts. *Mechanical Systems and Signal Processing*, 17(1):163–170, 2003. https://doi.org/10.1006/mssp.2002.1555.

[86] Enrique García-Macías and Filippo Ubertini. Mova/moss: Two integrated software solutions for comprehensive structural health monitoring of structures. *Mechanical Systems and Signal Processing*, 143:106830, 2020. https://doi.org/10.1016/j.ymssp.2020.106830.

[87] Gabriele Comanducci, Filipe Magalhães, Filippo Ubertini, and Álvaro Cunha. On vibration-based damage detection by multivariate statistical techniques: Application to a long-span arch bridge. *Structural health monitoring*, 15(5): 505–524, 2016. DOI: 10.1177/ToBeAssigned.

[88] Filippo Ubertini, Gabriele Comanducci, Nicola Cavalagli, Anna Laura Pisello, Annibale Luigi Materazzi, and Franco Cotana. Environmental effects on natural

frequencies of the san pietro bell tower in perugia, italy, and their removal for structural performance assessment. *Mechanical Systems and Signal Processing*, 82:307–322, 2017. https://doi.org/10.1016/j.ymssp.2016.05.025.

[89] Luis F Ramos, Leandro Marques, Paulo B Lourenço, Guido De Roeck, A Campos-Costa, and João Roque. Monitoring historical masonry structures with operational modal analysis: two case studies. *Mechanical systems and signal processing*, 24(5):1291–1305, 2010. https://doi.org/10.1016/j.ymssp.2010.01.011.

[90] Keith Worden, Graeme Manson, and Nick RJ Fieller. Damage detection using outlier analysis. *Journal of Sound and vibration*, 229(3):647–667, 2000. https://doi.org/10.1006/jsvi.1999.2514.

[91] Michèle Basseville, Laurent Mevel, and Maurice Goursat. Statistical model-based damage detection and localization: subspace-based residuals and damage-to-noise sensitivity ratios. *Journal of sound and vibration*, 275(3-5): 769–794, 2004. https://doi.org/10.1016/j.jsv.2003.07.016.

[92] Etienne Balmès, Michèle Basseville, Frédéric Bourquin, Laurent Mevel, Houssein Nasser, and Fabien Treyssède. Merging sensor data from multiple temperature scenarios for vibration monitoring of civil structures. *Structural health monitoring*, 7(2):129–142, 2008. https://hal.inria.fr/inria-00164852.

[93] Dionisio Bernal. Kalman filter damage detection in the presence of changing process and measurement noise. *Mechanical Systems and Signal Processing*, 39 (1-2):361–371, 2013. https://doi.org/10.1016/j.ymssp.2013.02.012.

[94] E Peter Carden and Paul Fanning. Vibration based condition monitoring: a review. *Structural health monitoring*, 3(4):355–377, 2004. DOI: 10.1177/1475921704047500.

[95] Peter Van Overschee and BL0888 De Moor. *Subspace identification for linear systems: Theory—Implementation—Applications*. Springer Science & Business Media, 2012.

[96] Carlos Ventura, Palle Andersen, Laurent Mevel, and Michael Döhler. Structural health monitoring of the pitt river bridge in british columbia, canada. In *WCSCM-6th World Conference on Structural Control and Monitoring*, 2014. https://hal.inria.fr/hal-01011750.

[97] LA Bisby, P Eng, N Banthia, L Bisby, R Britton, R Cheng, A Mufti, KW Neale, J Newhook, K Soudki, et al. An introduction to structural health monitoring. 2005.

[98] M Preeti, Koushik Guha, KL Baishnab, Kalyan Dusarlapudi, and K Narasimha Raju. Low frequency mems accelerometers in health monitoring–a review based on material and design aspects. *Materials Today: Proceedings*, 18:2152–2157, 2019. https://doi.org/10.1016/j.matpr.2019.06.658.

[99] K Guru Manikandan, K Pannirselvam, Jack J Kenned, and C Suresh Kumar. Investigations on suitability of mems based accelerometer for vibration measurements. *Materials Today: Proceedings*, 45:6183–6192, 2021. https://doi.org/10.1016/j.matpr.2020.10.506.

[100] Fanis Moschas and Stathis Stiros. Experimental evaluation of the performance of arrays of mems accelerometers. *Mechanical Systems and Signal Processing*, 116:933–942, 2019. https://doi.org/10.1016/j.ymssp.2018.07.031.

[101] G Standoli, E Giordano, G Milani, and F Clementi. Model updating of historical belfries based on oma identification techniques. *International Journal of Architectural Heritage*, 15(1):132–156, 2021. https://doi.org/10.1080/15583058.2020.1723735.

[102] Francesco Benedettini and Carmelo Gentile. Operational modal testing and fe model tuning of a cable-stayed bridge. *Engineering Structures*, 33(6):2063–2073, 2011. https://doi.org/10.1016/j.engstruct.2011.02.046.

[103] Ministero delle infrastrutture e dei trasporti, d.m 17 gennaio 2018 "aggiornamento delle norme tecniche per le costruzioni,". *Suppl. Ordin. Alla "Gazzetta Uff. n. 42 Del 20 Febbraio 2018- Ser. Gen.*, 2018.

[104] Ministero delle infrastrutture e dei trasporti, circolare 21 gennaio 2019 n. 7 c.s.ll.pp. istruzioni per l'applicazione dell'aggiornamento delle 'norme tecniche per le costruzioni'. *Di Cui Al D.M. 17/ 01/2018 (in Italian). Suppl. Ord. Alla G.U. n. 35 Del 11/2/19*, 2019.

[105] Rosario Ceravolo, Giuseppe Pistone, Luca Zanotti Fragonara, Stefano Massetto, and Giuseppe Abbiati. Vibration-based monitoring and diagnosis of cultural heritage: a methodological discussion in three examples. *International Journal of Architectural Heritage*, 10(4):375–395, 2016. https://doi.org/10.1080/15583058.2013.850554.

[106] Edwin Reynders, Jeroen Houbrechts, and Guido De Roeck. Fully automated (operational) modal analysis. *Mechanical systems and signal processing*, 29: 228–250, 2012. https://doi.org/10.1016/j.ymssp.2012.01.007.

[107] Richard S Pappa, Kenny B Elliott, and Axel Schenk. Consistent-mode indicator for the eigensystem realization algorithm. *Journal of Guidance, Control, and Dynamics*, 16(5):852–858, 1993. https://doi.org/10.2514/3.21092.

[108] Gabriele Marrongelli, Filipe Magalhães, and Álvaro Cunha. Automated operational modal analysis of an arch bridge considering the influence of the parametric methods inputs. *Procedia engineering*, 199:2172–2177, 2017. https://doi.org/10.1016/j.proeng.2017.09.170.